FACULDADE DE ENGENHARIA DA UNIVERSIDADE DO PORTO

On the Forces of the Puboviscera Muscle: A Biomechanical Analysis

Mariana Masteling Pereira

Integrated Masters Degree in Bioengineering

Supervisor: Prof. James A. Ashton-Miller

Supervisor: Prof. Renato Natal Jorge

September, 2016

On the Forces of the Puboviscereal Muscle: A Biomechanical Analysis

Mariana Masteling Pereira

Integrated Masters Degree in Bioengineering

September, 2016

Abstract

Introduction: Ten to 15 % of women are injured giving vaginal birth to their first baby. These tears in the pubovisceral portion of their pelvic floor (or levator ani) muscle are not repaired. If the muscle is torn from the bone, then it stays detached. This has been shown to be a major cause of genital prolapse later in life. In this work, which was conducted during my stay at the University of Michigan in Ann Arbor, I was first asked to estimate how much tensile force the pubovisceral muscle normally carries in activities of daily living.
Methods: In the first part of this dissertation I conducted biomechanical analyses to estimate the force carried by the PVM during a selection of increasingly strenuous daily activities. In the second part of this dissertation I measured the maximum anatomic cross-section of the PVM muscle in 24 selected women with intact pelvic floor muscles. By multiplying that area by the maximum specific force developed by striated muscle, one can arrive at a second, completely, separate estimate of the maximum force the PVM is called upon to carry in vivo. The second estimate of maximum muscle force was then used as a check on the magnitude of the biomechanical force estimate.
Results: The biomechanical analyses predicted that each of the PVM sides (left and right) must carry 29, 46 and 60 N of force for the 5^{th}, 50^{th} and 95^{th} percentile woman under static loading conditions, and 48, 78 and 98 N of force under dynamic conditions. Likewise, the 5^{th}, 50^{th} and 95^{th} percentile unilateral PVM has an anatomic cross-sectional area of 0.80, 1.22, 1.79 cm^2 developing a maximum tensile force under eccentric contraction conditions of 40, 67 and 94 N, respectively.
Discussion: The biomechanical and anatomic cross-sectional area-based estimates of maximum dynamic tensile PVM force are in reasonable agreement. However, our knowledge of the detailed functional anatomy of the PVM and its distal attachments and surrounding structures is fairly rudimentary so this is a first estimate that needs to be revisited in the light of more detailed anatomic studies.
Conclusions: The right and left PVM resist up to 48, 78 and 98 N in the 5^{th}, 50^{th} and 95^{th} percentile woman during dynamic activities of daily living.

Financial Acknowledgements

The travel and living costs for Ms. Mariana Masteling to conduct this research were supported by a scholarship to Ms. Masteling from the Fulbright Foundation. Drs. Ashton-Miller and DeLancey participation in this research was supported by US Public Health Service grant from ORWH, SCOR P50 HD044406 "Birth, Muscle Injury and Pelvic Floor Dysfunction" (Project 1) and a donation from the Haas Family Foundation.

Acknowledgments

First I would like to start by thanking Professor Renato Natal. In a biomechanics class he had asked any students interested in biomechanics research to approach the lectern after the lecture. A number of us did just that. He asked what I was interested in. I replied that I liked to play the euphonium in my village band, and that the instrument requires one to blow hard and therefore develop a lot of intraabdominal pressure in order to play high notes. He thought for a moment and then asked the bold and awkward question "Mariana, are you incontinent?". This thesis is a result of that question. Secondly, would like to thank Prof. James Ashton-Miller and Dr. John DeLancey for allowing me to learn from them, giving me new perspectives on the world and research and trusting me with this opportunity.

To the Fulbright Program, there are not enough words to summarize how thankful I am for this opportunity. Thank you for giving me "the chance to develop as a researcher and as a young Portuguese girl who just wants to change the world".

An acknowledgement to everyone in the Pelvic Floor Research Group of the University of Michigan and in the Biomechanics Research Lab for teaching me so many things! Thank you Paige, Payam, Kayla, Dan, Bing, Lahari and Ali!

For my family and friends, thank you! Thank you for making me believe "nothing is impossible"!

BEST Porto, in so many different ways, you made me a better person and gave me a bunch of wonderful friends.

To my American buddies, thank you guys! You made this journey remarkable and unbelievable! I already miss you!

Six years, two schools, four countries, five cities, two continents, lots of knowledge, friends and love later, here I am! Without any single one of you that crossed my path, this would not have been possible. This is my work, but you made me what I am!

Obrigada Amigos!

Mariana

Contents

List of Figures

List of Tables

Abbreviations and Symbols

AA	African American Women
ALOA	Absolute Limits of Agreement
CSA	Cross Sectional Area
DICOM	Digital Imaging and Communications in Medicine
EA	European American Women
LA	Levator Ani Muscle
MRI	Magnet Ressonance Imaging
IAP	Intraabdominal Pressure
PFM	Pelvic Floor Muscles
PRM	Puborectal Muscle
PVM	Puboviscerial Muscle

Chapter 1

Introduction

Injuries sustained while giving birth to a child vaginally have been linked to the development of pelvic floor dysfunction later in life (8) representing a 4-to 11-fold increased risk in developing prolapse and urinary and fecal incontinence to a lesser extent later in life (9).

The injuries sustained during vaginal delivery include tears to a portion of the levator ani muscle (LA). Following the Terminologia Anatomica (10), the levator ani muscle has three subdivisions – the pubococcygeal muscle (whose origin and insertion are more correctly indicated by the newer term pubovisceral muscle) , the iliococcygeal muscle and the puborectal muscle (detailed in Chapter 2). The LA is the main soft tissue structure that supports the weight of the abdominal contents and maintains closure of the levator hiatus at the bottom of the female pelvis under static and dynamic loading. When LA injuries occur they are thought to occur because of excessive tensile levator stretch during vaginal delivery; this has been estimated to reach twice the value normally tolerated by striated muscle in non-pregnant women (11; 12). More specifically, toward the end of the second stage of labor the most ventral pubovisceral part of the levator ani muscle (PVM), can be partially or even completely torn from its origin on the posterior aspect of the pubic bone (13) and even the pubic bone can sustain injury (14). These PVM tears can result in lasting pelvic floor dysfunction in the form, for example, of genital prolapse (15)

Pelvic floor dysfunction adversely affects the quality of life of women (16), leading to more than 356 000 surgical procedures to be performed in 2010 in the U.S. (17). Indeed, it has been estimated that the number of surgeries may reach 600,000 procedures in 2050 (17). As many as 24% of U.S, women undergo surgery for these conditions during their lifespan (18). Unfortunately, up to 40% of these women will have to undergo repeat surgery because the first operation fails (19; 20) As many surgeries are performed for pelvic floor dysfunction as are performed for breast cancer (21), and twice as many as for prostate cancer (21); facts that emphasize the wide scope of this problem. The annual cost of the prolapse operations alone exceed $1 billion in 2001 and is expected to raise (22). Although severe morbidity from pelvic dysfunctions are rare, patients score significantly worse in pelvic floor distress inventories (23) and have a negative self-perception of their body image (24). In addition the increase costs associated with treatments, make pelvic floor dysfunction a common and significant public health issue (23).

A wide range of conservative and surgical treatment offerings are available for women with a pelvic floor dysfunction. For example, physiotherapy in the form of pelvic floor exercises (25) is commonly offered to rebuild and strengthen damaged pelvic floor muscles. This might make logical sense for a muscle with a partial injury in that one tries to strengthen what remains of that muscle if it has the same biomechanical function. If the part that remains has a different function, it is less clear whether just strengthening what remains can help. And if the muscle in question is completely detached from the bone, no amount of physical therapy can restore the lost function. Therefore, when conservative therapy fails, surgery might be an option. In the recent past such surgery might have involved the use of a vaginal mesh implant, but recent studies have pointed to mesh failure rates of over 40% (20). Indeed, there are 20,000 mesh claims for up to $830 million in the U.S. (26). These recent facts create the need to explore other techniques for repairing the PVM. But first, one needs to be able to understand the characteristics of the PVM that one wants to replace. As we shall see one of these is how much force it is required to transmit in daily life.

The anatomy and function of the pelvic floor muscles can be studied using modern imaging techniques as MRI, transperineal or endovaginal ultrasonography or using digital palpation (27). Although these techniques are providing useful new information, to date there is no simple and rapid method for quantifying important functional muscle characteristics such as the cross-sectional area of the muscle. Such information is fundamental for designing better surgical operations and evaluating the rehabilitation of these muscles.

Presently, if the PVM is torn completely form the pubic bone on one or both sides of the midline it is not repaired surgically, perhaps because the risks of infection and other adverse events are considered to outweigh any possible functional benefit (28). However, it is becoming clear that the PVM normally plays an important role as a "lifter" of the anterior pelvic floor (6). When the PVM is completely torn from the pubic bone on one side this lifting function is impaired; when the PVM is torn on both sides its lifting function is lost. This lifting function is distinct from the levator hiatus "closing" function provided by the puborectal muscle, which is never injured during vaginal birth (29). Therefore, there is an argument that replacing the lost PVM lifting function might be advisable from a surgical point of view if the risks of short or long term complications can be brought low enough to be reasonable. Drs. DeLancey, Fenner and Ashton-Miller have submitted an invention disclosure to the University of Michigan outlining a PVM implant design to substitute for the lost PVM lifting function. An essential question is this: How strong such an implant needs to be to replace the lost functions of, say, both the left and right PVM? This master's dissertation addresses that very question using three different approaches.

Chapter 2 and 3 address, respectively, the anatomy and dysfunctions of the female pelvic floor. Chapter 4 describes the testing of a first hypothesis: it is possible to estimate the loading on the pubovisceral muscle using standard biomechanical approaches. Chapter 5 relates to that hypothesis: it is possible to estimate the maximum tensile force developed by the PVM if one can identify the anatomical margins of the PVM and thereafter measure its cross-sectional area in a plane normal to its morphologically parallel muscle fibers. One would then invoke the muscle physiologists' measure of maximum specific force (force/unit area) for striated muscle and multiply this by the PVM anatomic cross-sectional area to find the maximum tensile force it can develop from a physiological perspective. In Chapter 6, the hypothesis is tested that that force measurements obtained using an instrumented speculum can be used to estimate PVM force in the manner of (30). The results from chapters 4- 6 are described in 7, followed by the general discussion of these results in chapter 8, and Conclusions in chapter 9.

Chapter 2

Female Pelvic Floor

The normal female pelvic floor (FPF) is an elegantly complex structure that effortlessly supports and provides positioning for the pelvic organs (31; 32). It is a fibromuscular system of organs and their vascular attachments, supported by a network of muscles, attached to each other and to the pelvic bones by condensations of fascia and fibromuscular tissues, that runs from the symphysis pubis to the coccyx and sacrum, forming the inferior and dorsal walls of the pelvis, doming into the abdominal cavity (33; 34).

The principal striated muscle of the pelvic floor is the levator ani muscle (LA) that provides structural support to the urethra, bladder, vagina and rectum. The LA complex is a U-shaped soft tissue loop that allows the pelvic organs to maintain its position by keeping the urogenital hiatus closed and compressing the vagina, urethra and rectum against the pubic bone. This continuous tonic activity, similar to the continuous activity of the external anal sphincter muscle, closes the lumen of the distal vagina, eliminating any opening within the pelvic floor through which prolapse could occur (8). Two layers of connective tissue cover this LA muscular complex, the superior and the inferior fascia of the levator ani. Together the fascia and the muscle complex form the pelvic diaphragm (8).

The LA can be divided in three sections (1):

- **iliococcygeus:**forms a relatively flat, horizontal shelf and connects both ischial spines, attaching bilaterally to the obturator internus fascia, along the arcus tendineous levator ani.

- **pubovisceral (PVM)** (also known as pubococcygeal) : arises from the pubic bone on either sides attaching to the walls of the pelvic organs and perineal body. It has three subdivisions which are considered portions of the PVM rather than distinct muscles: a) puboperineal (insertion into the perineal body); b) pubovaginal (inserting into the vaginal wall); and c) puboanal (inserting into the intersphincteric groove of the anal canal).

- **puborectal (PRM):** forms a sling around and behind the rectum, some fibers merge with the external anal sphincter. The anterior/interior portion, attaches to the pubis near the bilateral aspects of the symphysis. Its insertion is located more caudally than the PVM.

The urethra, vagina and rectum, pass through an opening in the levator ani called urogenital hiatus. The rectum rests on top of the rear portion of the levator ani complex, and fits in the groove in the midline. The vagina rests on top of the rectum, and is attached bilaterally to the pelvic sidewall along the arcus tendineus fascia, a fascial condensation that runs over the levator muscle anteriorly, and over the obturator internus muscle posteriorly. The bladder and urethra rest on top of the anterior vaginal wall, from which they physically derive (8)(Figure 2.1)..

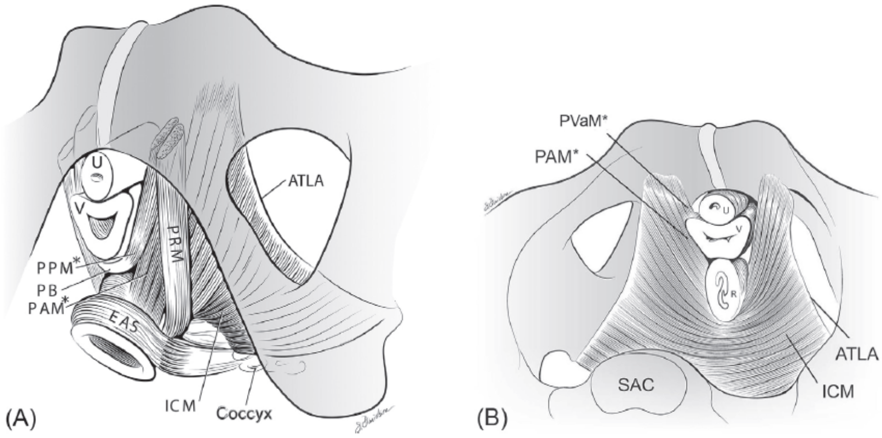

Figure 2.1: (a) Schematic view of the LA muscles from below after the vulvar structures and perineal membrane have been removed showing the arcus tendinous levator ani (ATLA); external anal sphincter (EAS); puboanal muscle (PAM); perineal body (PB) uniting the two end of the puboperineal muscle (PPM); Iliococcygeal muscle (ICM); puborectal muscle (PRM). The urethra and vagina have been transected just above the hymenal ring. (b) shows the levator ani muscle seen from above looking over the sacral promontory (SAC) showing the pubovaginal muscle (PVM). The urethra, vagina, and rectum have been transected just above the pelvic floor. The internal obturator muscles have been removed to clarify levator muscle origins. Puboanal muscle (PAM); arcus tendinous levator ani (ATLA); Iliococcygeal muscle (ICM). Adapted with permission from (1).

Chapter 3

Pelvic Floor Dysfunction

3.1 Introduction

Female pelvic floor (FPF) dysfunction is multifactorial, including factors as parity, age, high impact sports, chronic straining and hormonal status (35) with birth-related injuries playing an important role (15) . This dysfunction is a major public health problem because it decreases patients' quality of life (36; 37; 38; 39) (and there is a lack of information related to symptoms, condition and treatment options in the public domain (40). Pelvic floor dysfunction is the reason of 11% of the women that undergo surgery in the USA. In case of prolapse, more than 200,000 operations are performed each year, with an annual cost for ambulatory care treatment of the condition of $300 million (41) and a total cost exceeding $1bilion in the United States only(22).

During labor the descent of the fetal head and the maternal expulsive efforts distend the pelvic floor to a degree that can increase the chance of anatomic and functional changes in the future (42). The degree of pelvic floor muscle damage is dependent upon specific traumatic events during a first vaginal delivery (43) and not pregnancy or the number of vaginal deliveries (44; 45). Injury is more evident in women who have had long, active second-stage labors or heavier babies (34) and are at older age at first birth (46; 47). In conjunction with vaginal delivery, pelvic floor soft tissue trauma can involve injuries of the perineum, vagina, anal sphincter, pelvic floor muscles and innervating nerves (48).

3.2 Levator Ani Trauma

The main muscle component injured during childbirth are the fibers of the PVM because it is stretched more than any other parts of the levator muscle to more than 3 times its resting length as the fetal head is crowning during the second stage of labor (11). It is easy to see why when the levator hiatus area in young nulliparous women varies from 6 to 36 cm^2 on Valsalva maneuver (46) and minimum fetal head area is about 64 cm^2 (Equation 4.6) (49).

$$A=\pi * (D/2)^2 \approx \pi * 9^2/4 \approx 64 cm^2 (3.1)$$

LA injuries are described using different terminologies including terms like “tear”(50), “defect”(29), “avulsion”(13) and “injury”(43). These might suggest an all or nothing phenomenon, although deficiency implies a measurable gradient of muscle loss (27). In the present work levator ani “tear” will be used, as it refers to the physical phenomenon that causes the injury (14). Major tears of the levator ani muscle can be defined as an abnormal or loss of attachment of the muscle towards the pubic bone, with visible muscle loss at its specific site, either unilaterally or bilaterally (8). Tears have a marked effect on hiatal dimensions and pelvic organ support, appearing in 13-36% in primiparous women delivering vaginally (51). When they occur, tears are observed in the pubovisceral muscle (PVM).

Despite injury most women with major LA defects after vaginal delivery are still able to contract their PFM, although with pronounced lower PFM strength and endurance than women without major defects (52). There is the suggestion that uninjured pelvic floor muscle fibers might be able to compensate somewhat for a loss in PFM strength even in early stage after delivery (51), although methods with greater specificity may be required to quantify exactly where such compensation occurs – it may be difficult or even impossible for the ilococcygeal muscles to compensate for lost PVM lifting function in the case of a bilateral PVM avulsion, for example. MRI studies of LA muscle injuries reveal two patterns: one that involves gross architectural distortion of the anatomy and one that reveals loss of muscle substance, but maintenance of the overall architecture (13). These lead to two LA injury categories:

- **Type I injuries** are confined to individual portions of the PFM in which a portion of the muscle is missing: the levator arch remains intact but some substance of the muscle is lost. Histologically, this attachments are in form of a scarf enthesis as it is an enthesis where two heterogeneous materials (PFM and pubic bone) meet in an oblique angle.

- **Type II injuries** involve detachment of the catenary-like levator arch from the pubic one by excessive tension created in this region during vaginal birth. They involve loss of normal architecture of the pelvis sidewall due to loss of attachment. Changes on the overall architecture of the region is seen, as example, the abnormal appearance of the vagina, spilled lateral and posteriorly from its original position, that might be responsible for the additional risk of prolapse (Figure 3.1).

If a woman has a Type I injury after her first birth is at increased risk for Type II in subsequent births (53).Concerning treatment, for Type I injuries, when the overall muscle attachment remains intact, exercise may certainly help re-innervation of injured fibers and hypertrophy adjacent muscle to compensate for injury. Although, Type II injuries, do not benefit from exercise and early exercise might exacerbate the separation between the muscle and its insertion (13)

3.3 Prolapse

Prolapse is the abnormal movement and deformation of the female pelvic organs (54) (Figure 3.2). A PVM tear impairs the ability of the vaginal walls to resist caudal forces that include

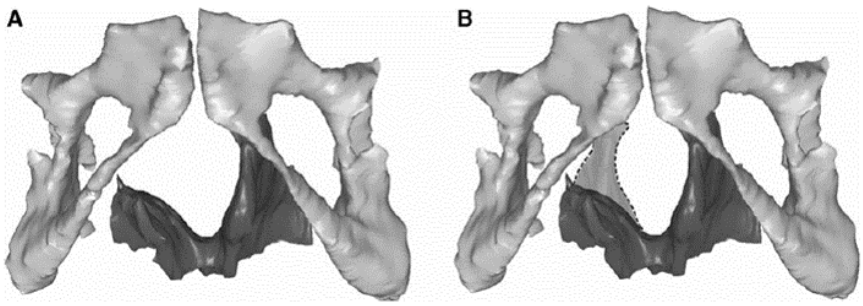

Figure 3.1: (a) 3D model showing the pubic bone and LA muscle with a right unilateral PVM tear – a type II injury. (b) The dashed region shows the expected location of the missing muscle, by reflecting the muscle from the normal side across the midline. Reproduced with permission from (2).

gravity, inertial forces, and intra-abdominal pressure, without incurring excessive movement (55). A more distensible levator hiatus is associated with risk of pelvic organ prolapse (42) and is more common in women after a vaginal delivery than after cesarean section (42). There are three main types of prolapse (56) (Figure 3.2):

- **rectocele:** prolapse of the posterior wall of the vagina and consequent prolapse of the rectum.
- **cystocele:** prolapse of the anterior wall of the, as result, the bladder and urethra may prolapse into the vagina
- **uterine prolapse:** descent of the uterus below its normal location. This is highly associated with cystocele (57; 58)

Clinically, these lesions occur in a variety of combinations. In certain instances of prolapse of these three types, the small intestine and abdominal distend the space between the uterus and the rectum. This is called an entereocele single structure, but rather by combinations of failure in different anatomical sites: up to as many as 20, along with impairment of the LA muscle (54).

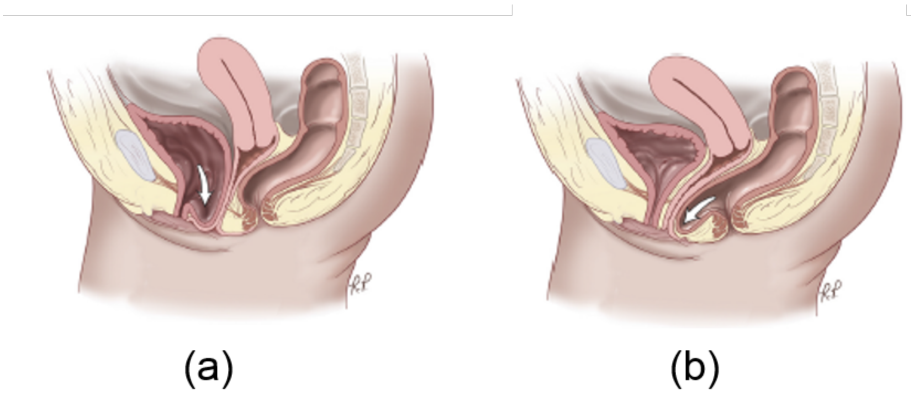

Figure 3.2: (a) Cystocele; (b) Rectocele. Adapted from (3)

Chapter 4

Loads on the Pelvic Floor

The main pelvic floor muscle function is to support the pelvic organs and abdominal contents during activities of daily living. These activities engender changes in the load applied to the pelvic floor and therefore the tension required of its constituent muscles to provide that support (Figure 4.1).

In this chapter the goal is to understand the static and dynamic loads the PVM needs to withstand during a range of activities. We test the hypothesis that it is possible to use biomechanics principles to calculate the loads on the PVM during activities of daily living. The chapter is divided in three parts: morphological characterization, assessment of the applied loads, and the levator plate model.

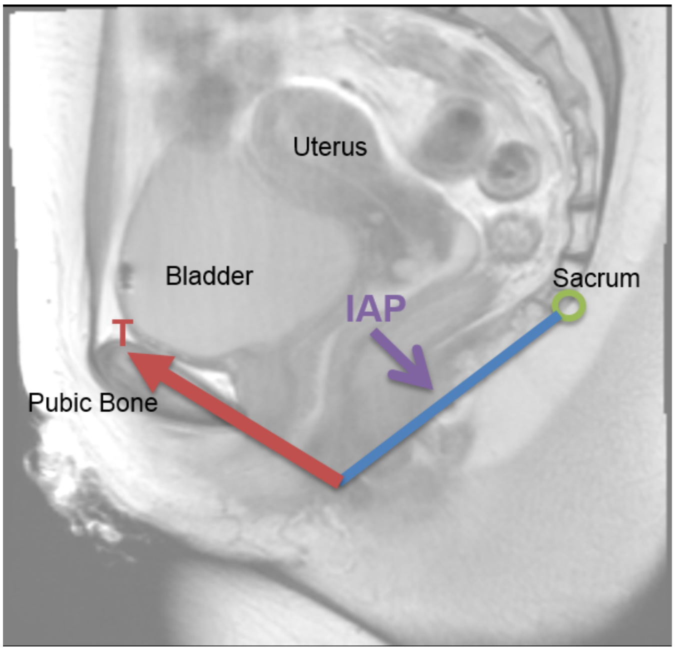

Figure 4.1: Sagittal view of the pelvic floor. With schematic representation of the applied forces (green) to the levator plate (blue) and tension to be sustained by the PVM (red).

4.1 Morphological Characterization

The first step in this analysis is to calculate the load applied to the pelvic floor by the abdominal contents above the pelvic floor. One therefore needs to know the cross-sectional area occupied by the PVM and if one knows the height of the abdominal contents acting on that area, one can calculate the hydrostatic pressure acting on the pelvic floor.

4.1.1 Volume Calculation

The abdominal volume can be calculated as 4.1:

$$V_{abdominal} = A_{pelvicfloor} * h_{abdomen} \tag{4.1}$$

Using data from Baragi et al. (5) who performed an extensive study of the dimensions of 80 female pelvic bones divided in European-American (EA) and African-American (AA) (fig 2) and from the Natick report, an anthropometric report of both female and male soldiers (4) (Figure 4.2), one is able to estimate the volume of the abdominal contents above the pelvic floor for women in the 5^{th}, 50^{th} and 95^{th} percentiles. It was assumed for simplicity that a woman in the 5^{th} percentile for area would also be in the 5^{th} percentile for abdominal height.

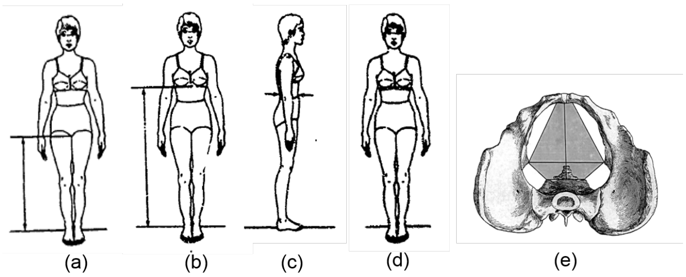

Figure 4.2: (a) Height pubic symphysis to the ground; (b) height of xiphoid process of stern to the ground; (c) depth abdomen; (d) perimeter at level just below bra cups. Adapted from (4); (e) Pelvis with Baragi's Area in grey. Adapted from (5).

Three different abdominal volumes were calculated (Table 4.3). The Pelvic Floor Area, which we shall call "Baragi's area" (Figure 4.2), was found from the data published both for European-American (EA) and African-American (AA) women (Table 4.1 and Table 4.2), considering the smallest area from the two for the 5^{th} percentile (AA women), and the biggest from the two, for both the 50^{th} and 95^{th} percentile (EA women). The 5^{th} percentile was calculated as mean - 2*standard deviation (mean - 2*SD), the 50% as the mean and the 5^{th} as the mean plus 2 times standard deviation (mean + 2*SD) (Table 4.1).

Abdominal height was calculated as the difference between the height of the xiphoid process of sternum from the ground (Figure 4.2 (b)) and the height of the pubic symphysis from the ground (Figure 4.2) (Equation 4.2).

$$h_{abdominal} = h_{xiphoid process} - h_{pubic\ symphysis} \tag{4.2}$$

Table 4.1: Pelvic Floor Cross-Sectional Area (5). In this and the following tables, see text for abbreviations

	EA				AA			
	mean	min	max	SD	mean	min	max	SD
Total area (cm^2)	93.7	75.78	121.35	9.7	88.96	71.27	113.11	10.29

A ratio was created to compare the results from both ellipse, circumference and hexagonal cylinder volumes to assess which volume gives a more reasonable result (Table 4.3 and Table 4.4). Considering the total body volume range between 37 and 65 liters (59), the torso being 50-55% in weight of the whole body (60) and the human body density to be similar to water (992.2 kg/m^3 at 40°C), one finds that the most reasonable ratio is the one considering the use of the Baragi hexagonal cylinder (Table 4.5). For this reason, it is the one that was used in the remaining calculations.

4.1.2 Area of PVM exposed to Intraabdominal Pressure

The cross-sectional area of the PVM that is exposed to intraabdominal pressure in the transverse plane can be estimated from the Baragi Area using certain landmarks (Figure 4.3) and triangle similarity postulates and theorems (Appendix A). For simplicity it was assumed that the width of the most cranial portion of the PVM was 2 cm and that the PVM tapered to a point at the perineal body on the midline. These estimates lead to an approximate unilateral average area exposed to intraabdominal pressure of 3.2, 6.0 and 8.9 cm^2 for, respectively, a 5^{th}, 50^{th} and 95^{th} percentile women. (Table 4.6). [Note: In the end we did not use this exposed PVM area for any further calculations but have left it in here only for academic interest.]

4.2 Biomechanical Analysis of Loads Applied to the Pelvic Floor by Daily Activities

The loads on the pelvic floor were calculated using two different approaches (Table 4.7):

- Using published intraabdominal pressure (IAP) data ((61; 62; 63) and Baragi's area dimensions (5) for: coughing, Valsalva, lifting (2kg and 20.4kg), running and jumping;

Table 4.2: Baragi Pelvic Floor Cross-Sectional Area expressed in percentiles

	EA			AA		
	5^{th}	50^{th}	95^{th}	5^{th}	50^{th}	95^{th}
Area (cm^2)	74.3	93.7	113.1	68.38	88.96	109.54

	EA+AA		
Area (cm^2)	68.38	93.7	113.1

Table 4.3: Different possible approaches for the abdominal volume calculation

<table>
<tr><th>Assumed Shape</th><th>Inferior base (pelvis)</th><th>Superior base (thorax)</th><th>Height</th></tr>
<tr><td>Ellipse based on external diameters of the torso at the sternum level</td><td rowspan="3">Baragi's Area (5)</td><td>Inferred from perimeter at sternum level and abdominal depth and analyzed as it is an ellipse (Figure 4.2 (c) and (d))</td><td rowspan="3">Abdominal Height from (4)</td></tr>
<tr><td>Circumference based on external diameters of torso at the sternum level</td><td>Inferred from perimeter at sternum level and analyzed as it is a circumference (Figure 4.2(d))</td></tr>
<tr><td>Hexagonal "Cylinder" based on the Baragi pelvic floor area</td><td>Baragi'sArea</td></tr>
</table>

Table 4.4: Abdominal Volume dimensions. Data from the Natick Report (US Army Natick Research and Development Command 1977). Last three rows are calculated dimensions. $h_{sternum}$, h_{hip}, $h_{abdomen}$ are the height of the sternum and hip from the ground, $h_{abdomen}$ is the difference between the previous heights. $P_{sternum}$ is the perimeter of the thorax at the level of the sternum, $d_{sternum}$ is the anterior posterior diameter at the same level. $r_{sternum}$ is the radius at the stern level $r_{sternum} = d_{sternum}/2$; $A_{sternum(ellipse)}$ is the cross-sectional area of the abdominal contents of the level of the stern assuming it to be an ellipse, $A_{sternum(circumference)}$ is the same calculation assuming it to be a circumference. Measures followed by an asterisk (*) represent dimensions interfered and calculated from available data. The other rows are original data from the Natick Report(4).

Abdominal dimensions	Units in cm		
	5^{th}	50^{th}	95^{th}
$h_{sternum}$	105.8	115.2	118.9
h_{hip}	69.5	76.1	83.9
$h_{abdomen}$ *	36.3	39.0	35.0
$P_{sternum}$	67.4	74.5	83.4
$d_{sternum}$=thicknesss$_{sternum}$	15.3	18.0	22.3
$r_{sternum}$*	7.7	9.0	11.1
$A_{sternum}$ (ellipse) *	315.0	399.5	528.1
$A_{sternum}$* (circumference) *	361.1	441.1	553.1

Table 4.5: Ratio between different volume calculation approaches and the total body volume

	Ratio (%)		
	5^{th}	50^{th}	95^{th}
Ratio ellipse	14	15	14
Ratio circumference	15	16	14
Ratio hexagonal "cylinder"	5	6	5

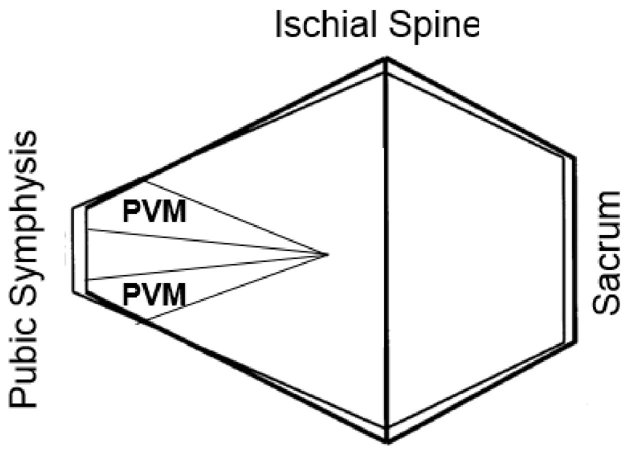

Figure 4.3: Baragi's Area with the indication of the surface area occupied by each PVM based on anatomical landmarks using MRI scans. Double line represent the area of both European and African-American. Adapted from (5)

- Using pelvic kinematics, the loads during a jump landing were calculated with data from (64) , estimating the pelvis deceleration from a graphical analysis of the difference in velocity during the time of impact. Difference in velocity (m/s) is given by the hip marker height at the peak height and at the point of impact in meters, divided by flight time in seconds (Equation 4.3). The acceleration (m/s^2) is the velocity difference divided by impact time (Equation 4.4). The load on the Baragi Area in an upright posture is given by hydrostatic load of the abdominal contents acting above that area; in a dynamic activity, one would add the dynamic load given by the mass of the abdominal contents times the calculated acceleration of the pelvis (Equation 4.5).

$$\Delta v_{pelvis} = \frac{\Delta d_{pelvis}}{t} \tag{4.3}$$

Table 4.6: Approximate PVM area in cm^2 expressed as a percentage of the total Baragi's Area

	Area in cm^2		
	5^{th}	50^{th}	95^{th}
Unilateral Area PVM (cm^2)	3.2	6.0	8.9
% total area	9%	13%	16%

Table 4.7: Loads applied to the Baragi Area in different daily activities

			Area EA (m^2)			Area AA (m^2)		
			5^{th}	50^{th}	95^{th}	5^{th}	50^{th}	95^{th}
Baragi 2002(5)			0.00743	0.00937	0.01131	0.006838	0.008896	0.010954
		Pressure	Force (N)					
		kPa	5^{th}	50^{th}	95^{th}	5^{th}	50^{th}	95^{th}
Egger 2015(61)	Cough	9.4	70	88	106	64	84	103
Egger 2015(61)	Valsalva	12.2	91	114	138	83	109	134
Mouritsen 2007(62)	Lifting 2kg	2.6	19	24	29	18	23	28
O'Dell 2007(65)	Lifting 20.4kg	7.0	52	66	79	48	62	77
Egger 2015(61)	Running	6.5	48	61	74	44	58	71
Egger 2015(61)	Jumping	8.6	64	81	97	59	77	94
			m pelvic contents (kg)					
			5^{th}	50^{th}	95^{th}	5^{th}	50^{th}	95^{th}
Natick report(4)			2.7	3.6	3.9	2.5	3.4	3.8
			Force (N)					
		a (m/s^2)	5^{th}	50^{th}	95^{th}	5^{th}	50^{th}	95^{th}
Mizner 2008(64)	Jump Landing	11.97	58	79	86	54	75	83

$$a_{pelvis} = \frac{\Delta v_{pelvis}}{t_{impact}} \tag{4.4}$$

$$F = m * (a_{pelvis} + g) \tag{4.5}$$

For future calculations the loads were divided in static and dynamic loads and the following types of activities were chosen as representing a variety of daily activities affecting loads on the pelvic floor. Static loads were summarized as (Table 4.8):

- Static standing: weight of the cylinder of water on the top of the Baragi area.
- Valsalva Maneuver: the load from the intraabdominal pressure reported by (61).

Dynamic loads were also calculated:

- Coughing: the load from the intraabdominal pressure reported by (61).
- Jump Landing: from the hip kinematics reported from (64).

Table 4.8: Calculated loads on the pelvic floor, for European-American (EA) and African-American (AA) women by percentile, according to the type of activity.

		EA			AA		
		5^{th}	50^{th}	95^{th}	5^{th}	50^{th}	95^{th}
Statics	Standing	26	36	39	24	34	37
	Valsalva	91	114	138	83	109	134
Dynamics	Cough	70	88	106	64	84	103
	Jump Landing	58	79	86	54	75	83
	Jump Landing + Valsalva	149	193	224	137	184	217

- Jump Landing + Valsalva: as worst case scenario when a person is performing a Valsalva maneuver when landing from a jump, resembling when one lands from a jump with a maximal abdominal muscle cocontraction. This might happen if one was inexperienced and afraid when landing a parachute jump, for example.

4.3 Use of the Levator Plate Model for Calculating PVM loads

The pelvic floor can be modeled as a trap door (2), with the hinge at the sacrum (figure 4.4(a)). IAP is applied on the Levator Plate that is supported/lifted by the PVM, one on each side of the pubic symphysis. Four different models were tested:

[I]All loads applied to the Pelvic Floor supported by the PVM, without co-contraction of the Iliococcygeal muscle All loads applied to the Pelvic Floor supported by the PVM, assuming co-contraction of the Iliococcygeal muscle PVM only supports the loads applied anteriorly to the ischial spines Assuming hinge at the ischial spines

4.3.1 Model I: All loads applied to the Pelvic Floor supported by the PVM, without co-contraction of the Iliococcygeal muscle

Most conservative approach for calculating maximum left and right PVM force required to equilibrate pelvic floor under superincumbent loading – no iliococcygeal muscle co-contraction assumed (Figure 4.4 and Table 4.9).

The PVM tension needed unilaterally to withstand IAP was calculated using the moments of force from T and P about the sacrum (Equation 4.6). One can consider the angle that the PVM makes between its two arms on both side of the pubic symphysis (Equation 4.7). This leads to a final equation, Equation 4.8.

$$F * c - 2 * T * cos\,\Theta = 0 \tag{4.6}$$

$$T = \frac{T}{cos(\Upsilon/2)} \tag{4.7}$$

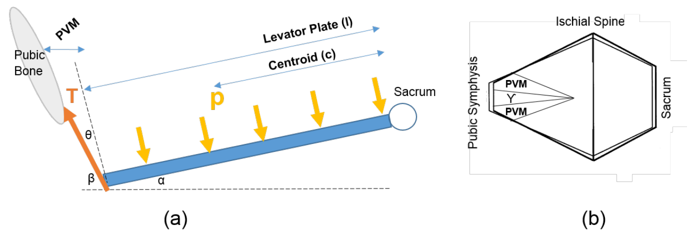

4.

Figure 4.4: Levator Plate Model: (a) showing the distributed pressure load, p, acting as a superincumbent load on the levator plate with a cross-sectional area equal to the Baragi Area. The pressure load can also be represented by a single point load, F, acting normal to the levator plate at the centroid of the Baragi Area. F is not shown here for clarity. The superincumbent load imposes a turning moment about the sacrococcygeal junction (labeled "Sacrum") which must be resisted by the left and right PVM forces, T, which act an angle to a normal to the levator plate in the mid-sagittal plane, and at an another angle to the midline sagittal in the axial plane. (b) Angle is the angle between the two insertions onto the each side of the pubic symphysis, adapted from (5).

$$T = \frac{F * c}{2 * l * cos\ \Theta * cos(\Upsilon/2)} \tag{4.8}$$

F represents the loads on the Baragi Area. T is the tension each PVM needs to withstand during different activities. is the fiber direction of the puborectal muscle, muscle that better represents the direction of the levator plate angle. β is the fiber direction of the PVM. Θ is the angle between a normal to the levator plate and T. The levator plate, l, is the distance from the sacrum at the level of the sacrococcygeal joint. Centroid, c, is the distance from the sacrococcygeal joint to the centroid of the Baragi Area. The angles α and β were described by (6) and Θ is given by equation 4.9. Angle Υ was calculated using axial MRI scans. Levator plate dimensions were estimated as the distance from the posterior limit of the urogenital hiatus and the sacrum. The centroid distance was calculated using equation 4.10, were y_i is the y coordinate of component i and A_i the area of the same component (Figure 4.5).

$$\Theta = 90^\circ - \alpha - \beta \tag{4.9}$$

$$c = \frac{y_i A_i}{A_i} \tag{4.10}$$

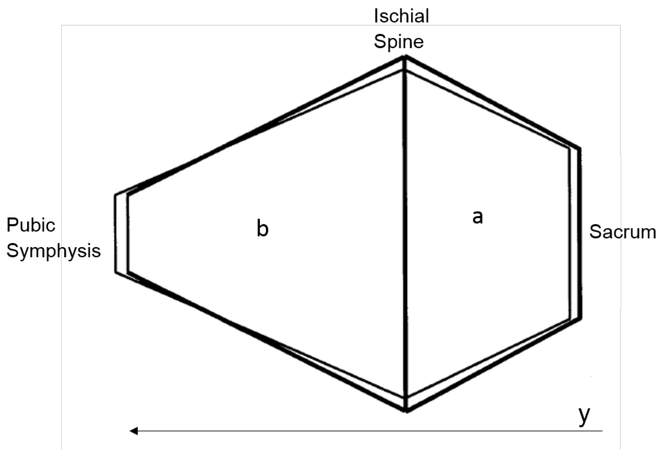

Figure 4.5: To calculate the centroid of the Baragi Area. The total area is divided in two components (a and b). Using Equation 4.10, the centroid concerning the y coordinate can be calculated.

4.3.2 Model II: All loads applied to the Pelvic Floor supported by the PVM, assuming co-contraction of the Iliococcygeal muscle

Less conservative approach for calculating maximum PVM force, T, required to equilibrate levator plate under superincumbent loading – PVM and Iliococcygeal co-contraction assumed whereby the vertical component of the left or right Iliococcygeal muscle-equivalent force, I, is arbitrarily assumed to equal to half the left or right PVM force, T (Equation 4.11 and 4.12 and Tabel 4.10)

$$F * c = 2 * T * cos\,\Theta + I * c \tag{4.11}$$

$$T = \frac{(F - I) * c}{2 * l * cos\,\Theta * cos(\Upsilon/2)}, \quad with\ I = 0.5F \tag{4.12}$$

Table 4.9: Results of the Most Conservative Model, Levator Plate Model I, Predictions of Left and Right PVM Force, T, in the Absence of Any Iliococcygeal Muscle Force. Units are in N.

		Model I					
		EA			AA		
		5^{th}	50^{th}	95^{th}	5^{th}	50^{th}	95^{th}
Statics	Standing	10	14	17	8	14	16
	Valsalva	33	46	60	29	44	57
Dynamics	Cough	26	35	46	23	34	44
	Jump Landing	21	32	37	19	30	35
	Jump Landing + Valsalva	55	78	98	48	74	92

Table 4.10: Results of the Less Conservative Levator Plate Model II Predictions of Left and Right PVM Force, T, in the Presence of Iliococcygeal Muscle Co-contraction. This Model Considers Load-Sharing by the PVM and Iliococcygeal Muscles. Units are in N.

		Model II					
		EA			AA		
		5^{th}	50^{th}	95^{th}	5^{th}	50^{th}	95^{th}
Statics	Standing	5	7	8	4	7	8
	Valsalva	17	23	30	15	22	28
Dynamics	Cough	13	18	23	11	17	22
	Jump Landing	11	16	19	9	15	18
	Jump Landing + Valsalva	27	39	49	24	37	46

4.3.3 Model III: PVM only supports the loads applied anteriorly to the ischial spines

Alternative less conservative model for calculating left and right PVM forces, T, required to equilibrate the superincumbent pelvic floor loading on the Baragi area lying only anterior to the ischial spines (Equation 4.13 and Table 4.11).

$$T = \frac{F * ratio * c}{2 * l * cos\,\Theta * cos(\Upsilon/2)}, \quad with\ ratio = A_{anterior}/A_{Baragi} \tag{4.13}$$

4.3.4 Model IV: Assuming hinge at the ischial spines.

Alternative (levator plate conservative) model for calculating left and right PVM forces, T, required to equilibrate the superincumbent levator plate loading on the Baragi area anterior to the ischial spines when the levator plate only extends to, and is considered hinged at the ischial spines. (he Iliococcygeal muscles are assumed to equilibrate the loads on the Baragi area posterior to the ischial spines (Figure 4.6 and Table 4.12).

4.3.5 Summary

Summary data of the four approaches can be found in table 4.13 and table 4.14.

Table 4.11: Results of the Levator Plate Model III Predictions of Left and Right PVM Force, T in which only the Superincumbent Load Acting on the Levator Plate Anterior to the Ischial Spines was Assumed to Resisted by the Left and Right PVM Forces, F. Units are N.

		Model III					
		EA			AA		
		5^{th}	50^{th}	95^{th}	5^{th}	50^{th}	95^{th}
Statics	Standing	5	8	8	4	8	10
	Valsalva	14	20	23	10	20	27
Dynamics	Cough	14	20	23	10	20	27
	Jump Landing	14	18	19	8	18	22
	Jump Landing + Valsalva	29	38	42	18	38	49
Ratio of the Baragi area anterior to the ischial spine as a proportion of the total Baragi Area		0.56	0.57	0.50	0.43	0.59	0.62

Table 4.12: Results of the Levator Plate Model IV Predictions of Left and Right PVM Force, T in which the levator plate hinge is located at the ischial spines instead of the sacrococcygeal joint. Units are N.

		Model IV					
		EA			AA		
		5^{th}	50^{th}	95^{th}	5^{th}	50^{th}	95^{th}
Statics	Standing	5	6	7	4	6	7
	Valsalva	16	21	25	15	19	24
Dynamics	Cough	12	16	19	11	15	19
	Jump Landing	10	14	16	9	13	15
	Jump Landing + Valsalva	26	35	41	24	33	39

Table 4.13: Comparison of the Calculated Unilateral PVM Force Results for the Four Levator Plate Models, I-IV, under Maximal Static Loading for Women of the Given Percentile. Units are N

Statics		Percentile		
		5^{th}	50^{th}	95^{th}
Valsalva	: PVM-Only Equilibration of the Baragi Area Loading	29	46	60
	Model II: PVM and Iliococcygeal Co-contract to Equilibrate the Baragi Area Loading	15	23	30
	Model III: PVM Only Equilibrates Anterior Baragi Area Loading	10	20	23
	Model IV: PVM Only Equilibrates “Shortened” Levator Plate (to Ischial Spines)	15	21	25
MVC	Force Calculated from CSA to find Maximum Isometric Contraction Force (1*MVC)	20	33	47
Mean Measured Instrumented Speculum Force (N) Measured During Maximal Voluntary Static Contraction Divided by Two			4	

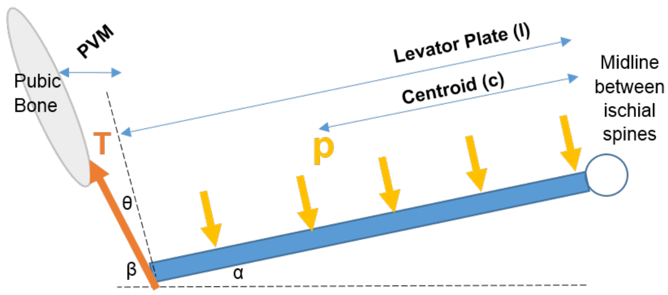

Figure 4.6: Levator Plate Model: showing the distributed pressure load, p, acting as a superincumbent load on the levator plate with a cross-sectional area equal to the Baragi Area. The pressure load can also be represented by a single point load, F, acting normal to the levator plate at the centroid of the Baragi Area. F is not shown here for clarity. The superincumbent load imposes a turning moment about the ischial spines which must be resisted by the left and right PVM forces, T, which act an angle to a normal to the levator plate in the mid-sagittal plane, and at an another angle to the midline sagittal in the axial plane.

Table 4.14: Comparison of the Predicted Unilateral PVM Force (N) Results for the Four Levator Plate Models, I-IV, under Maximal Dynamic Loading for Women of the Given Percentile.

Dynamic		Percentile		
		5^{th}	50^{th}	95^{th}
Valsalva	Model I: PVM-Only Equilibration of the Baragi Area Loading	48	78	98
	Model II: PVM and Iliococcygeal Co-contract to Equilibrate the Baragi Area Loading	24	39	49
	Model III: PVM Only Equilibrates Anterior Baragi Area Loading	18	38	42
	Model IV: PVM Only Equilibrates "Shortened" Levator Plate (to Ischial Spines)	24	35	41
MVC	Calculated PVM Force (N) from CSA to find Maximum Isometric Contraction Force and then Double It (2*MVC) to Estimate Maximum Eccentric Muscle Force	40	67	94
The Force equal to Twice the Measured Instrumented Speculum Force (N) Measured During Maximal Voluntary Contraction Divided by Two			7	

Chapter 5

Measuring the Anatomic Cross-Sectional Area of the PVM in MRI scans of Living Women

5.1 Introduction

As discussed in the Introduction (Chapter 1), there is a need for a reliable and reproducible method for measuring the anatomic cross-sectional area of the PVM on MRI scans in vivo. If one assumes that the PVM muscle is parallel fibered and not pennate or bipennate (66; 6), then one could could use muscle physiological principles to estimate the maximum tensile force developed by the muscle under static conditions from its anatomic maximum cross-sectional area multiplied by its specific force (maximum tetanic force per unit cross-sectional area of striated muscle) developed during a maximum isometric contraction(67).Since muscle physiologists have demonstrated that the maximum dynamic tensile force in a maximally activated muscle under lengthening or eccentric conditions is less than or equal to twice its isometric force (68), one could estimate that a PVM muscle has to carry twice times the maximum isometric contraction force. So knowing the anatomic cross-sectional area of the PVM gives one a reliable way of calculating the maximum force it is called upon to carry in daily life.

There are limitations with the published data of PVM cross-sectional area. In part this is because it is only recently that the true line-of-action of the PVM muscle fibers has been directly measured (6); this was found to be significantly different from that of the puborectal that is almost never injured during childbirth (28). In addition, the PVM cross-sectional area varies along its length, much as does the biceps muscle, with the cross-sectional area being much smaller near its pubic origin, presumably due to the higher Type 1 collagen content at the pubic aponeurosis (69). So, it is important to measure the cross-sectional area at the right point along the muscle length. This has not been done before.

The goal of this chapter was therefore to make accurate measurements of maximal PVM cross-sectional area in living women. We developed a method using 3D Slicer 4.5.0-1 (Bringham and

Women's Hospital, Boston, MA, USA) and ImageJ (version 1.50i; National Institutes of Health, Bethesda, MD; available at http://rsb.info.nih.gov/ij) was developed. This chapter addresses the development of a series of five steadily improving intermediate methods (Methods #0 through #5) which led to the final method (Method #6) we actually used for measuring PVM cross-sectional area. The six different methodological iterations include:

- Method #1: how does one estimate muscle strength
- Method #2: how to define PVM fiber direction
- Method #2: creation of 3D models and the mechanisms of rotating the imaging planes
- Method #3: defining the angle to rotate to
- Method #4: definition of the anatomical visual limits of the PVM
- Method #5: final method

This chapter also includes the experimental design and institutional review board approval and description of the statistical analysis performed.

5.2 Experimental Design

This study used a cross-sectional design with a single experimental group. The experimental group consisted of 24 primiparous women who underwent cesarean section (C-Section) about 7 months prior to MRI scanning; these were selected from the EMRLD study (50; 70). The EMRLD study images were used because of their image quality which were taken on a 3T GE machine (see below) using 2 mm slice thickness. Primiparous women who underwent C-Section were selected because they never pushed to the end of the second stage of labor and so are not expected to have sustained birth-related injuries to the pelvic floor.

For the method development and anatomical characterization phase of this study a second set of "practice" images were used: these were from women with a unilateral levator ani tear and from primiparous women who had undergone an elective C-Section. The first sub-group of these "practice" images were selected from OPAL study because unilateral tear reveals the difference in morphology between an intact PVM on the one side when compared with a torn PVM on the other side (15). The shape of the missing muscle reveals the margins of the normal PVM where its margins might otherwise be confused with adjacent muscle. The second "practice" sub-group were from EMRLD study (50; 70). These two studies are described in the next two paragraphs.

OPAL (Organ Prolapse and Levator) study is a University of Michigan institutional review board approved case-control study with the aim of elucidating the role of the levator ani muscle injury in the pathophysiology of pelvic organ prolapse. Cases were recruited from the Urogynecology Clinic of the University of Michigan and controls by advertisement in the local community. It recruited 247 women between November 2000 and November 2008. Each woman underwent a

MRI in the axial, sagittal and coronal planes using a fast spin proton density technique (echo time: 15ms, repetition time: 4000ms) in the supine position. Scans were performed on a 1.5T superconducting magnet (Signa; General Electric Medical Systems, Milwaukee, WI, USA). Image spacing was 5mm: slice thickness of 4mm and 1mm gap; field of view: 160x160 mm; imaging matrix: 256x256 (15). From the total dataset, 11 subjects evaluated as having a unilateral tear were used.

EMRLD (Evaluating Maternal Recovery from Labor and Delivery) is a study approved by the University of Michigan institutional review board with the aim of characterize pelvic floor injury after labor with serial MRI. Primiparous were recruited between January 2004 and April 2012 before hospital discharge if identified to be of high-risk for pelvic floor injury. Two MRI scans were performed, the first about 6 weeks after birth and a second, around 7 months' post-partum. MRI were made with a 3T scanner (Achieva, Philips Healthcare, The Netherlands) with an eight-channel cardiac coil positioned over the pelvis. Coronal, Axial and Sagittal sequences were made (Echo time: 30ms; Repetition Time: 2100-2500ms), with image spacing of 2mm, filed of view 18cm; image matrix: 256x256; number of signal averages: 2. The subjects that underwent a C-Section (n=24) and had a second time point MRI were used, as healing is expected to be complete by then. From this women 7 had an elective C-Section and 17 had an active second stage of labor prior to C-Section.

5.3 Methods:

5.3.1 Method #1: How to measure muscle strength?

Functional muscle strength is limited by subjective effort and is of special importance in muscles like the LA whose activity is difficult to control volitionally (71). Instead of measuring force directly, one can measure the muscle cross-sectional area which directly allows us to estimate the maximal contractile force that can be developed in the direction of the fibers, independent of the effort level. In this study it was assumed that the fibers of the PVM are parallel fibered from origin to insertion such that a plane that is taken normal to these fibers represents the anatomic cross-sectional area. The maximum specific contractile force of striated muscle is about 2.8 $Kgf(cm^2)$(Equation 5.1) (67; 68).

$$F(Kgf) = CSA(cm^2) * 2.8(Kgf(cm^2)) \tag{5.1}$$

The maximum anatomic CSA is then measured perpendicular to the direction of its fibers, at its largest point.

5.3.2 Method #2: PVM Fiber Direction

Betschart et al. (6) studied the fiber direction of the different levator ani muscle fiber directions, calculating the PVM fiber direction angle as 41° with the horizontal plane (Figure 5.1).

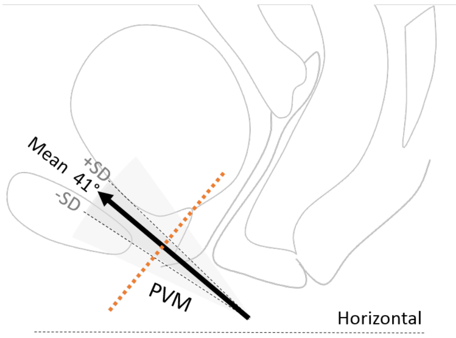

Figure 5.1: Fiber direction of the PVM. Orange dashed line represents the normal plane to the fiber direction. Adapted with permission from (6)

The Pelvic Floor Research Group of the University of Michigan, has chosen to use the computer modeling and visualization software called "3D Slicer" (Bringham and Women's Hospital, Boston, MA), an open source modeling software. Although it takes a little longer to learn, they had found it to provide greater flexibility for making non-standard custom measurements of morphology than commercial modeling packages such as Mimics (Materialise, Leuven, Belgium). Slicer has two commands that lead to plane rotations: "transform" and "reformat" (72; 73). Both developed for slice alignment, when the default slice alignment is not successful or enough. The first has the ability to change the relative position of different label marks, models or regions of interest and allows us to keep track of the changes, and get back to original position. The second, changes the relative position of the planes and changes are not trackable through the software. Both commands were used to obtain the normal angle to the fiber direction. But, after careful analysis of the resultant image, it was understood, that both commands were not producing a useful result. They rotated the whole stack of slices to the given angle and did not cut though the stack (Figure 5.2).

5.3.3 Method #3: Model creating and OsiriX

- Approach 1: It was understood that the software would not allow us to cut through the plane orthogonally due to its voxel characteristics. So it was decided to try another approach. The approach would include label the LA in all its extension using both coronal and axial slices using the model creation tools to build a model. The models were then exported the model to another 3D modeling software like SolidWork (SolidWorks, Dassault Systemes SolidWorks Corp, France) or COMSOL Multiphysics (COMSOL AB, Stockholm, Sweden) to cut a plane normal to the fiber direction. This was time consuming and had errors associated with it: these included unwanted labeling and smoothing associated with importing to different software (Figure 5.3).

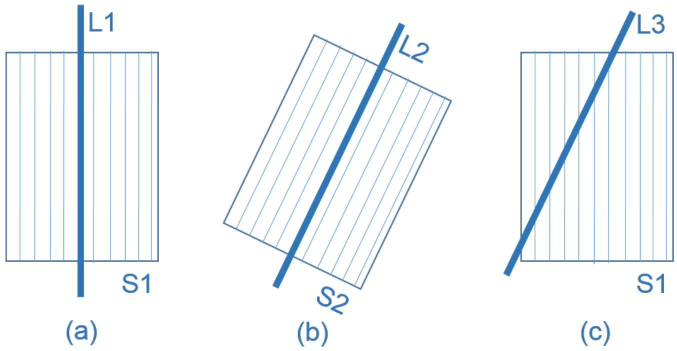

Figure 5.2: (a) Original slices stack (S1) and cutting plane (L1) (b) When using either transform or reformat command, both image stack and cutting plane rotate the same angle (c) Our goal: cutting through the original image stack (S1) and having a cutting plane (L3) at a specific angle.

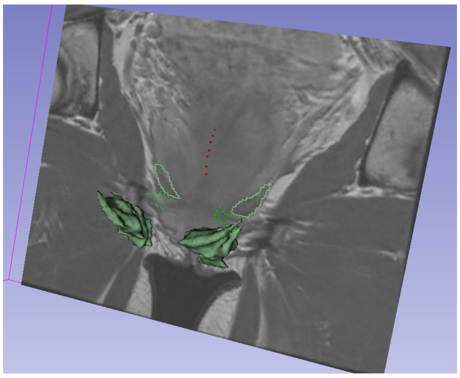

Figure 5.3: 3D Model creation using 3D Slicer

- Approach 2: To address these problems A different medical image analysis software was therefore tried, OsiriX (Pixmeo, Switzerland). OsiriX has in its standard modules, the component for angle rotation. The rotation is visible in the images, although based on a mouse rotation, making the angle shift is not clear and untrackable, meaning it is not possible to known to angle we have rotated too. This makes it difficult to use as a measurement tool.

5.3.4 Method #4: Rotating the Plane

As an open source software, Slicer, can be enriched for specific needs using 'extensions'. An extension called "AnglePlanes" was developed at the University of Michigan Dental School (74) to be able to cut through 3D models. This need led to the capability of using this extension to allow one to cut through a stack of images at a given angle (Figure 5.5).

This extension also allows one to upload a script with the angle information. However, working with the extension developer, it was concluded that the coding for achieving the angle by uploading a file would be more complex than changing it manually.

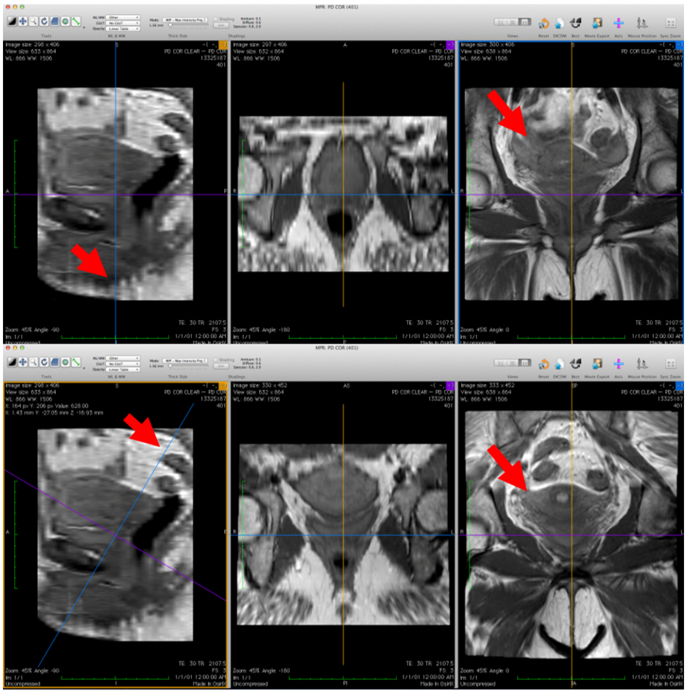

Figure 5.4: Plane rotation in OsiriX. Red arrows represent the angle rotated to.

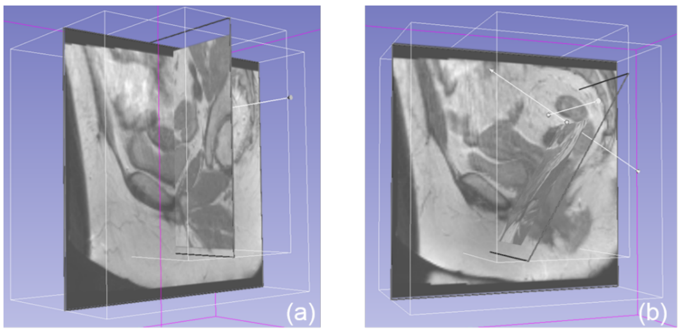

Figure 5.5: 3D view of MRI stack using 3D Slicer. (a) Sagittal and Coronal plane make a normal angle. (b) Coronal plane has been rotated to a normal angle to PVM's fiber direction

5.3.5 Method #4: How to define the rotation angle?

The PVM fibers make, on average, a 41^{o} angle with the horizontal plane (Betschart et al. 2014). However, there is variability between women. Therefore, it was decided to measure the specific angle for each subject.

The PVM fiber direction can be seen in both 5 mm thick images acquired with 1.5T magnet as well as 2mm thick slices made on a 3T magnet. As expected, the second provides to a more detailed image. The fiber direction are seen best in the sagittal scans that cut along the fiber direction, in a para–median sagittal plane, as illustrated in Figure 5.6.

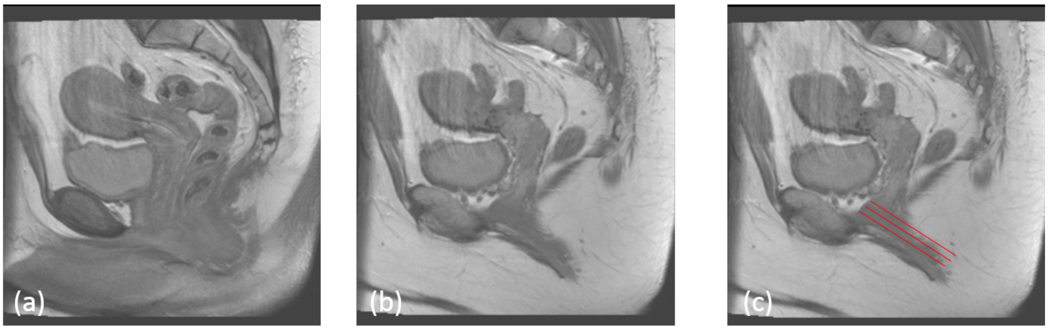

Figure 5.6: (a) Sagittal midline plane. (b) Para-medial plane where PVM fiber direction is identifiable (c) red lines represent the PVM fiber direction

To standardize the process, the angle was measured as the angle between the points located (Figure 5.7):

1. Pubic Bone
2. Location following the angle direction

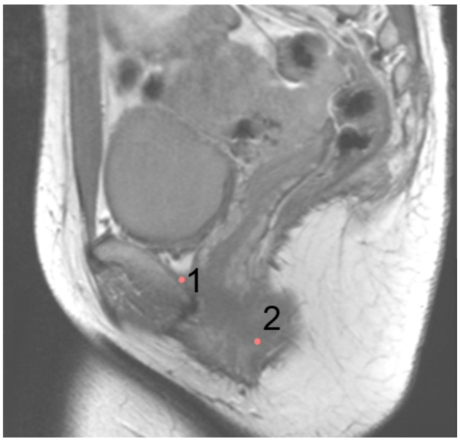

Figure 5.7: Fiducial placing for PVM fiber angle

5.3.6 Method #5: What portion of the LA is the PVM

After rotating the plane so that it is perpendicular to the fiber direction line it is necessary to export the image because Slicer does not allow labeling to be performed in this rotated plane becauseit cuts through the original voxels of the image. Therefore a second software , ImageJ a free software (version 1.50i; National Institutes of Health, Bethesda, MD; available at http://rsb.info.nih.gov/ij) was used for this purpose (Figure 5.8).

Next, we outlined the muscle. Although the medial, lateral, and inferior margins of the muscle are visible, In its upper portion The PVM merges with the iliococcygeal muscle and there is

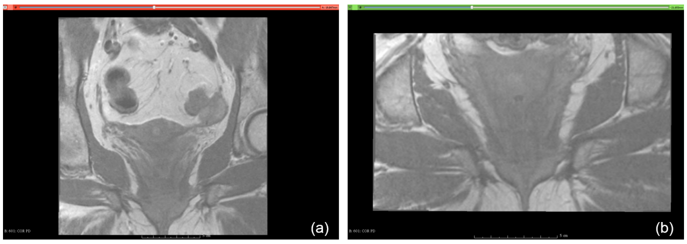

Figure 5.8: (a) Original coronal slices (b) Tip coronal slice view.

no consistently visible separation between them. Therefore we developed a set of anatomically-based principles to allow us to define the upper margin of the muscle. To accomplish this, several anatomical constraints were tested to define the limits of the PVM (Table 5.1).

Intuitively, the transition from the PVM to PRM is clear, as the physiognomy chance is quite obvious, as seen in figure 9. When moving posteriorly to the puborectal muscle, the fibers start to be less organized (Figure 5.9 (a)) and start stretch into a less parallel organization (Figure 5.9(b)).

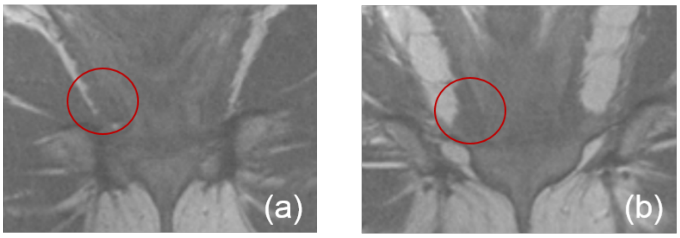

Figure 5.9: Different muscle morphology between an anterior point, that is only PVM (a) and a point where PRM fibers are already visible (b).

Using the coronal scans rotated to be normal to the PVM fiber direction, one started by defining the perineal body at the level of the perineal membrane as the posterior "stopping point". However, one realized that this point was always posterior to the point thought to be the posterior stopping point. In the case of C-section women, this distance was calculated by: identifying the scan I which the anterior wall of the perineal body is visible and by calculating the distance to the slice considered to be the stopping point (Figure 5.9). In the case of the unilateral tear women, the distance from the anterior wall of the perineal body to the first slide was used, when moving anterior-posteriorly, where the puborectal muscle was visible, meaning that is the transition point,

Table 5.1: Proposed and tested limits of the PVM

Anatomical structure	Comment
Obturator canal	Lies at the margin between the muscles. Is not easy to identify.
Anal sphincter	At the region of the anal sphincter, even considering its anterior limit, most of the fibers are already from the puborectal Muscle. Muscle physiognomy is clearly different than in a more anterior location.
Posterior urethral wall at its lower half	There are still PVM fibers after this limit.
Perineal body	Fibers of the puborectal start to be visible at this point.

as they are missing their PVM on the torn side. This average distance was calculated as 11 mm in 18 women.

Cranially to the PVM one finds the iliococcygeus muscle. The transition between the PVM and the iliococcygeus muscle was also found not to be clear. From his extensive surgical experience Dr. DeLancey defined the width of the PVM as being “two fingers”. In case of the unilateral tear women, the PVM is missing, but the iliococcygeus muscle is still present. The point this transition was seen and marked. Considering the first slide when moving posterior-anteriorly where the arcuate pubic ligament was visible, the vertical distance to that point was. The same procedure was adopted in women that underwent an elective C-section, but in those, it was considered the point where visually the start of the transition was visible (Figure 5.10). This distance was measured as averaging 19 mm in 18 women.

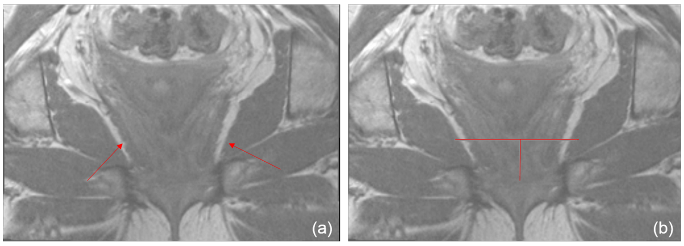

Figure 5.10: PVM width in the tipped coronal plane: (a) arrows show the normal indentation at the PVM/iliococcygeus transition. (b) marking off the 19 mm distance from arcuate pubic ligament.

After tracing the width limits using an onscreen ruler tool and identifying the posterior limit of the PVM, the slices between the defined posterior limit and the pubic bone were imported to ImageJ as separate images and converted into a stack in order to label the PVM (Figure 5.11). The CSA of interest is then found as the largest cross-section in each subject. A detailed protocol can be found in Appendix B.

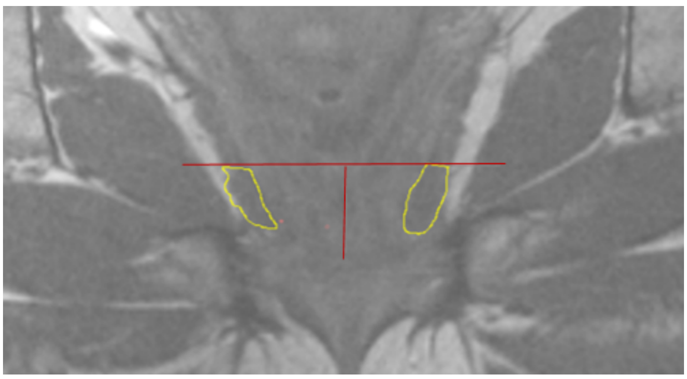

Figure 5.11: ImageJ Labeling example of the PVM in the tipped coronal plane

5.3.7 Method #6: Final Method for measuring PVM Anatomic Cross-sectional Area

The final method that was developed can be summarized as: Using 3D Slicer:

1. Import axial, sagittal and coronal images into 3D Slicer
2. Identify the PVM fiber direction, using a para-midline sagittal scan to calculate the angle it makes with a horizontal line/axial plane.
3. Rotate the coronal plane, using Plugin AnglePlanes (74), to normal angle to the PVM fiber direction.
4. Define a 19 mm vertical width at the arcuate public ligament posterior limit in the coronal images – cross-check for this point using sagittal plane. Trace an horizontal line at the 19 mm level.
5. Identify the slice located 11 mm anteriorly to the perineal body. Consider for labeling the slices comprise between the pubic bone and that reference point. Access each individual anatomy to identify guideline fitting.

Using ImageJ:

1. Label the PVM, as LA region contained within the previously defined limits

5.4 Statistical Analysis

After protocol training, CSA measurements using the final protocol were performed by two raters in two different time points. All statistical analyses were conducted using SPSS (version 23, IBM, Chicago, IL, USA) and p-values<.05 indicated statistical significance. All data are reported as mean standard deviation (SD) and percentiles in case of the area. Differences in area measurements between raters and between time points for the same rater were assessed with paired t-tests. Intraclass Correlation Coefficients (ICCs), (mode: two-way random; type: absolute agreement)(75), Bland-Altman plots(76)and absolute limits of agreement (ALOA) (mean$\pm$1.96 standard deviations of the difference) were used to assess measurement agreement between raters and within rater over time.

Chapter 6

Speculum measurements of maximum volitional levator ani contractile force in living women

The EMRLD study comprises, besides MRI scans, of a pelvic exam that called for a volitional pelvic floor contraction when an instrument speculum is inserted in the vagina. In each patient an instrumented speculum was used to measure the force generated by the LA during a maximum voluntary contraction of the pelvic floor (7). The instrumented speculum is made of two parallel aluminum bills, cantilevered and held substantially parallel to each other. The upper bill of the speculum is divided in two: the distal end of the upper bill is also rigidly connected to the lower bill, in order to avoid cross-talk from intraabdominal pressure (7) (Figure 6.1).

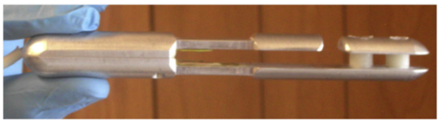

Figure 6.1: Photograph of the Speculum used in the measurements

The instrumented speculum was covered with a disposable condom and lubricant before insertion in the vagina. The ventral bill rests against the anterior vaginal wall, resisted by compression of the urethra against the pubis symphysis. The posterior bill was then pulled towards the anterior bill in the distal region of the vagina by the contraction of the pelvic floor muscles and the force with which the two speculum bills were compressed was measured by the instrumented speculum (7) (Figure 6.2).

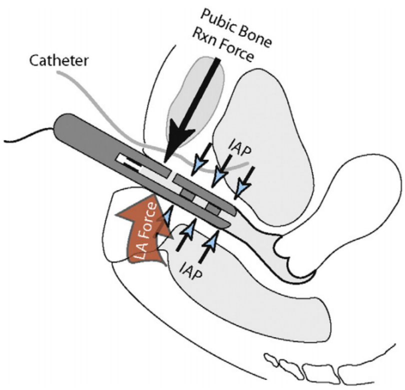

Figure 6.2: The upward red arrow (LA Force) illustrates the line of action of the levator ani force; the downward black arrow (Pubic Bone Rxn Force) shows the line of action of the corresponding reaction (Rxn) force from the inferior symphysis pubis. The short black arrows represent the IAP, acting normal to the upper and lower surfaces of the compound lower bill; these pressures null one another out so as to minimize the net force on that bill due to IAP. Minimizing this net force also minimizes the effect of IAP on the measured VCF. The short black lines near the root of each bill show the location of the strain gauges. Adapted with permission from (7).

Chapter 7

Results

7.1 Measurements of Pubovisceral Muscle Cross-Sectional Area

MRI scans of 24 primiparous women who had a Caesarean section but had not had a vaginal birth about 8.1 $\pm$ 2.2 months prior to scanning were used. The age of this group was 28.9 $\pm$ 6.4 years, the duration of second stage ranged from 0 to 636 minutes, and average body mass index (BMI) was 27.0 $\pm$ 6.9 kg/m^2. For the final results, the measurements of the two raters at the second time point were averaged for each subject. The mean of the maximum PVM CSA for the 24 subjects, measured by two different raters was 1.22 $\pm$ 0.25 cm^2, range [0.79 1.871]. The 5^{th}, 50^{th} and 95^{th} percentile were also calculated, being, respectively: 0.80 cm^2, 1.25 cm^2 and 1.79 cm^2 (Figure 7.1). The average fiber direction angle was 32 $\pm$ 6°, range 18 to 50°. Measurements between raters were considered similar and correlated at time-point one and time-point two (p=0.285; ICC=0.954 [0.898 0.980]) and (p=0.154; ICC=0.892 [0.796 0.952]). Measurements for both raters were found to be similar comparing the two time-points (p=0.093; ICC=0.886 [0.751 0.949]) and (p=0.244; ICC=0.904 [0.793 0.957]). Bland-Altman plots and ALOA for intra-rater and inter-rater reliability at time point one and two were plotted (Figure 7.2). The error of the measurements of the two raters at time point two was 7$\pm$ 5%.

7.2 Predicted Loads on the Levator Ani and PVM Forces

The predicted loads on the Baragi Area, range from 34 N while standing to 79 N in a jump landing and 114 N when performing a Valsalva Maneuver, for a 50% Percentile African-American women (Table 4.8). The expected loads supported unilaterally by the PVM using the Levator Plate Model are present in table 7.1(a replication of table 4.9) and the predicted unilateral loads using the CSA (Equation 4.8) in table 7.2 .

For comparison, the maximum force measured for the same subjects by the instrumented speculum was significantly less than these values was 6.7 $\pm$ 3.6 N, range [3 17], and its distribution concerning each subject PVM CSA can be seen in figure 7.3.

Table 7.1: Results of the Most Conservative Model, Levator Plate Model 1, Predictions of Left and Right PVM Force, T, in the Absence of Any Iliococcygeal Muscle Force. Units are in N.

		Model I					
		EA			AA		
		5^{th}	50^{th}	95^{th}	5^{th}	50^{th}	95^{th}
Statics	Standing	10	14	17	8	14	16
	Valsalva	33	46	60	29	44	57
Dynamics	Cough	26	35	46	23	34	44
	Jump Landing	21	32	37	19	30	35
	Jump Landing + Valsalva	55	78	98	48	74	92

Table 7.2: Predicted Unilateral PVM force based on measured PVM cross-sectional area (CSA). Units in N.

	Predicted unilateral PVM force (N) based on measured PVM		
	5^{th}	50^{th}	95^{th}
5% Relaxed in Supine Position	1	2	2
10% Relaxed Supine Position	2	3	5
Maximum Voluntary Contraction (MVC)	20	34	47
2* MVC	40	67	94

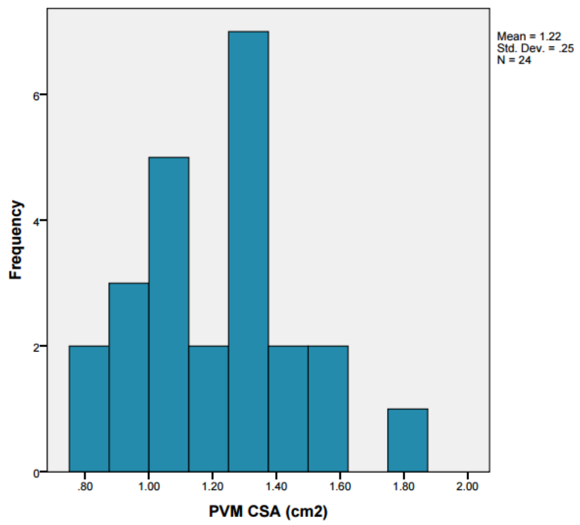

Figure 7.1: Histogram of measured unilateral PVM CSA

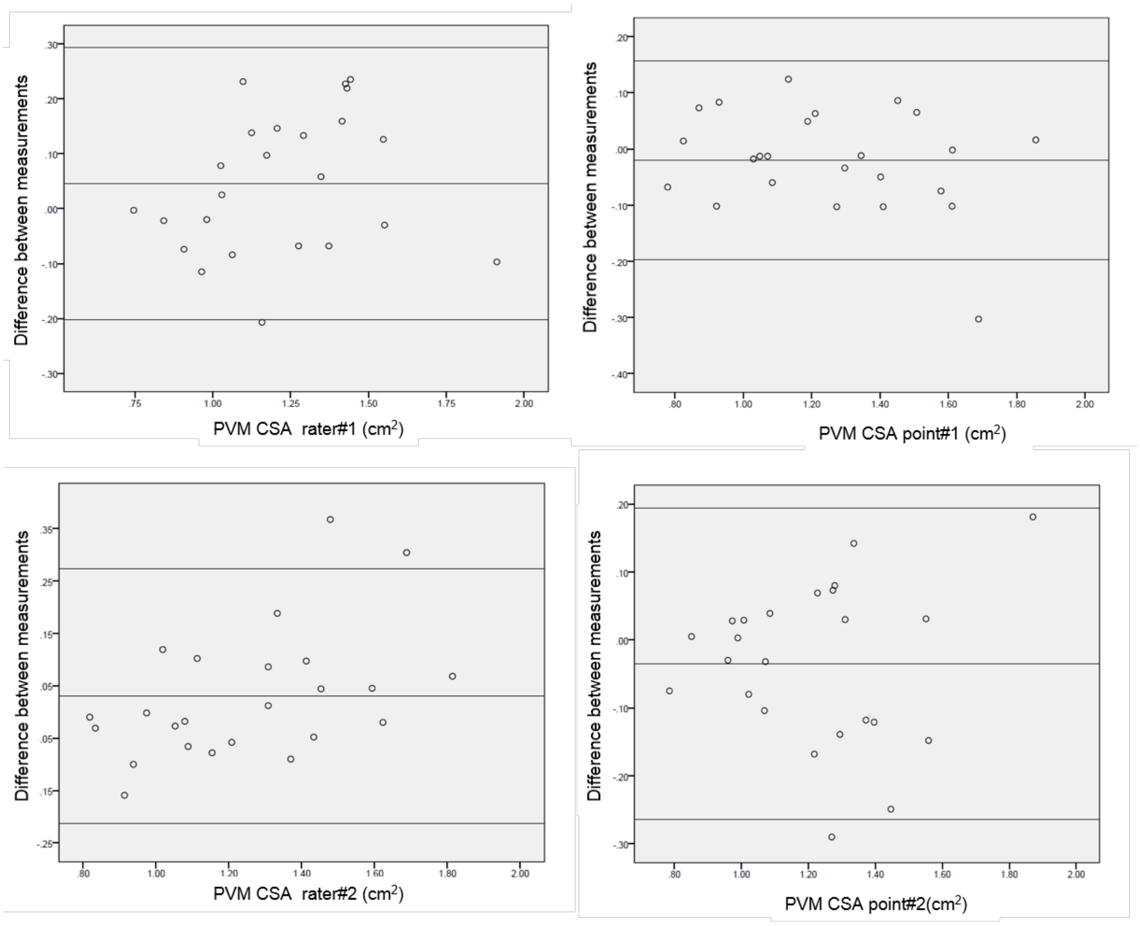

Figure 7.2: The Bland-Altman and ALOA plots.From left to right top to bottom. Intra-rater reliability for rater#1. Inter-rater reliability at time point #1. Intra-rater reliability for rater#2. Inter-rater reliability at time point #2.

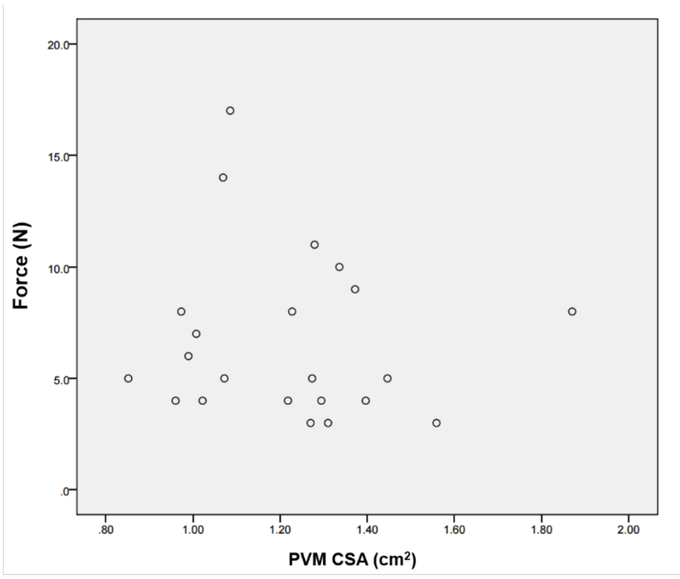

Figure 7.3: PVM CSA versus force measured with the instrumented speculum

Chapter 8

Discussion

8.1 What is new?

The method used to calculate the Pubovisceral Muscle cross-sectional area (Chapter 5) is the first, to our knowledge, to use a plane that is normal to the recently described PVM line-of-action and muscle fiber direction (6) in order to measure the CSA directly from the MRI data. The use of specific anatomical landmarks and measured distances to define the PVM anatomical limits has not been described in literature before. This is the first time that three different ways (i.e., biomechanical, physiological and intravaginal speculum) of estimating and/or measuring maximal PVM force have been compared.

8.2 How do the present results compare with published data?

Different research groups have worked on developing a strategy to describe levator ani muscle morphology (Table 8.1). Hoyte et al. (77) , Chen et al. (2) and Morris et al (71) analyzed the muscle as a complex and not a specific subdivision using different techniques. Hoyte et al. used manually segmented axial MRI and a mathematical approach to calculate the thickness in each point. Chen et al. and Morris et al. created three dimensional models after labeling the Levator Ani using all three orthogonal planes. Results for these techniques ranged from 0.5 - 1 cm for thickness and 2.5 – 4 cm^2- for the CSA of the levator ani. Those estimates are generally larger than our present estimates.

Table 8.1: Average levator ani cross-sectional area and median thickness using MRI

Present Result (cm^2)	Study	Average Unilateral PVM CSA (cm^2)	Median Unilateral Levator Ani Thickness (cm)
1.22	Hoyte et al. (77)		0.5 - 1.1
	Chen et al. (2)	2.47 (left side) 2.4 (right side)	
	Morris et al. (71)	4.06	

Table 8.2: Comparison of puborectal cross-sectional area and thickness using MRI and ultrasound

Study	Technique	puborectal area (cm^2)	puborectal thickness (cm)
Alt et al. (78)	MRI		0.72±0.20(left) 0.57±0.19 (right)
Fielding et al. (79)		4.4±0.7(left) 2.2±0.5 (right)	
Ackerman et al. (81)		5.2±1.6(left) 5.2±1.3(right)	
Kruger et al. (80)	Ultrasound		0.7±0.11

When considering measurements of sub-portions of the levator ani, the published results concern what the authors refer as the puborectal (Table 8.2). These authors are studying the portion of the levator ani muscle that is injured during childbirth and carefully performed MRI analysis shows that this is actually the PVM and so the label puborectal muscle may not be accurate. In the field the separate nature of these muscles has not always been recognized leading to confusion. Whether or not the technique includes part or all of the puborectal and pubococcygeal muscle may explain the wide range of measurements present in the literature (Table 8.2). Using MRI, Alt et al. (78)measured the thickness at the area surrounding the rectum in the axial plane, Fielding et al. (79) used the level of the transverse urethral ligament, at each side of the vagina, for the same measurement. Using ultrasound for the same measurement, Kruger et al. (80) used a plane approximately 1 cm above the levator hiatus. Ackerman et al. (81) measured the puborectal cross-sectional on axial scans at the level of the pubic symphysis and bladder neck.

The wide range of areas (2.44 cm^2 (2) to 5.2 cm^2 (81)and thickness measurements (0.6 cm (78) to 4.4 cm (79) present in the literature appear to be the result of using different techniques and protocols. Some of the variation is explained by the use of different imaging modalities, namely 3D/4D ultrasound imaging and MRI, and using different planes for measurements (80); in addition, variations in image quality, the use of different anatomical terminology for the same anatomical region, and the use of different landmarks adds to the variability. Most other authors do not use techniques that are limited to the PVM , but measure in a certain region that contains both muscles. This distinction is important because estimates about the force lost with PVM injury would be inaccurate if the uninjured puborectal muscle was also included.

Our results for cross-sectional area are smaller than published values (the present value of 1.22 $\pm$ 0.25 cm^2 vs 2.44 cm^2 (2) and 4.06 cm^2 (71)). This may be because the present measurements were restricted to the PVM, whereas the published data likely include other muscle, sometimes the iliococcygeus, but also the puborectal muscle in their measurements. The present use of a technique that analyses the CSA at a normal plane to the line-of-action of the PVM muscle fiber direction is likely the most anatomically and physiologically accurate technique achieved to date. For example, the other studies did not measure orthogonal to the line-of-action of the PVM muscle fibers.

8.2.1 Estimates of PVM contractile force

The PVM muscle CSA should yield a reliable estimate of the maximum isometric static force and dynamic eccentric contraction force that the PVM is dimensioned to withstand in daily life in each of these living women measured. These estimates, which do not depend on estimating Baragi area or assuming LA muscle co-contraction strategies, should be reasonably accurate as long as we have not overestimated the specific force for the PVM as being 2.8 Kg/cm^2 . It is possible PVM might have a lower specific force, but not likely they have a higher specific force than regular striated muscle. There are different types of striated muscle in the jaw muscles than regular striated limb muscles and this could be true of the LA, however there is no evidence of this in the PVM to date. Muscle physiologists need to measure the contractile properties of the PVM muscle *in vivo* in humans, a difficult experiment.

The instrumented speculum measures of PVM force could not have been influenced by the presence or absence of iliococcygeal muscle contraction because that muscle lies too far posterior to contribute to the measured force on the instrumented speculum. But the instrumented speculum measure of maximum voluntary levator force might be low because of the generally poor LA volitional motor control in healthy women. Indeed, 10% of healthy women cannot willfully contract their LA at all. As cases in point, the number of women with large PVM CSA values who could not generate much additional force on the instrumented speculum above when asked to contract (see scatter plot in Figure 7.3)could plausibly to be those with difficulty contracting their LA reliably.

The results of Model I are conservative in that the iliococcygeal muscle was assumed not to contribute to equilibrating superincumbent loads on the levator plate. The results of Models II - IV are less conservative, provide consistent PVM force values, and give surprisingly similar results in that PVM tension was approximately half that in Model I. While the inertial loads in Model I were reasonable (equivalent those in a 30 cm jump landing) we conclude the truth lies between Model I and Models II – IV.

As discussed in Chapter 5, the maximum contractile force of striated muscle is about 2.8 Kgfcm^2 (68; 67), normal muscular tension ranges from a value of perhaps 10% activity during the relaxed supine posture (82; 83) to twice maximum isometric contraction value during an eccentric or lengthening contraction (in case of an unexpected fall or landing).

For the PVM and its unilateral calculated area, these measurements of its maximum unilateral cross-sectional area translate to a range from 2 to 67 N on each side. For comparison, the Levator Plate calculations using Model I, in Chapter 4, provide a range from 14 to 78 N; the two sets of results agree quite well despite the considerable simplifications used in the Levator Plate Model.

Considering the speculum measurements, the average of forces in the studied subjects is substantially larger than the published data using the same device (6.2 $\pm$ 3.7N vs 3.8 $\pm$ 1.8 N) (7). The measured speculum force does not correlate with the PVM CSA (see Figure 7.3). This difference is expected because the published data concern women that have had vaginal deliveries, and besides which they are older and heavier than our sample. It is interesting that the instrumented speculum force measurements are significantly smaller than both Levator Plate Model and CSA PVM force predictions. The speculum measures the force developed by both the left and right PVM. The reason that the speculum forces are lower than the calculated PVM maximal force may be explained by the difficulty that many women have in volitionally contracting their pelvic floor muscle *maximally*. A volitional maximum PVM contraction is rarely called for in daily life and would likely require specialized motor training over a longer period. Most pelvic floor contractions are probably posturally-related and happen semi-automatically without thinking when jumping or speaking (83). Most tests of pelvic floor muscle strength are taken on a single day with little scope for practicing PVM motor control with feedback of knowledge of results over weeks in the same way that progressive resistance training can lead to dramatic increases in limb muscle strength of 50% over a four week period due to improved motor control (for example, (84)).

The three approaches above yield tensile force that are significantly lower than the maximum tensile strength of commercially available gynecological mesh used for implants (630 N/cm)(85).

8.3 Defining the anatomic margins of the PVM on MRI

The definition of the boundaries of the PVM is based on three different concepts: the angle of its line-of-action and hence its fibers, the definition of its cranial limit and the definition of the posterior limit.

The PVM fiber direction angle has been studied by Betschart et al.(6) and our angle is smaller than published ($32 \pm 6^\circ$ vs $41 \pm 8^\circ$). The protocol used had similarities to the published one: fiber direction calculated from the sagittal plane, but calculated the direction of the whole muscle and not of a specific muscular fiber. The scans were also not correct the scans for the PICS (Pelvic Inclination Correction System)(86). the fact that we did not include the PICS adjustment that creates a standard horizontal rather than the horizontal that is established by the scanner coordinate system, made the angle calculation relative to the horizontal axis of the scan for each individual subject, maintaining the whole alignment between the different planes, and using a subject-specific angle and not an average angle in each subject. The difference of 9° to our data, only implies an error of approximately 1% in the area measurement (AppendixC).

The cranial limit of the PVM is its transition into the Iliococcygeal muscle. Although this is clear in concept, during dissection, there is no feature that can always be see that would be visible in MRI that would allow this distinction to be consistently used to define the extent of the muscle. it is difficult to define the discrete portions of the LA. It is known that the Iliococcygeal muscle is not injured during childbirth, so, in women that have a unilateral tear, both Iliococcygeal and PVM are present in the healthy side. On the torn side only the Iliococcygeal (and the puborectal) muscle is present. This anatomical difference is what allowed us to calculate the width of the PVM. As, only 11 subjects with this uncommon characteristic were available, and their MRI slices were 5 mm thick, woman that had an elective C-section (without second stage of birth) for their only birth were also used. As in these newer scans, the slice thicknesses were 2 mm thick allowing for more detail to be seen in the alternative planes. In those women the transition between these two components of the PVM is also clear.

The same rationale was used for the identification of the posterior limit of the PVM. The anterior wall of the perineal body is an anatomical feature that is identifiable in the sagittal plane in all women. When one considers the stopping point to identify that region in ventral to which the scan plane contained only the PVM, it was seen that, the slice one would consider as stopping point was a two of slices before the perineal body. For this reason, this distance was calculated.

The definition of these limits, allows us to be systematic, but can represent an added error to the measurement. For specific woman the PVM could be bigger and its width might be more than 19 mm, or she may be smaller and it would be less than 19 mm. The same is true when considering the posterior stopping point. Even though there is the possibility of some added error from this assumption, on the other hand having a standard border for measurement avoids the errors of not knowing precisely where the muscle transition from PVM to iliococcygeal muscle occurs or where the puborectal muscle begins to overlap the PVM that would create its own uncertainty and variability.

8.4 General Discussion

8.4.1 Strengths & Limitations

The main strength of the method is the use of the plane normal to the muscle fiber direction to calculate the PVM CSA. This method also greatly reduces the time needed for obtaining result. It took about 30 minutes to perform the CSA measurement for each subject from DICOM import to obtaining the area value, this is significantly quicker than approaches that require model creation (2) that could require up to 8 hours per subject for all the labeling and computing steps. In addition, the ability to use the MRI images themselves avoids the error introduced by model creation where computer smoothing algorithms create an object that is not the same as the original muscle.

The labeling process itself, was supported by the definition of clear limits However, the PVM is a muscle comprised between different structures: obturator internus muscle, perineal membrane, vessels, organs and fat. Being able to identify it requires training by an experienced gynecologist with specialized anatomical and MRI knowledge. Considering trained raters and the use of high-quality images inter-rater differences were calculated as $7\pm5\%$. It is expected that in lower quality images the error to be higher.

The strength of the CSA protocol is also supported by the statistical analysis performed. The ratings were statistically different using paired t-tests and had high intraclass correlation coefficients (ICCs) when comparing two raters and within-rater over time. Comparison between raters had ICCs of 0.954 [0.898 0.980] and 0.892 [0.796 0.952] for, respectively, first and second time comparison. The difference in ICCs can be explained by the inherited variability of outlining a small structure that has indistinct visual borders. When comparing the two-time points within rater, rater#1 had an ICCs of 0.886 [0.751 0.949] and rater#2 had an ICCs of 0.904 [0.793 0.957]. Using the descriptive tools of Bland-Altman plots and the ALOA, one can see limited measurement bias for rater#2 and no bias in the measurements for rater#1. The presence of a slight proportional bias for rater#2 is not alarming, as the paired-tests indicated significant differences between raters were not found and the ICCs demonstrate high levels of associations between and within the raters. One of the reasons for this bias can be the be the small sample size as well as the reliability studies being performed on the same subjects as the one used for protocol training, once those are the only subjects with these characteristics in our database. The possibility of a slight proportional bias should be address in future uses of the method as one of its limitations.

8.5 How Do the Results Support or Refute the Hypotheses?

The present result supports the first and second hypothesis tested, respectively, that it is possible to estimate the load on the PVM using standard biomechanical approaches and that it is possible to identify the anatomical margins of the pubovisceral muscle and measure its cross-sectional area in a plane normal to its morphologically parallel muscle fibers. Considering the third tested hypothesis, a relation between the force measurements of the instrumented speculum and the applied loads and forces was not found. This simply means that the volitional instrumented speculum measurements may be measuring a fraction of the maximum PVM force and more research is needed to understand why. We presume this lack of correlation is due to lack of PVM motor control ability much as one may have difficulty maximally contracting (and arching) just one eyebrow muscle if one has never trained to do so.

8.6 How Strong does the Pubovisceral Muscle Need to be?

The biomechanical analyses predicted that the left and right PVM must carry 29, 46 and 60 N of force for the 5^{th}, 50^{th} and 95^{th} percentile woman under static conditions, and 48, 78 and 98 N of force under dynamic conditions. Likewise, the 5^{th}, 50^{th} and 95^{th} percentile unilateral PVM has an anatomic cross-sectional area of 0.80, 1.22, 1.79 cm^2, and an estimated produced force of 40, 67 and 94 N, respectively. These are the range of values in healthy younger women without PVM tears.

8.7 Suggestions for Future Work

The many assumptions underlying the Levator Plate Model should be revisited to see where obvious improvements can be made to refine the model. This dissertation represents a first attempt to define this model so it provides estimates of maximal PVM static and dynamic force, but upon reflection one can see there are a number of assumptions which could be refined. The method to calculate the PVM CSA could be improved to be more practical by being able to make the CSA measurements in only one software package with as little human intervention possible. However, to do that even better quality MR images will be needed along with a more detailed understanding of how the PVM and related structures insert onto the perineal body and lateral aspects of the anal sphincter.

Chapter 9

Conclusions

1. MRI measurements lead us to conclude that in this sample of 24 young women who have not given birth vaginally the PVM CSA ranges from 0.79 to 1.8 cm^2, with a mean 1.22 and SD of 0.25 cm^2.

2. Biomechanical analysis suggests the maximum unilateral force the PVM must carry is 29, 46 and 60 N of force in the 5^{th}, 50^{th} and 95^{th} percentile woman under static conditions, and 48, 78 and 98 N of force under dynamic conditions.

3. Muscle physiological arguments lead one to derive the maximum unilateral PVM force derived from multiplying the MRI CSA measurements by the maximum specific tension of striated muscle and the resulting forces proved to be consistent with the biomechanical predictions of PVM forces using the Levator Plate Model. The MRI measurements therefore validate the biomechanical predictions.

4. Measurements from an instrument speculum in women asked to contact their pelvic floor muscles 8months post-partum resulted in forces that are only 20% of those that potentially can be developed according to the biomechanical and physiological calculations.

Appendix A

Appendix I - PVM area onto Baragi's Area Calculation

Unilateral PVM area was calculated using dimensions from (5) and trigonometric postulates. Area is calculated using the sequence from equation A.1 to equation A.9. Equation A.10 is the ratio of the PVM area considering the Baragi Area.

$$psd_{ant} = \sqrt{pis^2 - \left(\frac{bis - psw}{2}\right)^2}$$

(A.1)

$$psd_{post} = \sqrt{iss^2 - \left(\frac{bis - sw}{2}\right)^2}$$

(A.2)

$$psd = psd_{ant} + psd_{post}$$

(A.3)

$$base_{2cm} = \frac{2 * psd_{ant}}{pis} \quad (A.4)$$

$$h = \frac{\frac{bis}{2}}{psd_{ant}} * \frac{4}{5} * psd_{ant} \quad (A.5)$$

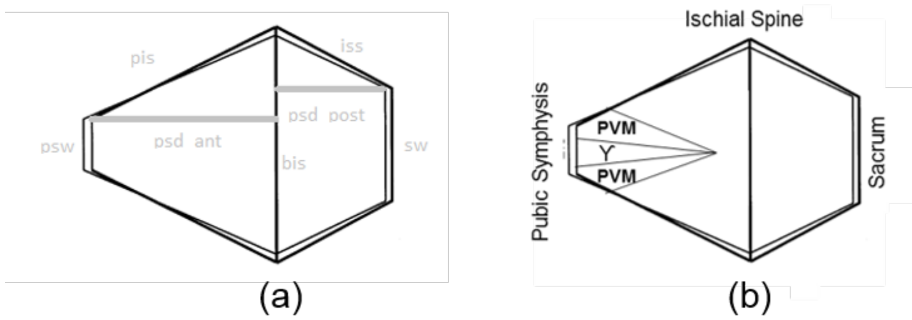

Figure A.1: (a) Baragi Area with indication of the different auxiliary components. Psw-pubic symphysis width ; Pis-pubis-ischial space; Psd -pubo-sacral distance; Psd ant- pubo-sacral distance anterior part; Psd post- pubo-sacral distance posterior part; Iss- ischial-sacrum space; Sw-sacral width; Bis-bi-ischial space. (b) Location of the PVM onto Baragi's Area. Drawings adapted from (5).

$$A_{hiatus} = \frac{0.5 * psd * 0.25 * psw}{2} \tag{A.6}$$

$$A_{triangle} = \frac{\frac{4}{5} * h - base_{2cm}}{2} \tag{A.7}$$

$$A_{total} = \frac{0.5 * psd + h}{2} * psd \tag{A.8}$$

$$A_{PVM} = A_{total} - A_{triangle} - A_{hiatus} \tag{A.9}$$

$$ratio = \frac{A_{PVM}}{0.5 * A_{Baragi}} \tag{A.10}$$

Appendix B

Appendix II: Pubovisceral Muscle Cross-Sectional Area Protocol

Detailed PVM CSA protocol, using 3D Slicer and ImageJ.

Plan:

1. Open DICOMs
2. Get PVM fiber direction
3. Tip Plane
4. Label in image J

1

Detailed Plan

1. Import DICOMs
2. Load DICOMs to slicer
3. Save mrml file in same folder as DICOMs
4. Open yellow view – sagittal – bit of mid-line check perineal membrane. Place fiducial on the Pubic Bone and other on the perineal membrane
5. Perineal membrane angle can also be made from the coronal, with marking it in difference slices. View in 3D view and check visually its slope and take the points to excel and get a angle (from the coordinates, make graph and get slope)
6. Insert coordinates to excel sheet - to get angle
7. Open plugin angle planes – rotate to angle
8. Open green slice –
   1. Mark with a vertical rule X distance from the perineal membrane
   2. Make the ruler project to all the other slices
   3. screen-shot it
9. Open ImageJ – drag images, add images to stack, set scale
10. Label PVM, press b to add label to the selection, when finished add selection to ROI and click measure
11. Copy results to excel sheet where you inserted the fiducials coordinates

2

1. Open DICOMs
2. Get PVM fiber direction
3. Tip Plane
4. Label in image J

3

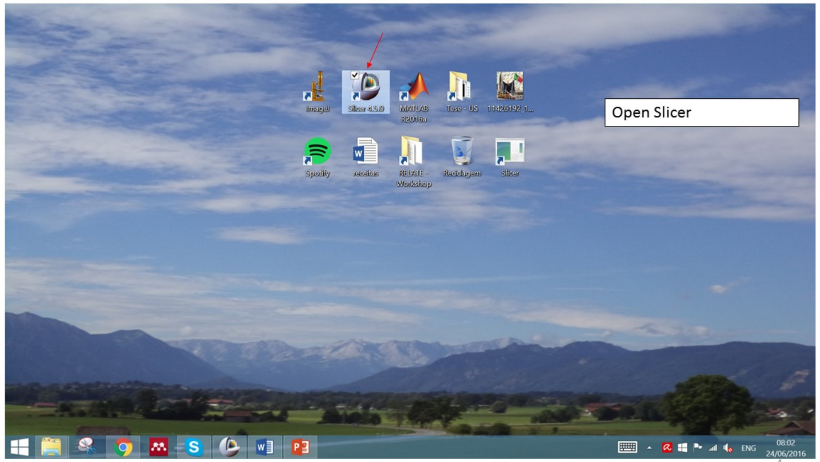

4

Open DICOMs || Open mrml file (when existing)

5

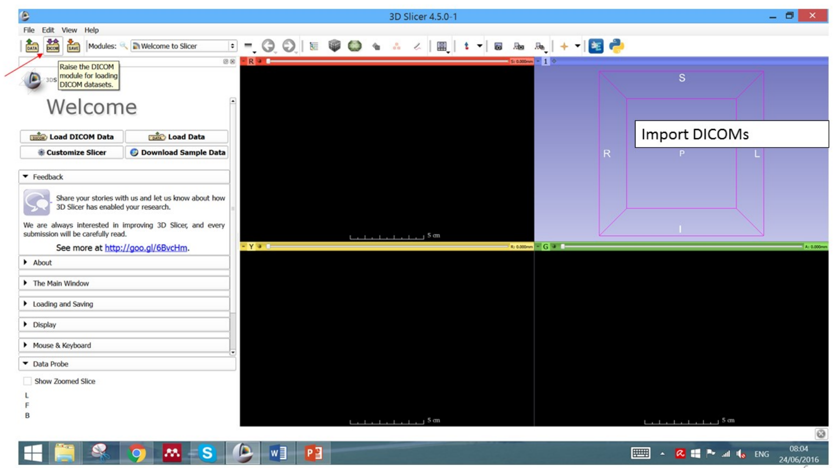

6

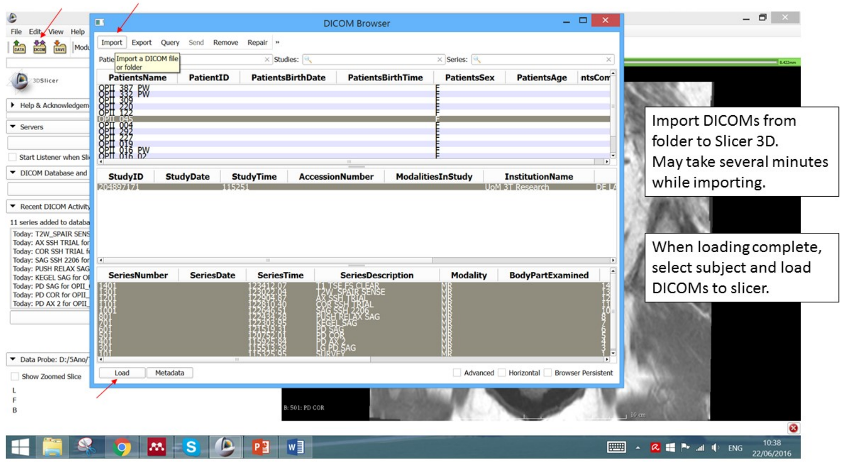

7

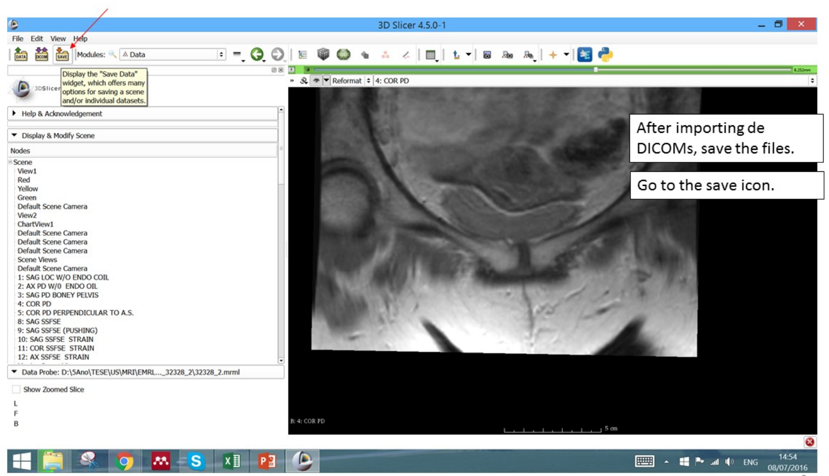

8

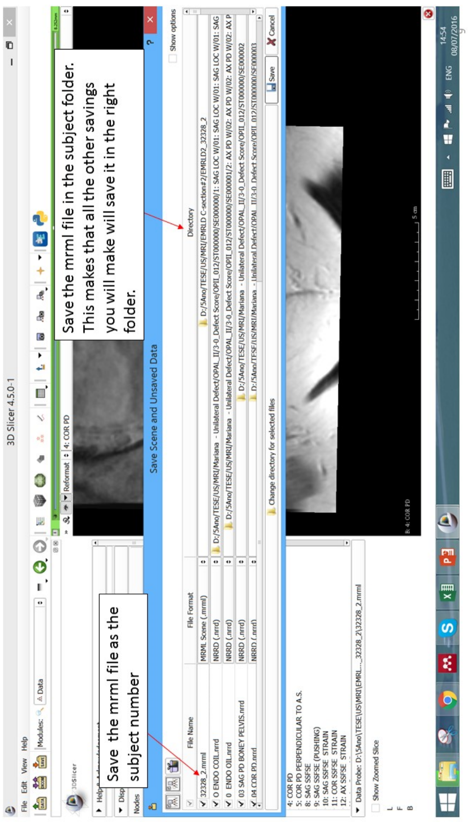
Save the mrml file as the subject number
Save the mrml file in the subject folder. This makes that all the other savings you will make will save it in the right folder.

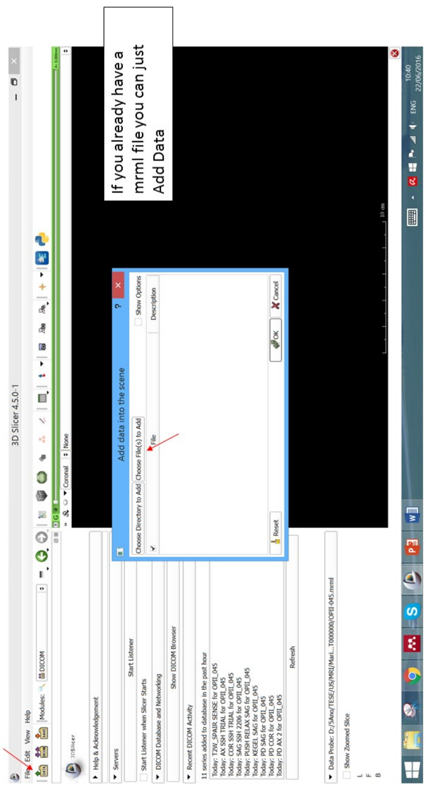
If you already have a mrml file you can just Add Data

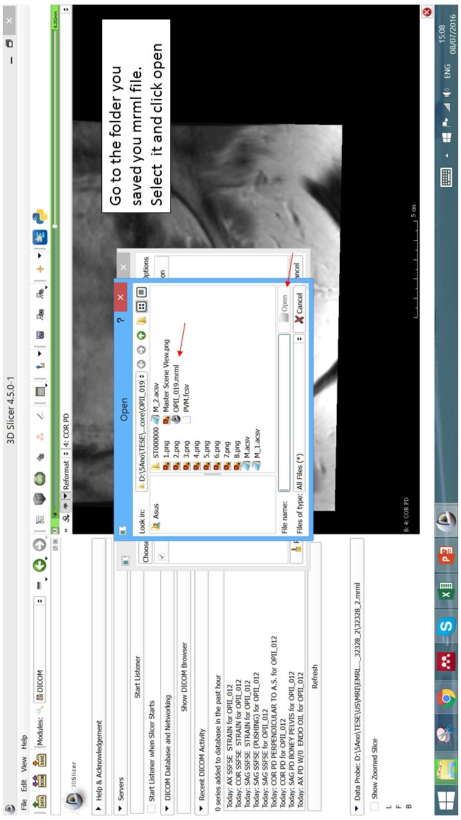
Go to the folder you saved you mrml file. Select it and click open

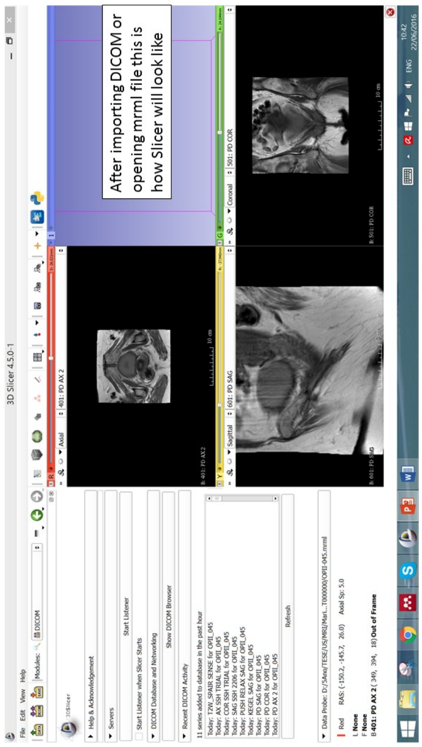
After importing DICOM or opening mrml file this is how Slicer will look like

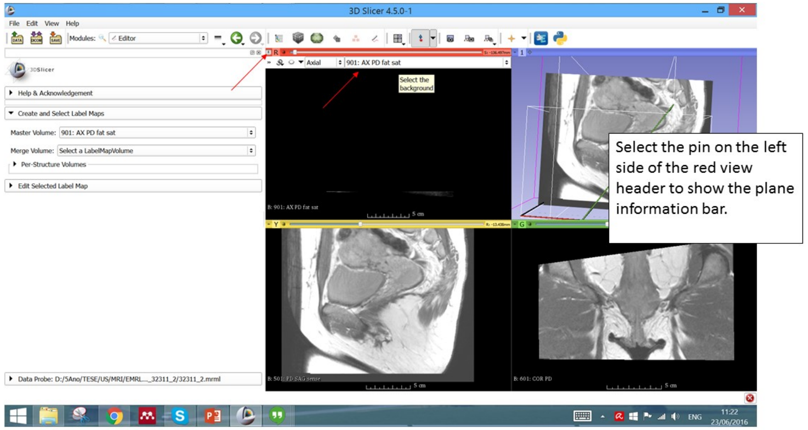

13

Confirm the alignment between the different planes. Use a bone, as soft-tissue can change configuration during acquisitions

15

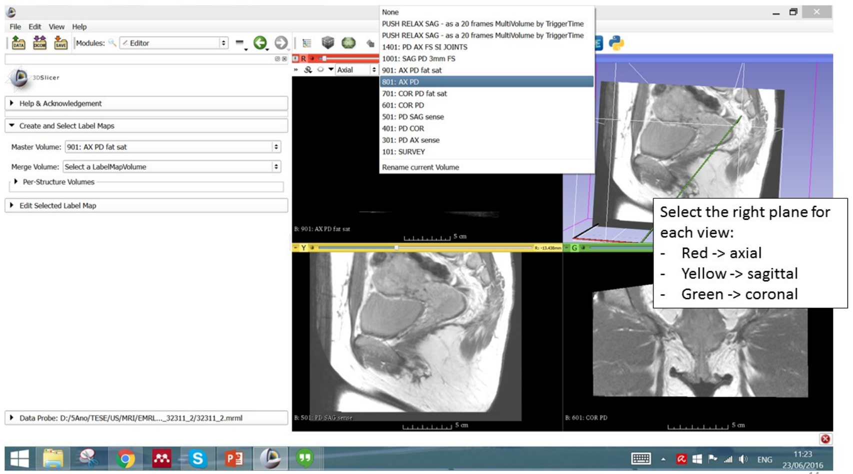

14

1. Open DICOMs
2. **Get PVM fiber direction**
3. Tip Plane
4. Label in image J

16

Check of PVM fiber direction

Plane will be rotated to a perpendicular of the PVM fiber direction, in order to get the smallest Cross-Sectional Area of the PVM

17

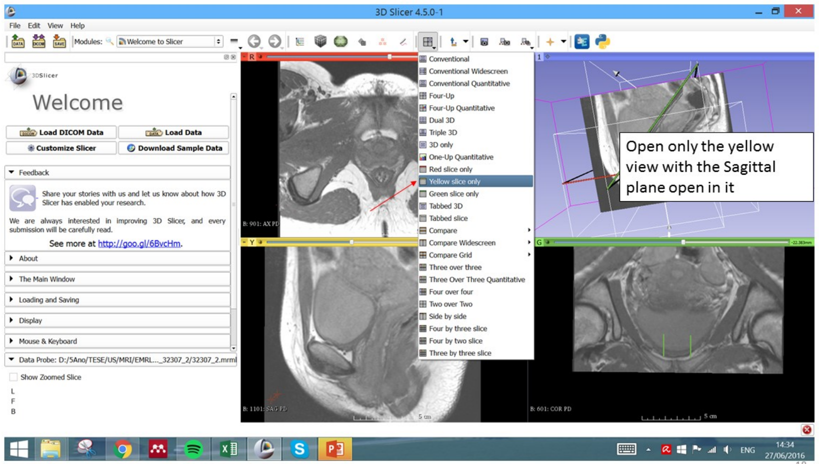

18

19

Place fiducials:

- to sense PVM fiber directions
- fiducial 1: on the pubic bone
- fiducial 2: follows the fiber direction, in relation with fiducial 1

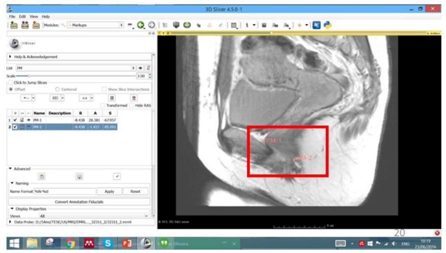

20

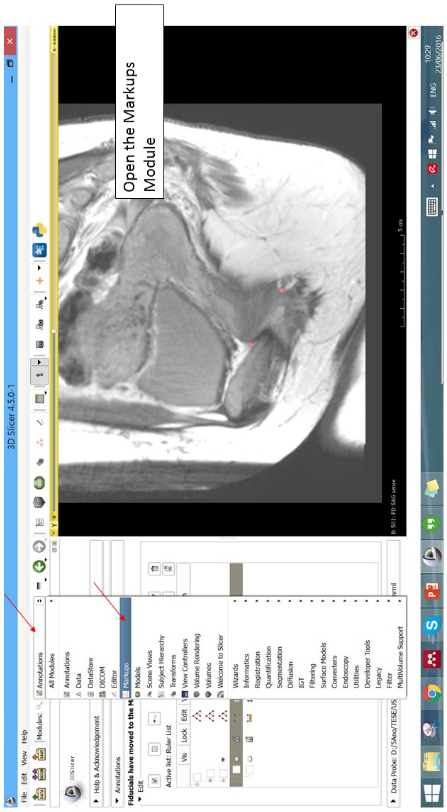
Open the Markups Module
21

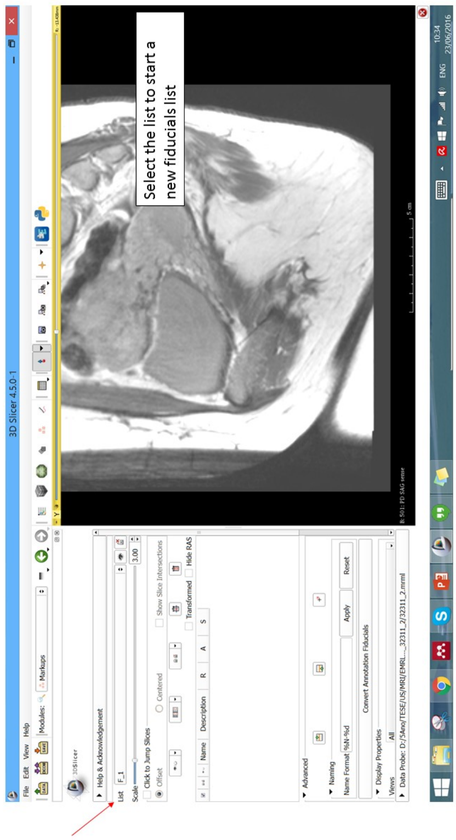
Select the list to start a new fiducials list
22

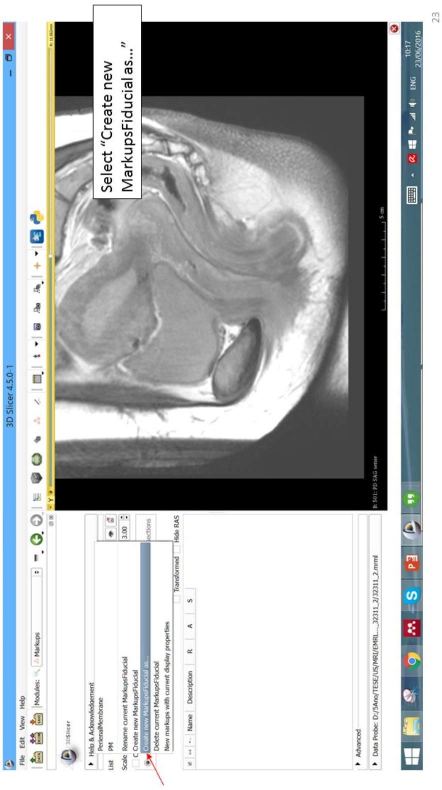
Select “Create new MarkupsFiducial as…”
23

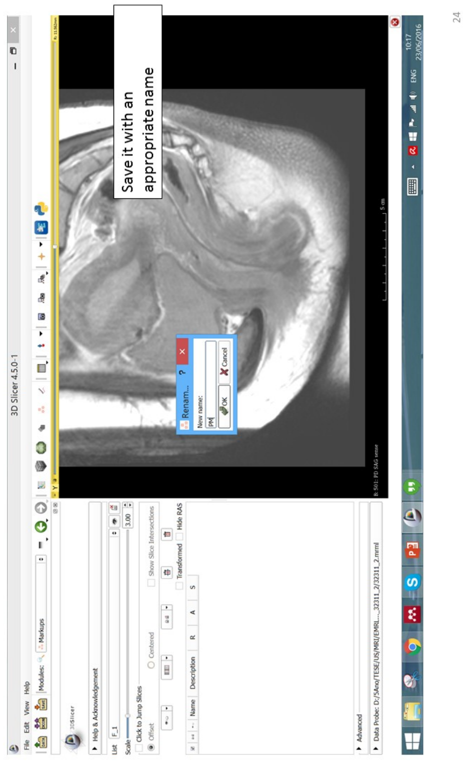
Save it with an appropriate name
24

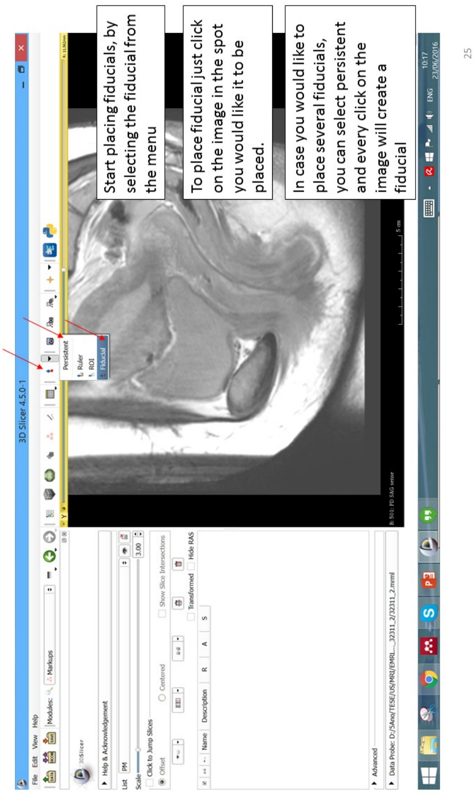
Start placing fiducials, by selecting the fiducial from the menu
To place fiducial just click on the image in the spot you would like it to be placed.
In case you would like to place several fiducials, you can select persistent and every click on the image will create a fiducial

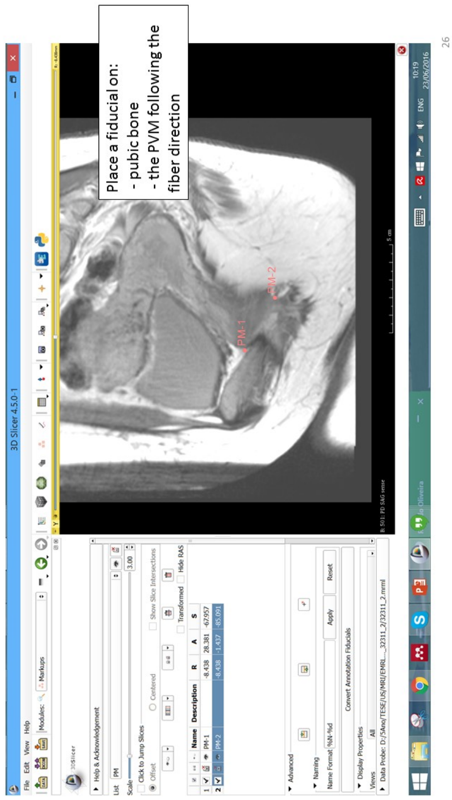
Place a fiducial on:
- pubic bone
- the PVM following the fiber direction

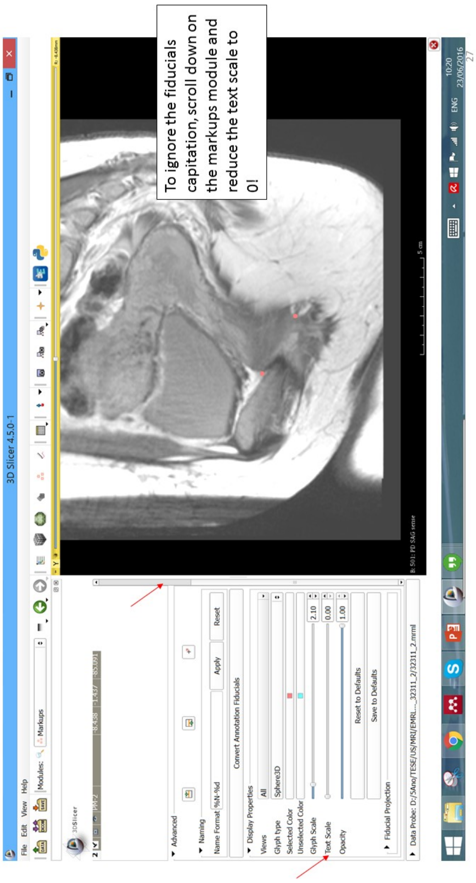
To ignore the fiducials capitation, scroll down on the markups module and reduce the text scale to 0!

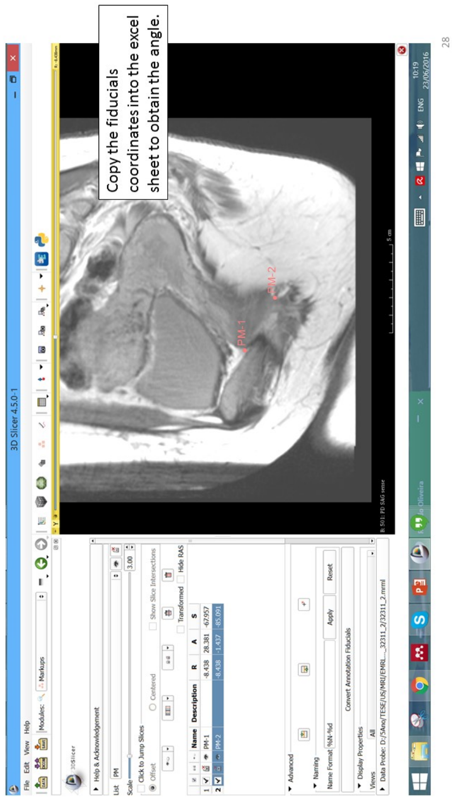
Copy the fiducials coordinates into the excel sheet to obtain the angle.

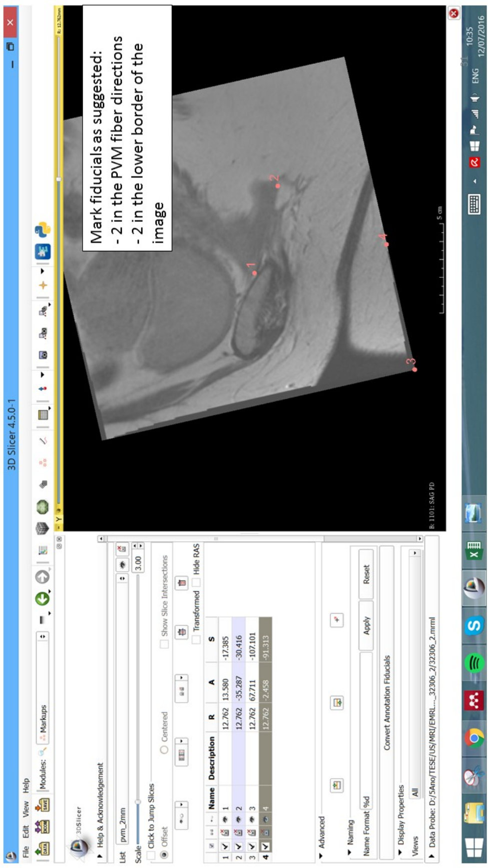

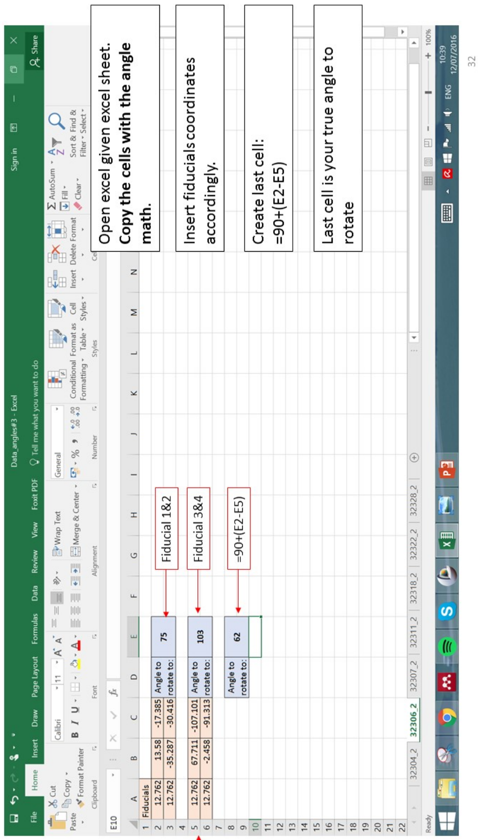

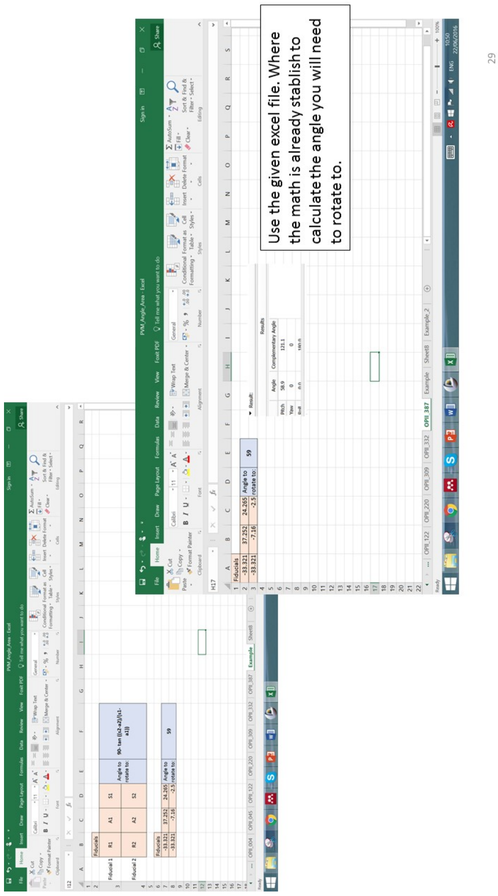

In case the Sagittal Plane is not parallel to the horizontal "line"

1. Open DICOMs
2. Get PVM fiber direction
3. Tip Plane
4. Label in image J

33

Angle Planes Extension

for 1st time users. After you installed once, it will be working for the next time you use slicer

34

Install Angle Planes extension
- only works with Slicer 4.5.0

35

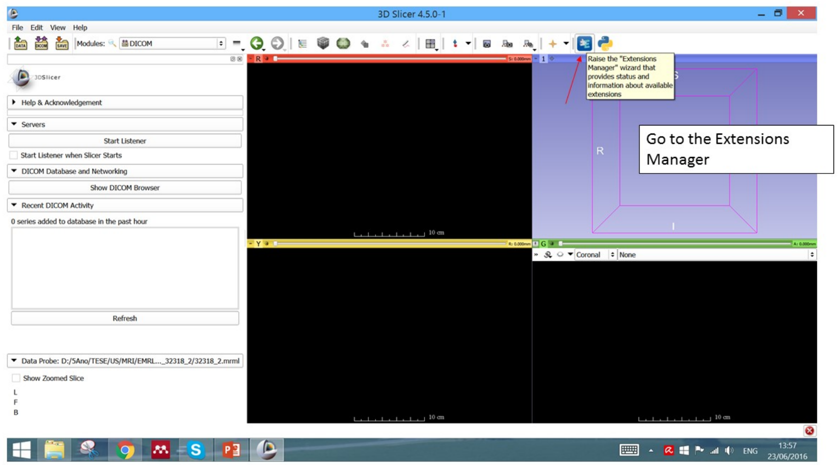

36

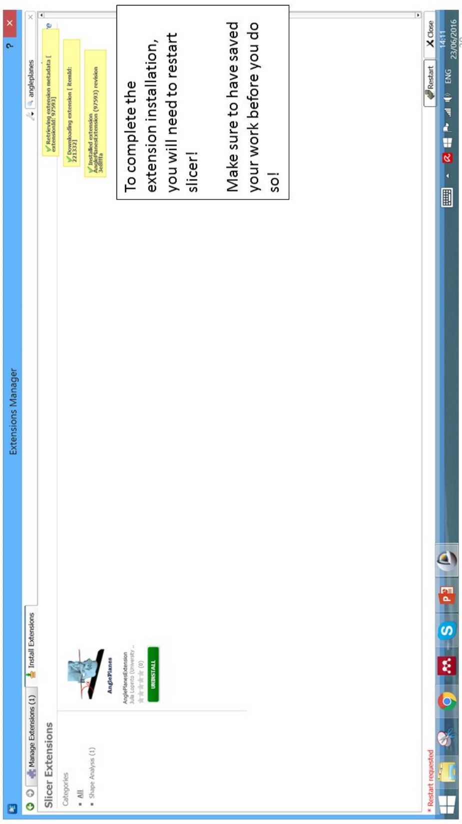
Extensions Manager
Slicer Extensions
To complete the extension installation, you will need to restart slicer!
Make sure to have saved your work before you do so!

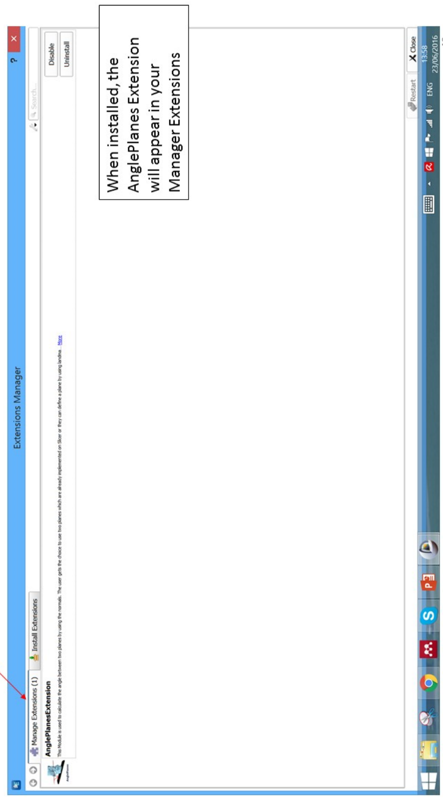
Extensions Manager
When installed, the AnglePlanes Extension will appear in your Manager Extensions

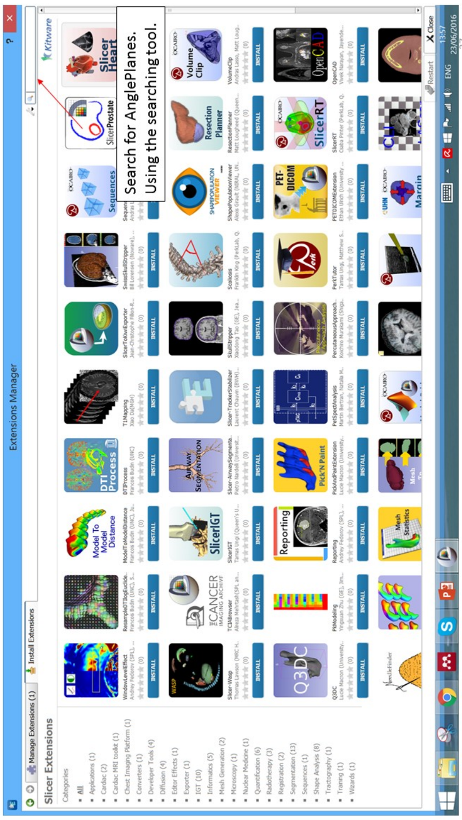
Extensions Manager
Slicer Extensions
Search for AnglePlanes.
Using the searching tool.

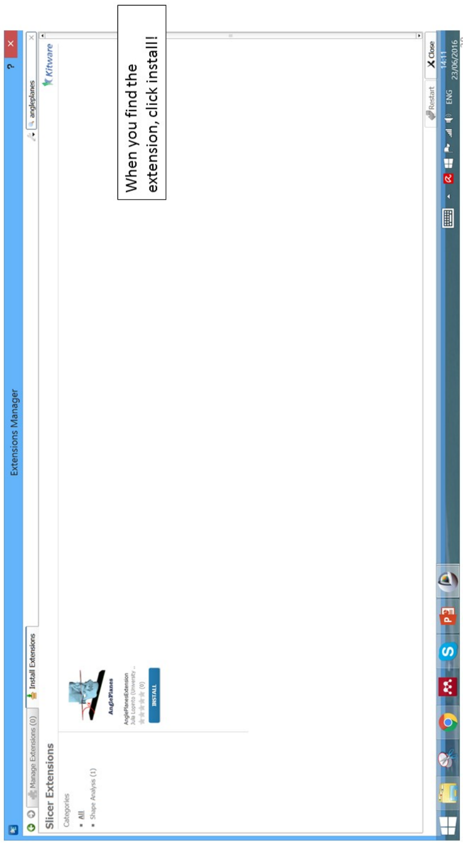
Extensions Manager
Slicer Extensions
When you find the extension, click install!

Using AnglePlanes extension to created a “tipped plane”

41

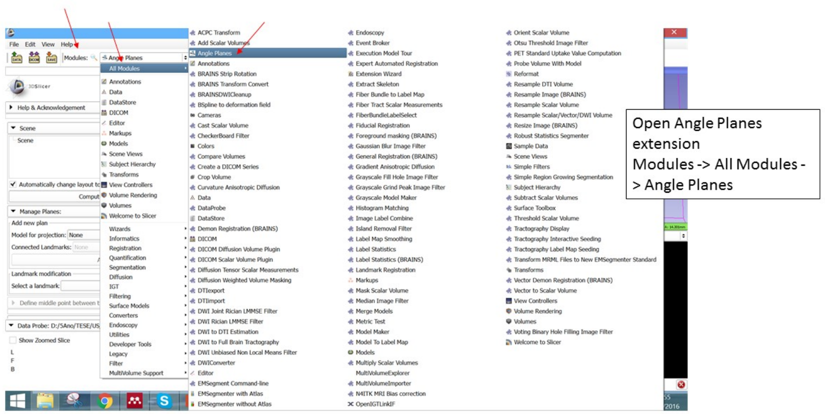

42

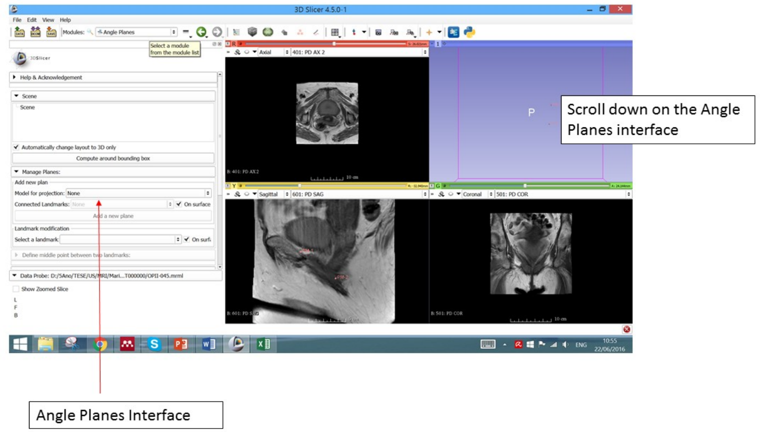

43

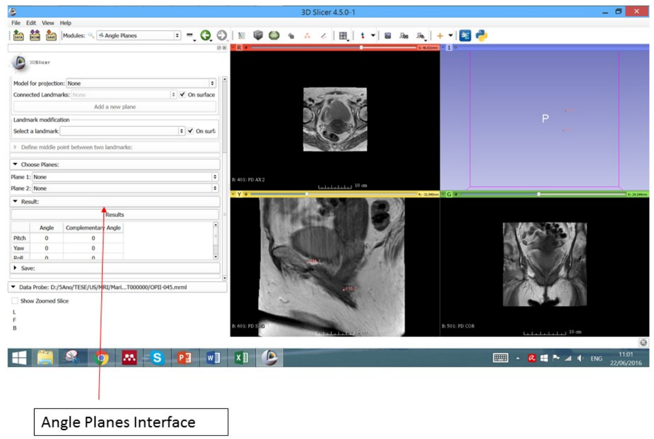

44

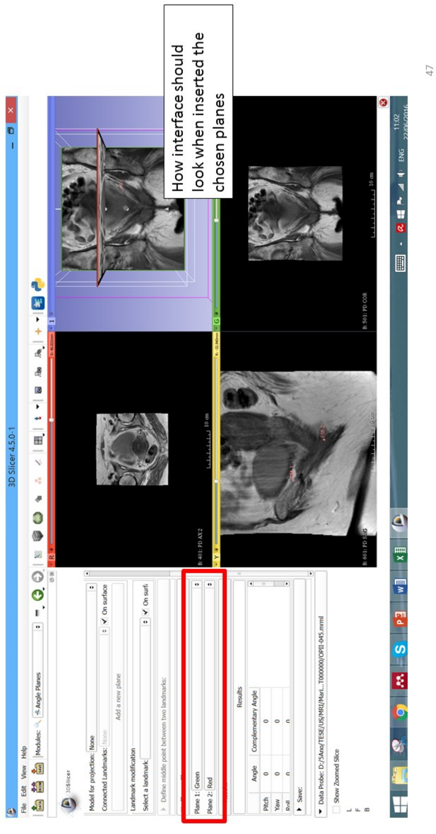
How interface should look when inserted the chosen planes
47

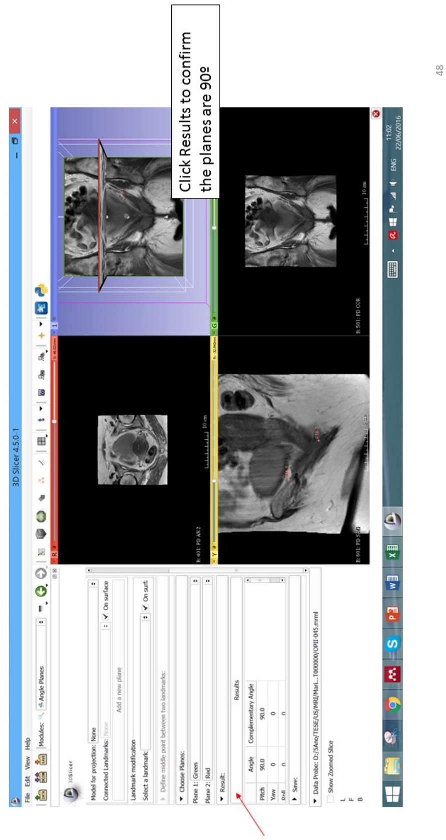
Click Results to confirm the planes are 90º
48

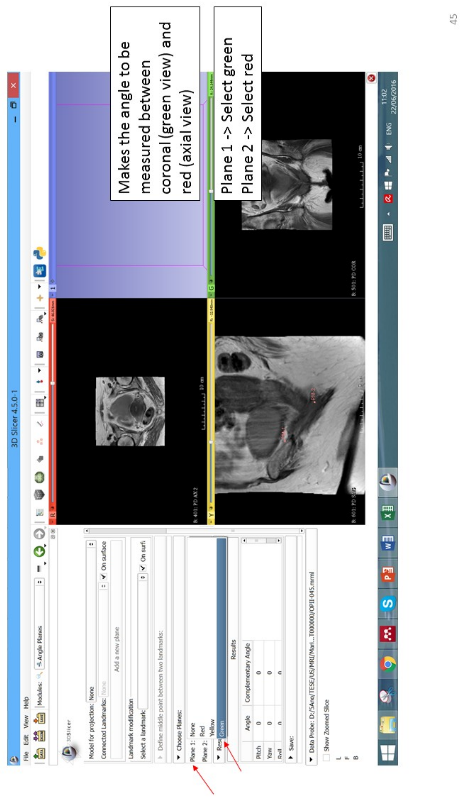
Makes the angle to be measured between coronal (green view) and red (axial view)
Plane 1 -> Select green
Plane 2 -> Select red
45

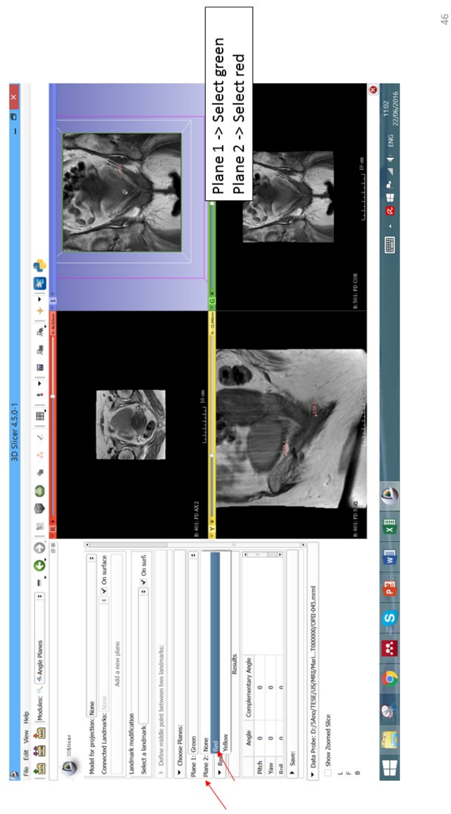
Plane 1 -> Select green
Plane 2 -> Select red
46

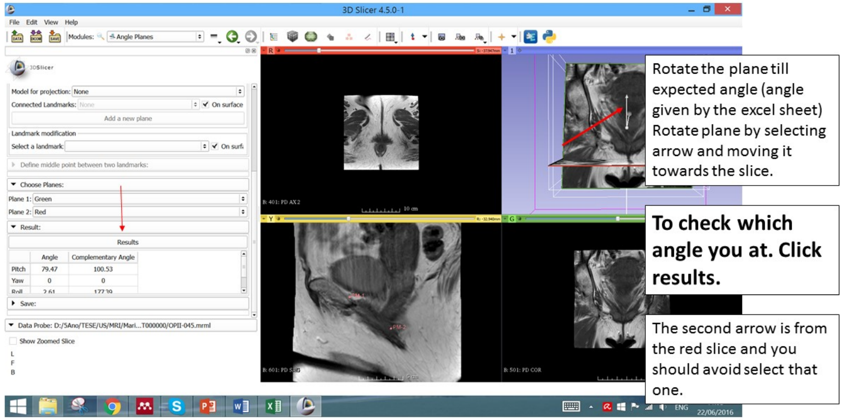

49

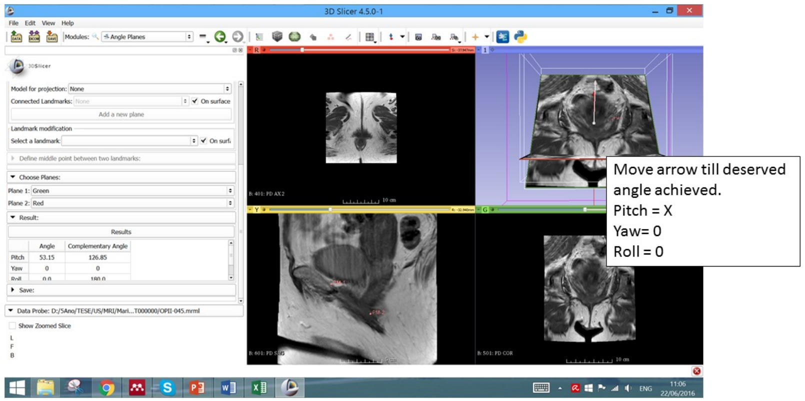

50

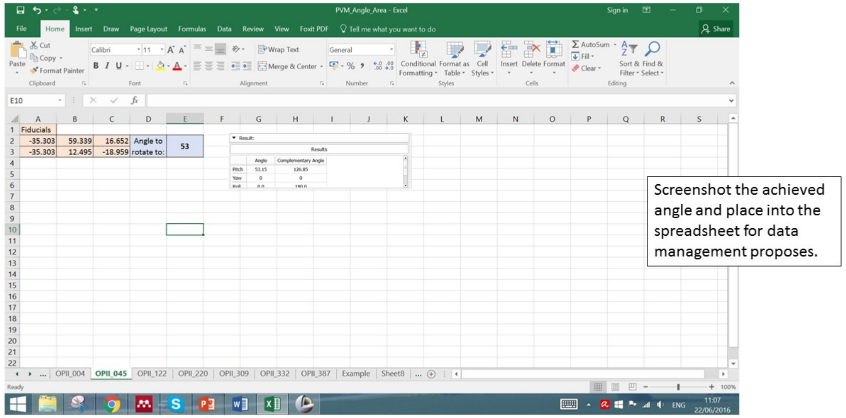

51

Define the **19mm vertical bar** that represents the width of the PVM

Bar should start:

- 1st slide when moving posterior-anterior you see the arcus pubic ligament. If not sure, checked it in the 3D view on the sagittal plane.
- bar placed in the mid point

52

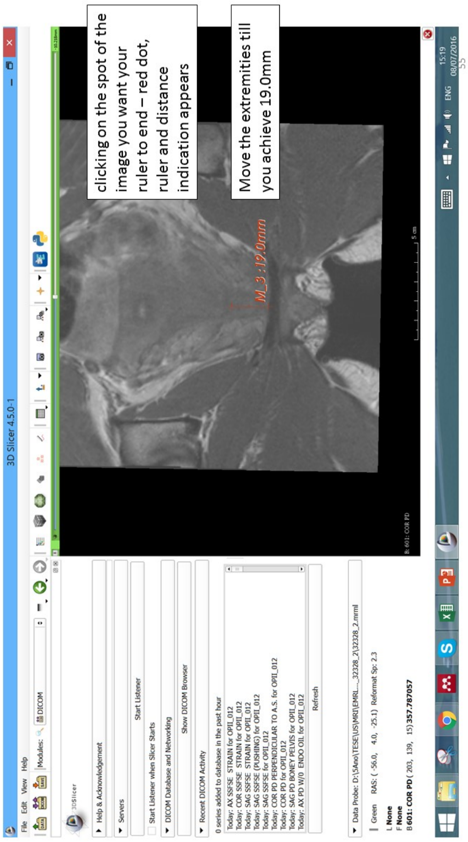
clicking on the spot of the image you want your ruler to end – red dot, ruler and distance indication appears
Move the extremities till you achieve 19.0mm

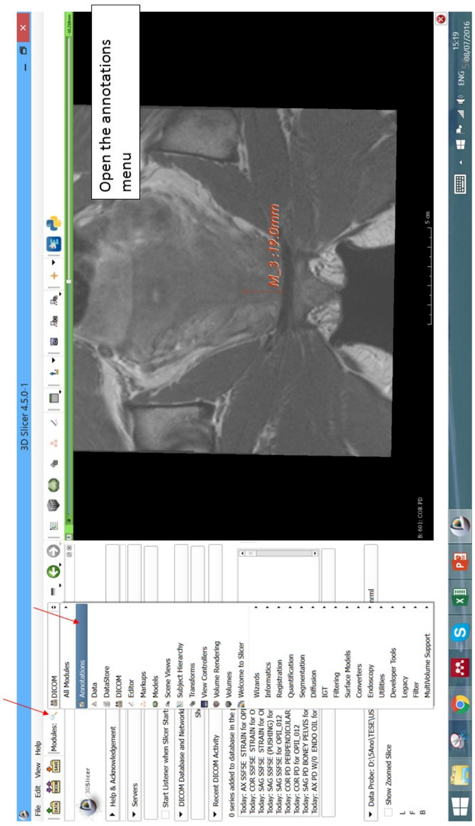
Open the annotations menu

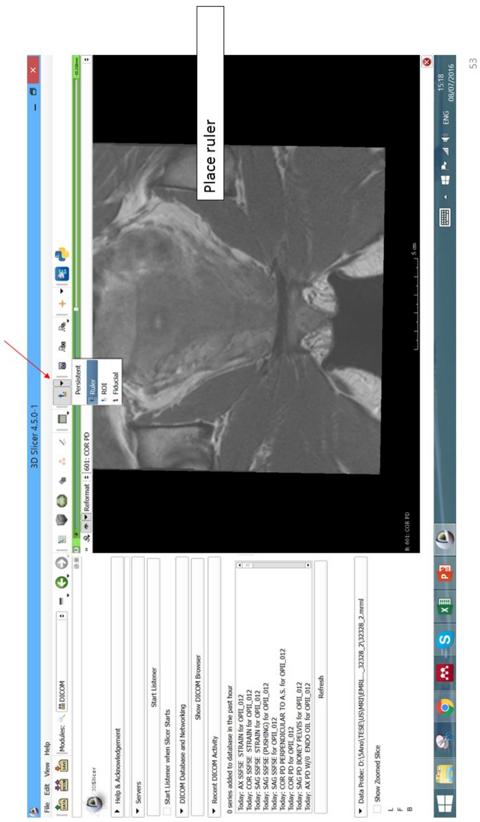
Place ruler


The ruler is traced by clicking on the spot of the image you want your ruler to start – red dot appears

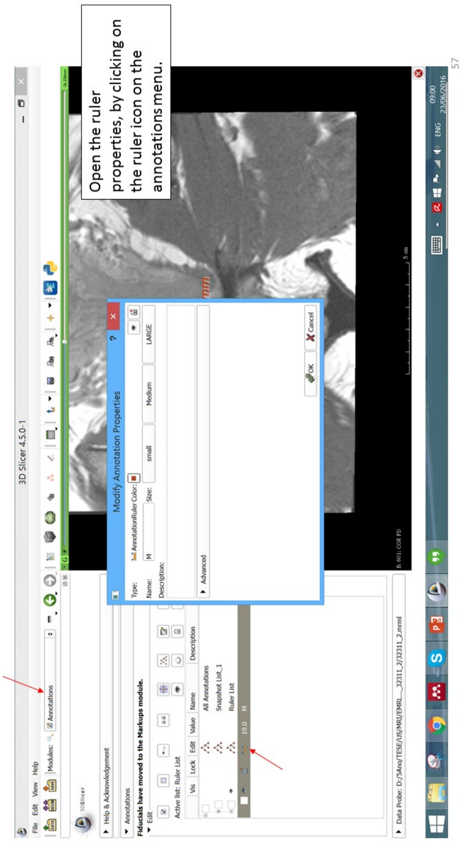
Open the ruler properties, by clicking on the ruler icon on the annotations menu.

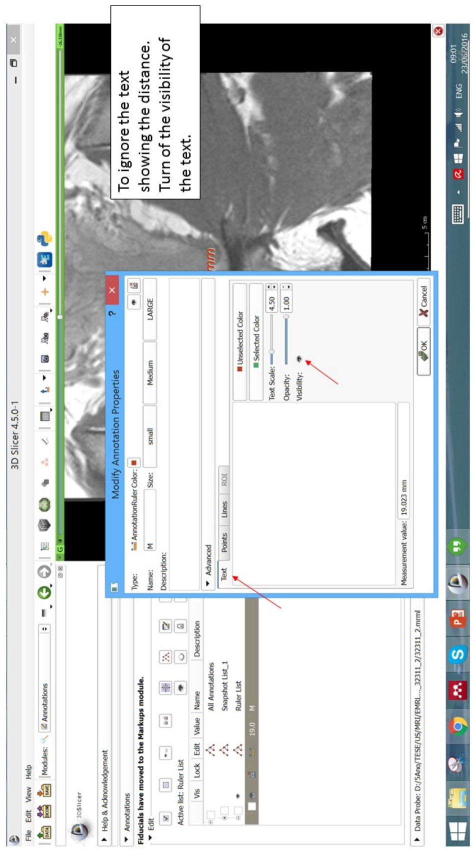
To ignore the text showing the distance. Turn of the visibility of the text.

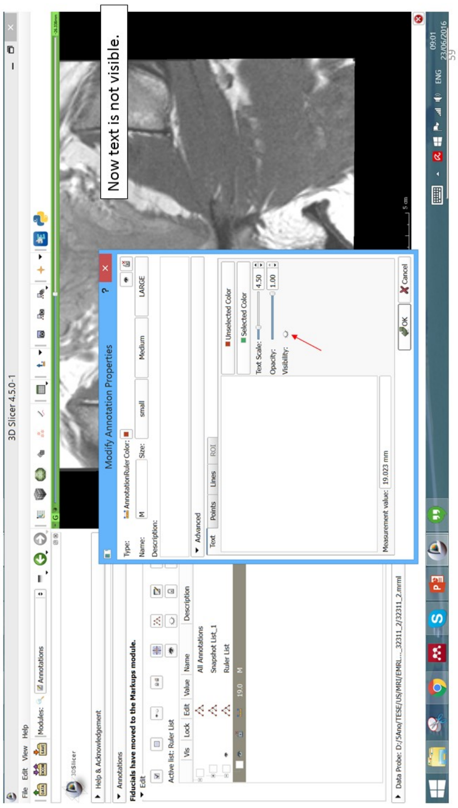
Now text is not visible.

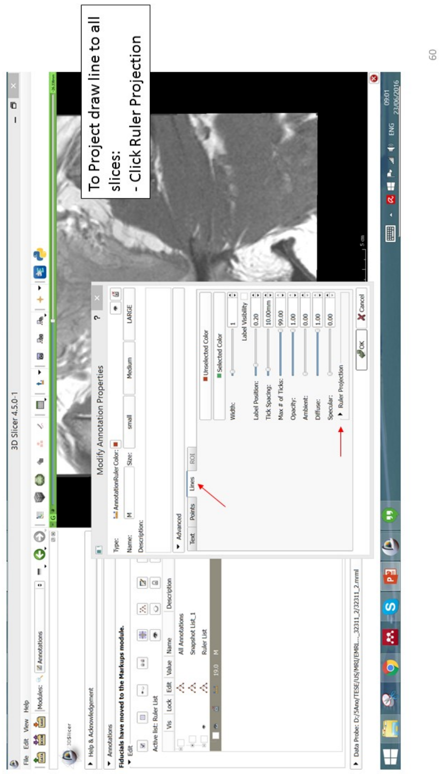
To Project draw line to all slices:
- Click Ruler Projection

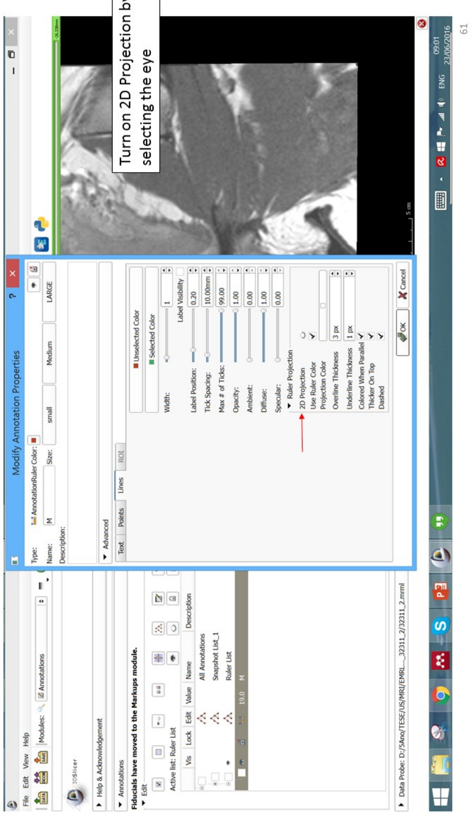
Turn on 2D Projection by selecting the eye

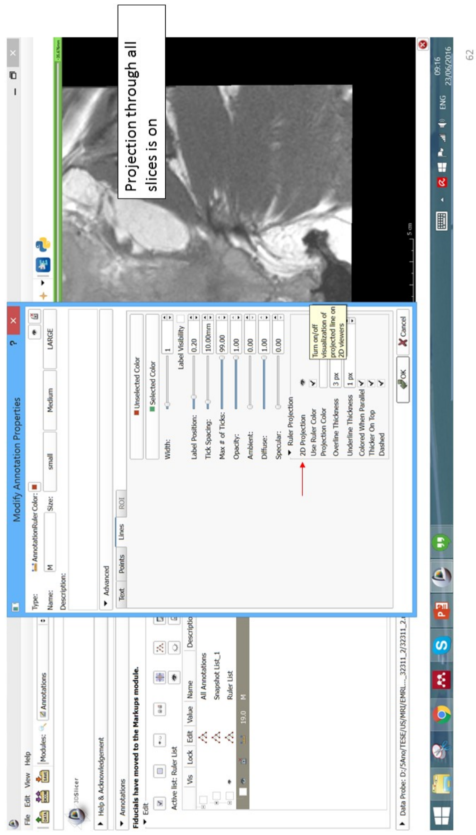
Projection through all slices is on

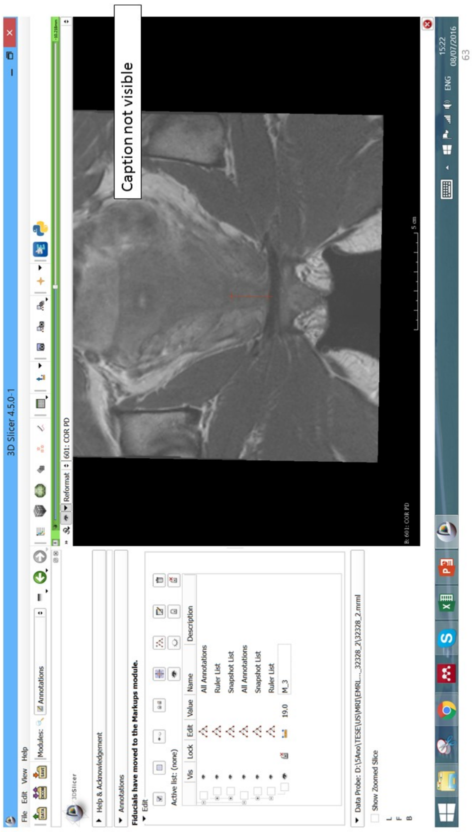
Caption not visible

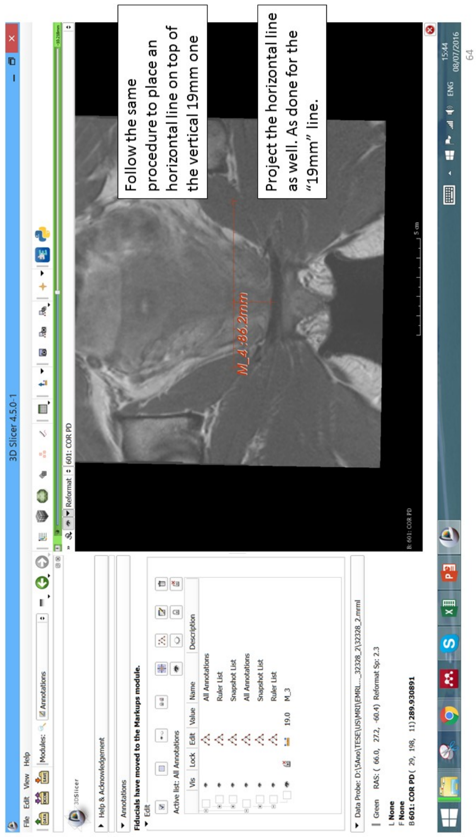
Follow the same procedure to place an horizontal line on top of the vertical 19mm one
Project the horizontal line as well. As done for the "19mm" line.

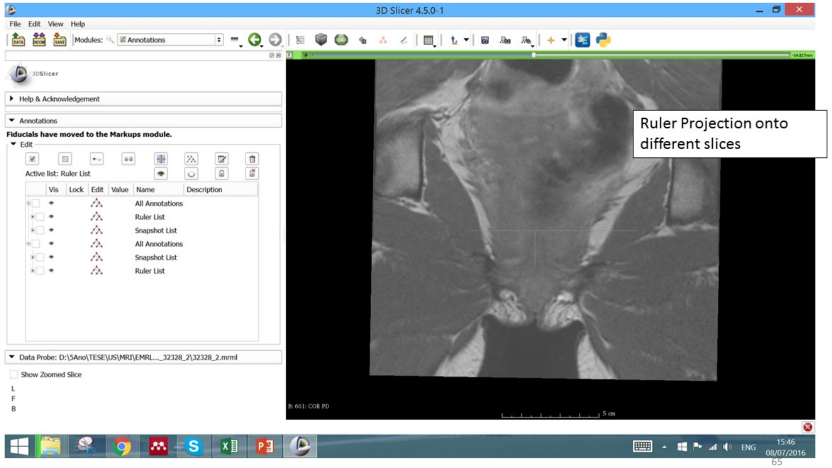

65

Save screenshots from Slicer so you can label the PVM in ImageJ.

As Slicer does not allow us to label in a tipped plane

67

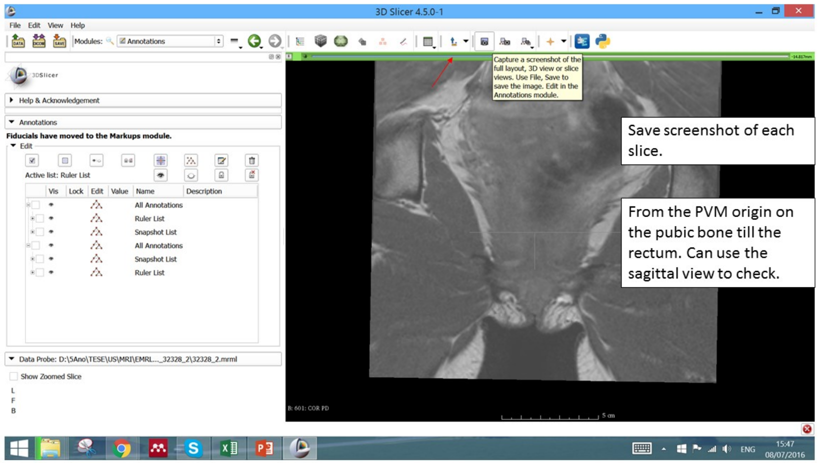

66

68

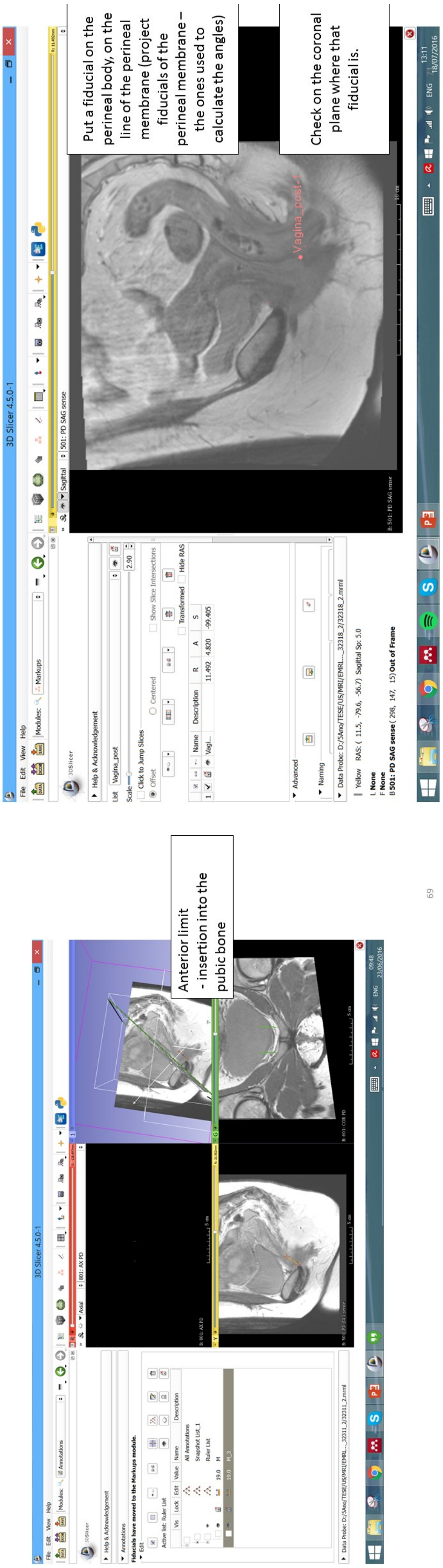
Put a fiducial on the perineal body, on the line of the perineal membrane (project fiducials of the perineal membrane – the ones used to calculate the angles)
Check on the coronal plane where that fiducial is.
Anterior limit - insertion into the pubic bone
69


From the fiducial plane. Go 11mm in front (closer to the pubic bone)
Posterior Limit
70

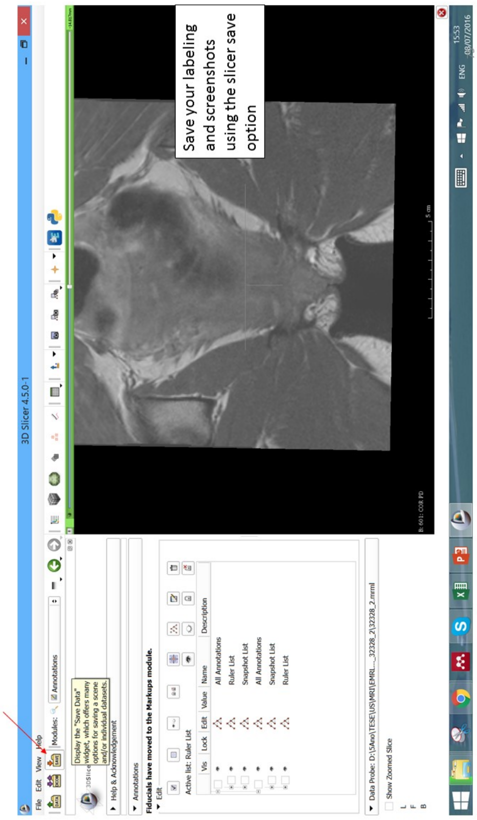
Save your labeling and screenshots using the slicer save option

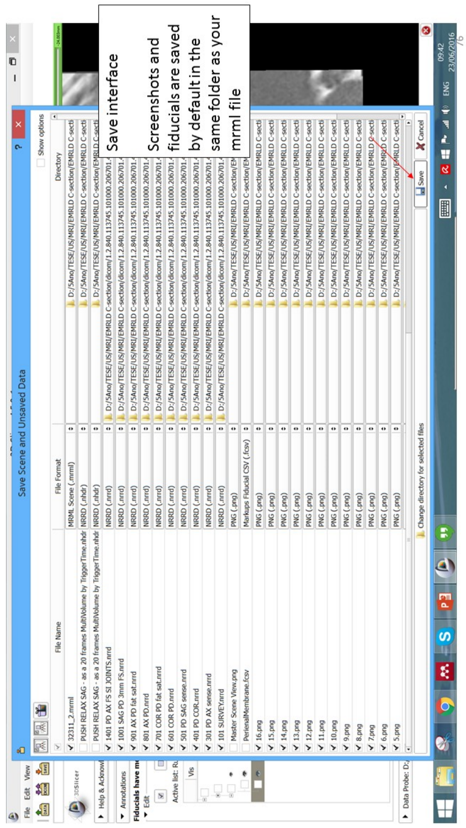
Save interface
Screenshots and fiducials are saved by default in the same folder as your mrml file

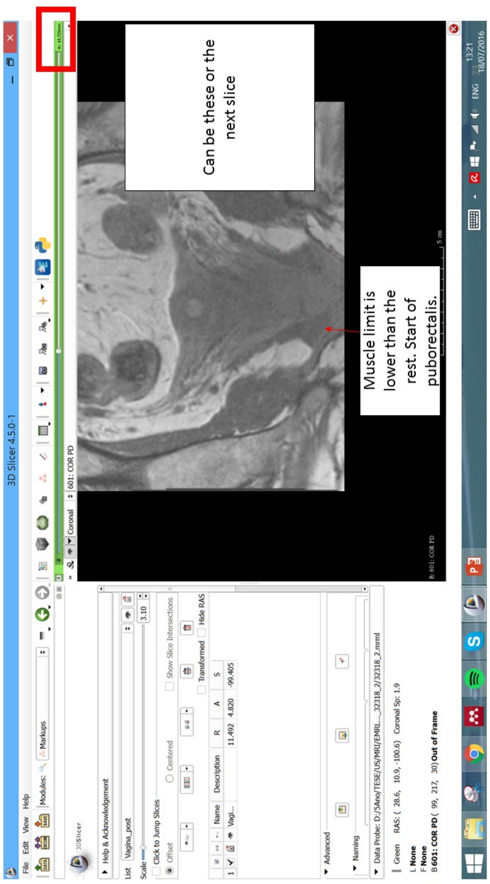
Can be these or the next slice
Muscle limit is lower than the rest. Start of puborectalis.

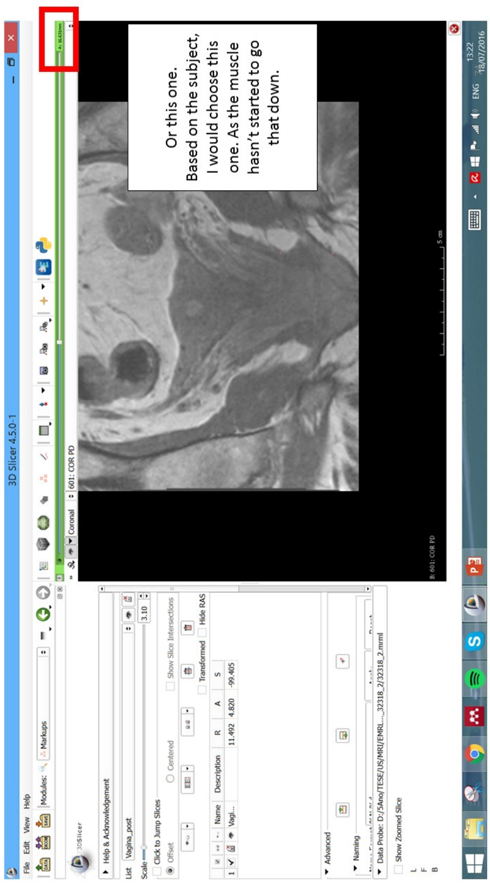
Or this one. Based on the subject, I would choose this one. As the muscle hasn't started to go that down.

1. Open DICOMs
2. Get PVM fiber direction
3. Tip Plane
4. **Label in image J**

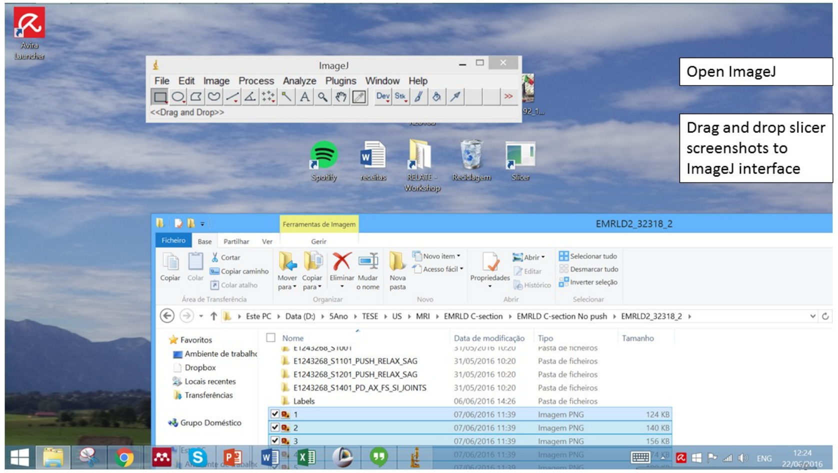

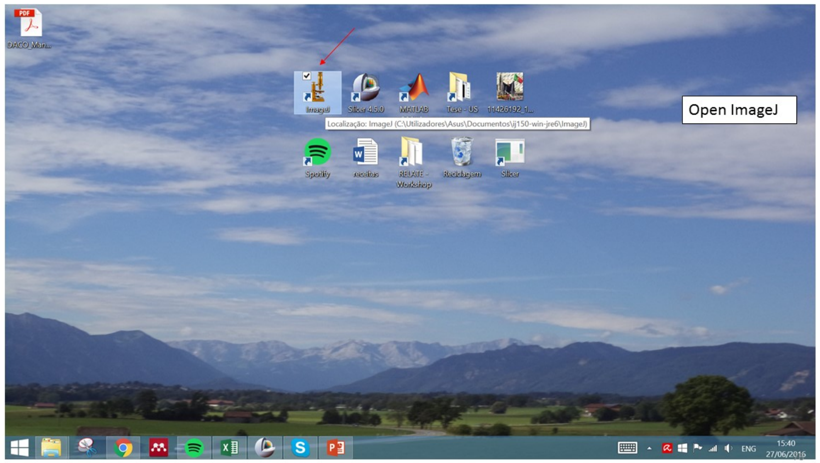

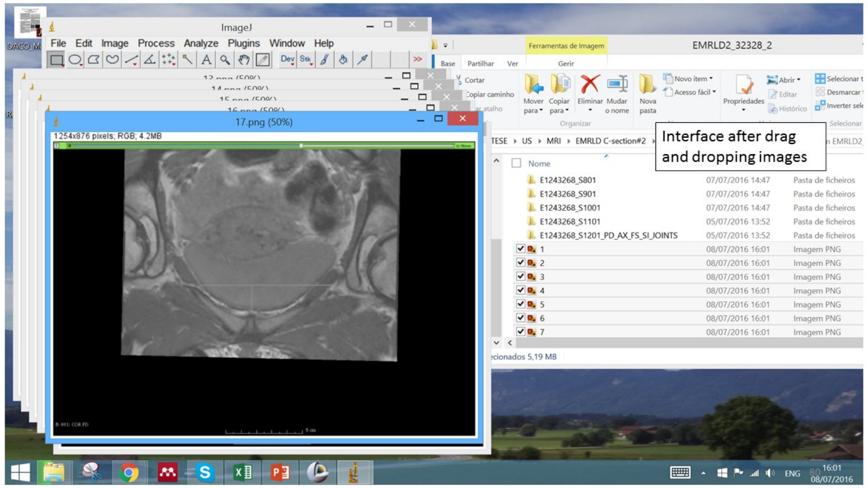

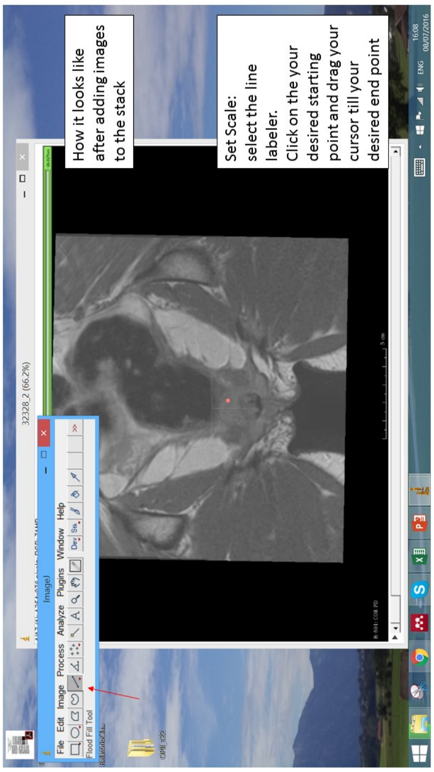
How it looks like after adding images to the stack
Set Scale: select the line labeler. Click on the your desired starting point and drag your cursor till your desired end point

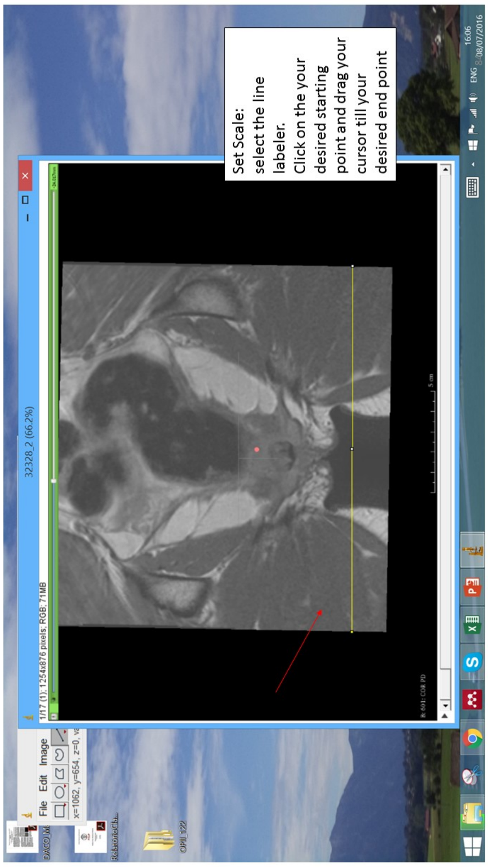
Set Scale: select the line labeler. Click on the your desired starting point and drag your cursor till your desired end point

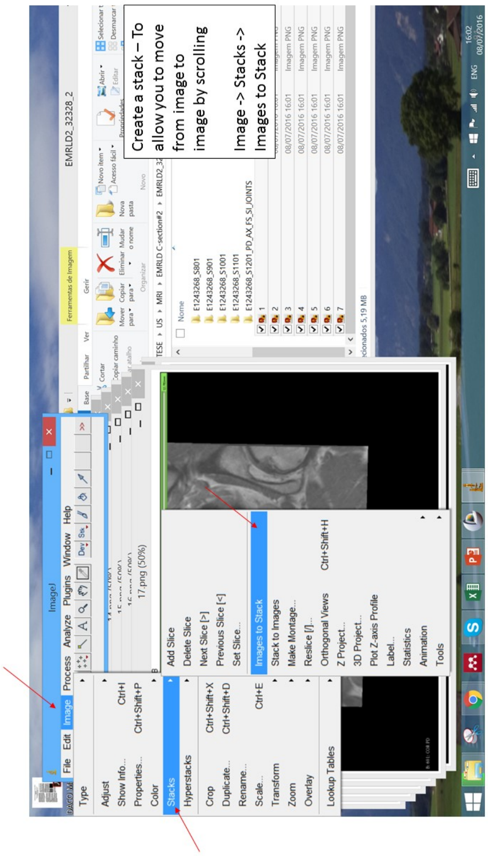
Create a stack – To allow you to move from image to image by scrolling
Image -> Stacks -> Images to Stack

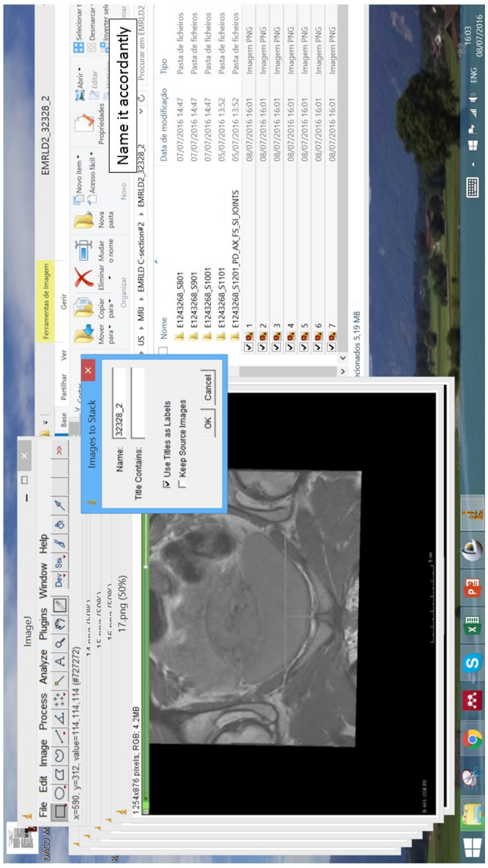
Name it accordantly

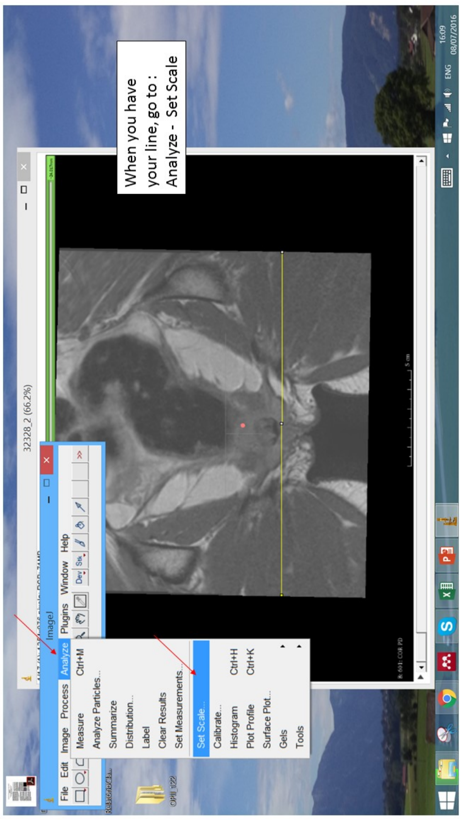
When you have your line, go to : Analyze - Set Scale

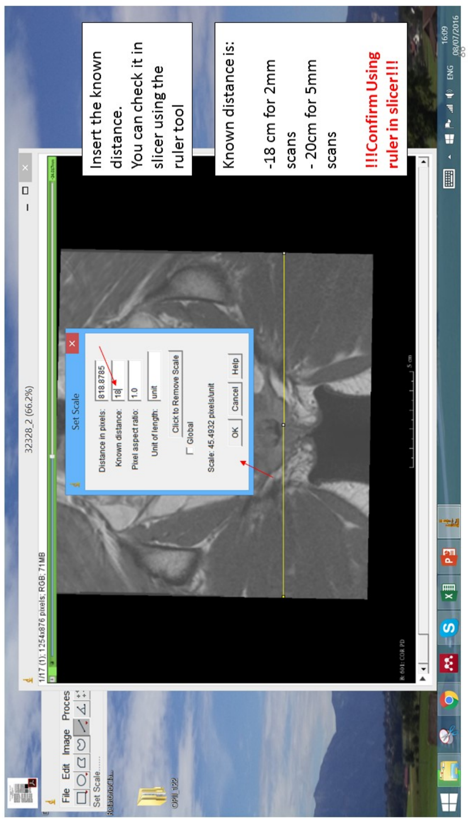
Insert the known distance.
You can check it in slicer using the ruler tool
Known distance is:
-18 cm for 2mm scans
- 20cm for 5mm scans
!!!Confirm Using ruler in slicer!!!

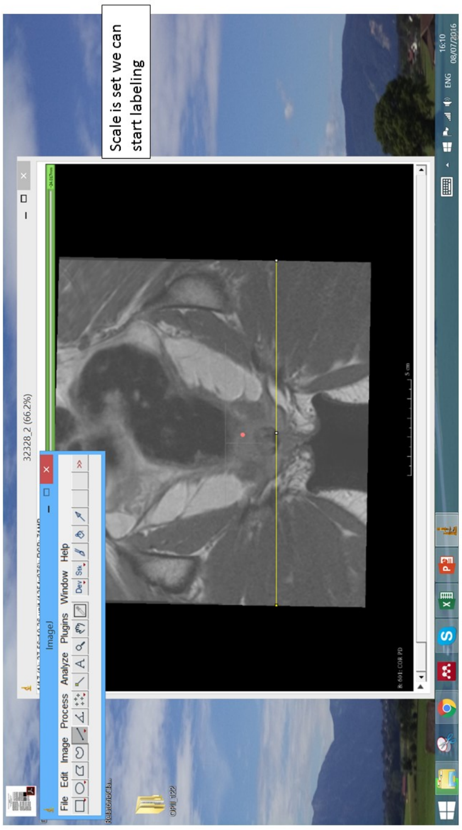
Scale is set we can start labeling

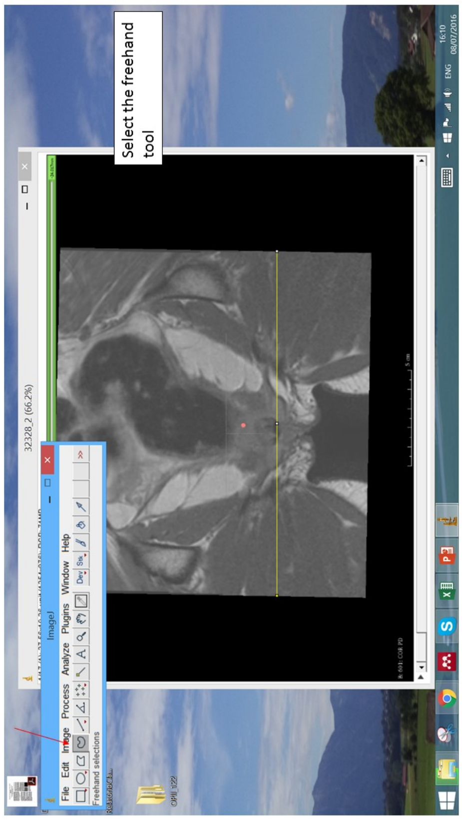
Select the freehand tool

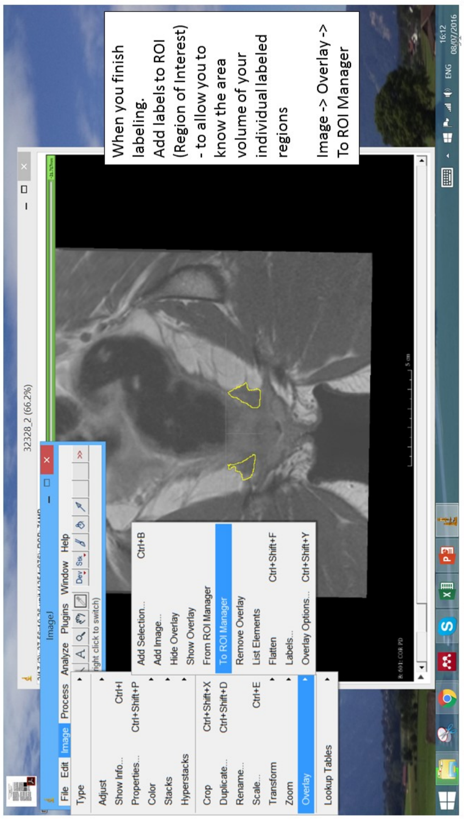
When you finish
labeling.
Add labels to ROI
(Region of Interest)
- to allow you to
know the area
volume of your
individual labeled
regions
Image -> Overlay ->
To ROI Manager

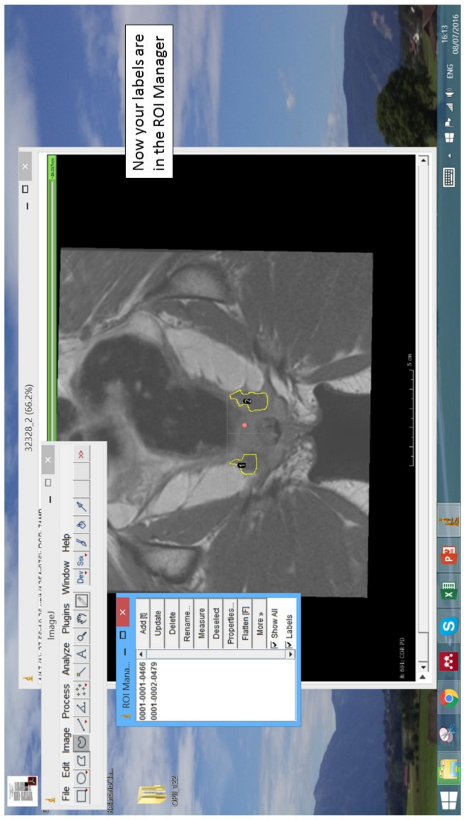
Now your labels are
in the ROI Manager

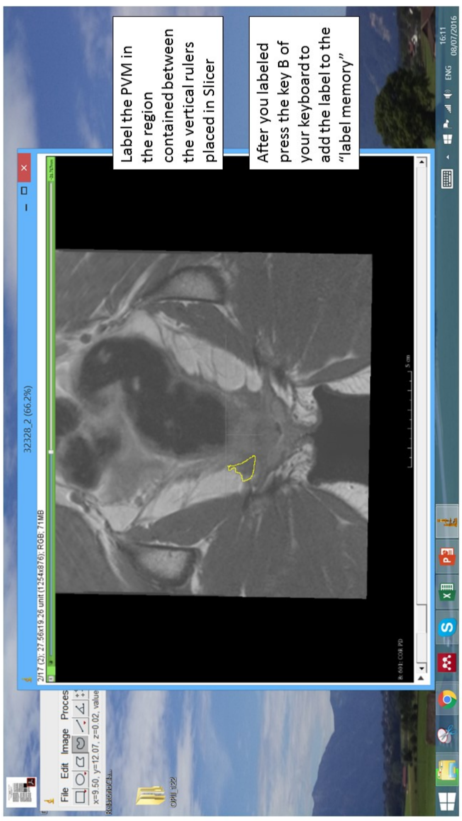
Label the PVM in
the region
contained between
the vertical rulers
placed in Slicer
After you labeled
press the key B of
your keyboard to
add the label to the
"label memory"

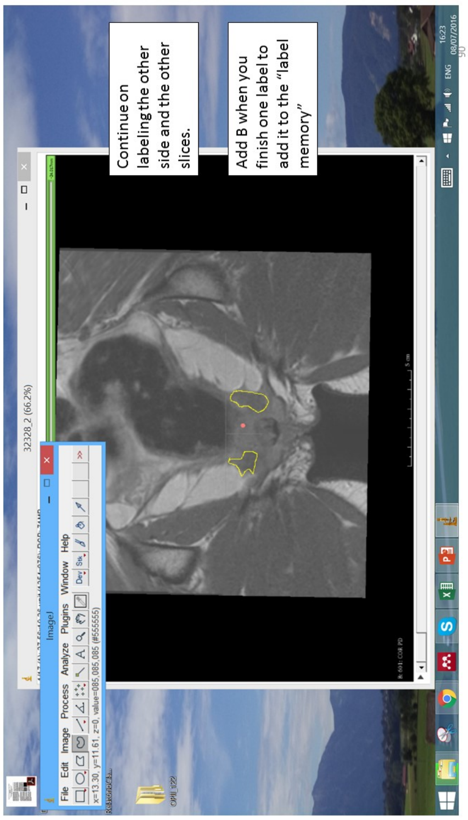
Continue on
labeling the other
side and the other
slices.
Add B when you
finish one label to
add it to the "label
memory"

The end!

Well done!

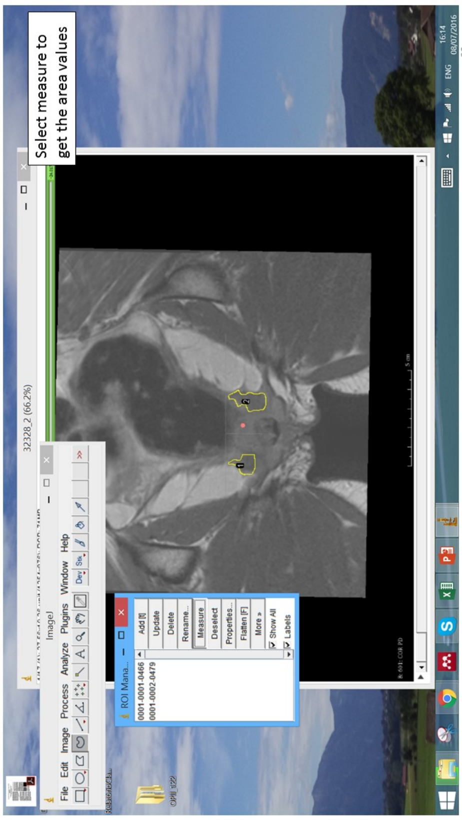

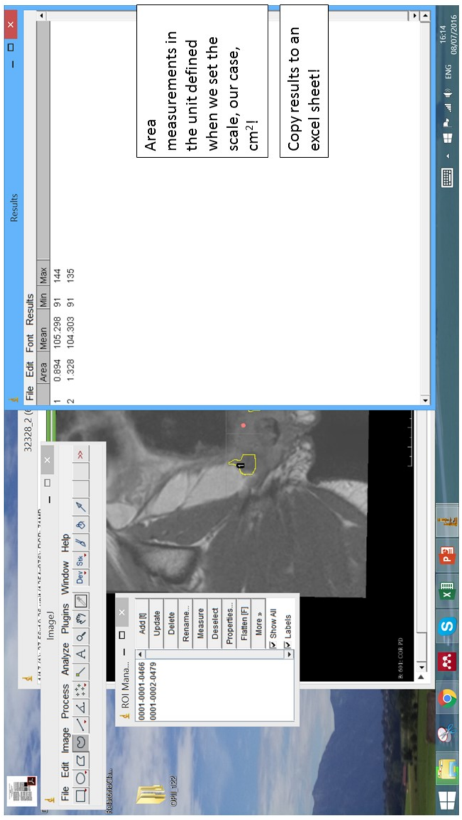

Appendix C

Appendix III - Ratio between areas

Calculting the ratio between the area of the base of the cube and the area of a plane cut at a angle α from the base of the cube.

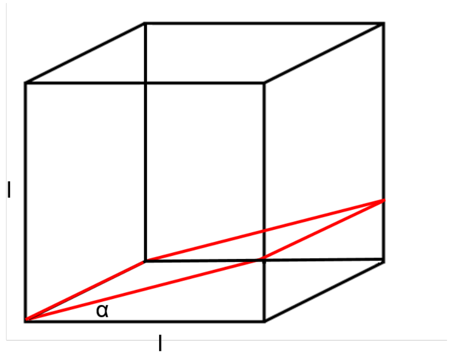

Figure C.1: Ratio between areas, represent by the ratio of the base of the cube and the area of a plane cut at an angle α from the base of the cube. The dimension of the cube's edge is given by l.

$$A_{cube} = l^2$$

(C.1)

$$A_{angleplane} = l * \frac{l}{cos\alpha}$$

(C.2)

$$\alpha = 9^{\circ} \tag{C.3}$$

$$\frac{A_{cube}}{A_{angleplane}} = \frac{l^2}{l * \frac{l}{cos\ \alpha}} = \frac{1}{cos\alpha} = \frac{1}{cos\ 9^\circ} \approx 1.01 \approx 1\%\ difference \tag{C.4}$$

References

[1] R. Kearney, R. Sawhney, and J. O. L. DeLancey, "Levator Ani Muscle Anatomy Evaluated by Origin-Insertion Pairs," *Obstetrics & Gynecology*, vol. 104, no. 1, pp. 168–173, 2004.

[2] L. Chen, Y. Hsu, J. A. Ashton-Miller, and J. O. L. DeLancey, "Measurement of the pubic portion of the levator ani muscle in women with unilateral defects in 3-D models from MR images," *International Journal of Gynecology and Obstetrics*, vol. 92, no. 3, pp. 234–241, 2006.

[3] J. Pizarro-Berdichevsky, M. M. Clifton, and H. B. Goldman, "Evaluation and Management of Pelvic Organ Prolapse in Elderly Women," *Clinics in Geriatric Medicine*, vol. 31, no. 4, pp. 507–521, 2015.

[4] US Army Natick Research and Development Command, "Anthropometry of women of the US Army," 1977.

[5] R. V. Baragi, J. O. L. Delancey, R. Caspari, and D. H. Howard, "Differences in pelvic floor area between African American and European American women," *Am J Obstet Gynecol*, no. July, pp. 111–115, 2002.

[6] C. Betschart, J. Kim, J. M. Miller, J. A. Ashton-Miller, and J. O. L. DeLancey, "Comparison of muscle fiber directions between different levator ani muscle subdivisions: In vivo MRI measurements in women," *International Urogynecology Journal and Pelvic Floor Dysfunction*, vol. 25, no. 9, pp. 1263–1268, 2014.

[7] J. A. Ashton-Miller, R. Zielinski, J. M. Miller, and J. O. L. Delancey, "Clinical Biomechanics Validity and reliability of an instrumented speculum designed to minimize the effect of intra-abdominal pressure on the measurement of pelvic fl oor muscle strength," *Journal of Clinical Biomechanics*, vol. 29, no. 10, pp. 1146–1150, 2014.

[8] J. A. Ashton-Miller and J. O. L. DeLancey, "Functional Anatomy of the Female Pelvic Floor," *Ann. N.Y. Acad. Sci.*, no. 1101, pp. 266–296, 2007.

[9] J. Mant, R. Painter, and M. Vessey, "Epidemiology of genital prolapse: observations from the Oxford Family Planning Association Study.," *British journal of obstetrics and gynaecology*, vol. 104, pp. 579–85, may 1997.

[10] F. C. o. A. Terminology, *Terminologia anatomica: international anatomical terminology*. Stuttgard, Germany: Thieme, 1998.

[11] K.-C. Lien, B. Mooney, J. O. L. DeLancey, and J. A. Ashton-Miller, "Levator Ani Muscle Stretch Induced by Simulated Vaginal Birth," *Obstetrics & Gynecology*, vol. 103, no. 1, pp. 31–40, 2004.

[12] D. Jing, J. A. Ashton-Miller, and J. O. L. DeLancey, “A subject-specific anisotropic visco-hyperelastic finite element model of the female pelvic floor stress and strain during the second stage of labor,” *J Biomech*, vol. 45, no. 3, pp. 455–460, 2011.

[13] J. Kim, C. Betschart, R. Ramanah, J. A. Ashton-Miller, and J. O. L. DeLancey, “Anatomy of the Pubovisceral Muscle Origin : Macroscopic and Microscopic Findings Within the Injury Zone,” *Neurourology and urodynamics*, pp. 1–7, 2014.

[14] J. M. Miller, L. K. Low, R. Zielinski, A. R. Smith, J. O. L. Delancey, and C. Brandon, “Evaluating maternal recovery from labor and delivery: Bone and levator ani injuries,” *American Journal of Obstetrics and Gynecology*, vol. 213, no. 2, pp. 188.e1–188.e11, 2015.

[15] J. O. DeLancey, D. M. Morgan, D. E. Fenner, R. Kearney, K. Guire, J. M. Miller, H. Hussain, W. Umek, Y. Hsu, and J. a. Ashton-Miller, “Comparison of levator ani muscle defects and function in women with and without pelvic organ prolapse,” *Obstet Gynecol*, vol. 109, no. 2 Pt 1, pp. 295–302, 2007.

[16] A.-c. Pizzoferrato and G. Bader, “Dynamic Magnetic Resonance Imaging and pelvic floor disorders : how and when ?,” vol. 2115, no. 14, 2014.

[17] K. Berzuk and B. Shay, “Effect of increasing awareness of pelvic floor muscle function on pelvic floor dysfunction: a randomized controlled trial,” *International Urogynecology Journal*, vol. 26, no. 6, pp. 837–844, 2015.

[18] I. E. Nygaard, F. L. Thompson, S. L. Svengalis, and J. P. Albright, “Urinary Incontinence in Elite Nulliparous,” *Obstetrics & Gynecology*, vol. 2, pp. 183–187, 1994.

[19] A. Olsen, V. Smith, J. Bergstrom, J. Colling, and A. Clark, “Epidemiology of surgically managed pelvic organ prolapse and urinary incontinence .,” *Obstetrics & Gynecology*, vol. 89, no. 4, pp. 501–506, 1997.

[20] R. M. Freeman, “Do we really know the outcomes of prolapse surgery?,” *Maturitas*, vol. 65, no. 1, pp. 11–14, 2010.

[21] S. H. Boyles, A. M. Weber, and L. Meyn, “Procedures for urinary incontinence in the United States, 1979-1997,” *American Journal of Obstetrics and Gynecology*, vol. 189, pp. 70–75, jul 2003.

[22] L. Suback, L. Waetjen, S. van den Eeden, D. Thom, E. Vittinghoff, and J. Brown, “Cost of pelvic organ prolapse surgery in the United States. - PubMed - NCBI,” *Obstet Gynecol*, vol. Oct, no. 98(4), pp. 646–51, 2001.

[23] C. Menon, F. Carpi, and D. De Rossi, “Concept design of novel bio-inspired distributed actuators for space applications,” *Acta Astronautica*, vol. 65, no. 5-6, pp. 825–833, 2009.

[24] J. E. Jelovsek and M. D. Barber, “Women seeking treatment for advanced pelvic organ prolapse have decreased body image and quality of life,” *American Journal of Obstetrics and Gynecology*, vol. 194, no. 5, pp. 1455–1461, 2006.

[25] E. Lamin, L. M. Parrillo, D. K. Newman, and A. L. Smith, “Pelvic Floor Muscle Training: Underutilization in the USA,” *Current Urology Reports*, vol. 17, no. 2, pp. 1–7, 2016.

[26] Food and Drug Administration, “FDA strengthens requirements for surgical mesh for the transvaginal repair of pelvic organ prolapse to address safety risks,” 2016.

[27] G. Rostaminia, M. Machiorlatti, S. A. Shobeiri, and L. H. Quiroz, "Variability of the pubic arch architecture and its influence on the minimal levator hiatus area," *International Journal of Gynecology & Obstetrics*, vol. 134, pp. 217–220, 2016.

[28] P. V. Tracy, J. O. Delancey, and J. A. Ashton-Miller, "A geometric capacity-demand analysis of maternal levator muscle stretch required for vaginal delivery," *Journal of Biomechanical Engineering*, vol. 138, no. February, 2016.

[29] J. U. o. M. DeLancey, "Why do women have stress urinary incontinence," *Neurourol Urodyn*, vol. 29, no. Suppl 1, pp. 1–12, 2012.

[30] D. M. Morgan, G. Kaur, Y. Hsu, D. E. Fenner, K. Guire, J. Miller, J. A. Ashton-Miller, and J. O. L. Delancey, "Does vaginal closure force differ in the supine and standing positions?," *American Journal of Obstetrics and Gynecology*, vol. 192, no. 5 SPEC. ISS., pp. 1722–1728, 2005.

[31] A. L. da Silva-Filho, P. a. L. S. Martins, M. P. Parente, C. S. Saleme, T. Roza, M. Pinotti, T. Mascarenhas, and R. M. Natal Jorge, "Translation of biomechanics research to urogynecology.," *Archives of gynecology and obstetrics*, vol. 282, pp. 149–55, aug 2010.

[32] C. Strauss, A. Lienemann, F. Spelsberg, M. Bauer, W. Jonat, and A. Strauss, "Biomechanics of the female pelvic floor: a prospective trail of the alteration of force-displacement-vectors in parous and nulliparous women.," *Archives of gynecology and obstetrics*, vol. 285, pp. 741–7, mar 2012.

[33] L. Hoyte and M. S. Damaser, "Magnetic resonance-based female pelvic anatomy as relevant for maternal childbirth injury simulations," *Annals of the New York Academy of Sciences*, vol. 1101, pp. 361–376, 2007.

[34] S. J. Madill and L. McLean, "A contextual model of pelvic floor muscle defects in female stress urinary incontinence: A rationale for physiotherapy treatment," *Annals of the New York Academy of Sciences*, vol. 1101, pp. 335–360, 2007.

[35] S. Brandão, T. Da Roza, M. Parente, I. Ramos, T. Mascarenhas, and R. M. Natal Jorge, "Magnetic resonance imaging of the pelvic floor: from clinical to biomechanical imaging.," *Proceedings of the Institution of Mechanical Engineers. Part H, Journal of engineering in medicine*, vol. 227, pp. 1324–32, dec 2013.

[36] A.-C. Pizzoferrato, K. Nyangoh Timoh, X. Fritel, E. Zareski, G. Bader, and A. Fauconnier, "Dynamic Magnetic Resonance Imaging and pelvic floor disorders: how and when?," *European journal of obstetrics, gynecology, and reproductive biology*, vol. 181, pp. 259–66, oct 2014.

[37] F. Yao, M. A. Laudano, S. Seklehner, B. Chughtai, and R. K. Lee, "Image-Based Simulation of Urethral Distensibility and Flow Resistance as a Function of Pelvic Floor Anatomy," *Neurourology and urodynamics*, no. April, 2014.

[38] E. Nystrom, H. Stenlund, and E. Samuelsson, "ICIQ Symptom and Quality of Life Instruments Measure Clinically Relevant Improvements in Women With Stress Urinary Incontinence," *Neurourology and urodynamics*, no. April, 2014.

[39] N. H. Fultz, G. G. Fisher, and K. R. Jenkins, "Does urinary incontinence affect middle-aged and older women's time use and activity patterns?," *Obstetrics and gynecology*, vol. 104, pp. 1327–34, dec 2004.

[40] M. Pakbaz, E. Rolfsman, I. Mogren, and M. LÖfgren, "Vaginal prolapse - Perceptions and healthcare-seeking behavior among women prior to gynecological surgery," *Acta Obstetricia et Gynecologica Scandinavica*, vol. 90, no. 10, pp. 1115–1120, 2011.

[41] V. W. Sung, B. Washington, and C. A. Raker, "Costs of ambulatory care related to female pelvic floor disorders in the United States," *American Journal of Obstetrics and Gynecology*, vol. 202, no. 5, pp. 483.e1–483.e4, 2010.

[42] C. Chaliha, "Postpartum pelvic floor trauma," *Current opinion in obstetrics & gynecology*, vol. 21, pp. 474–479, 2009.

[43] R. Kearney, J. M. Miller, J. A. Ashton-miller, and J. O. L. Delancey, "Obstetric factors associated with levator ani muscle injury after vaginal delivery," *Obstetrics & Gynecology*, vol. 107, no. 1, pp. 144–149, 2006.

[44] R. E. Allen, G. L. Hosker, A. R. Smith, and D. W. Warrell, "Pelvic floor damage and childbirth: a neurophysiological study.," *British journal of obstetrics and gynaecology*, vol. 97, pp. 770–9, sep 1990.

[45] D. Howard, J. O. L. Delancey, R. Tunn, and J. A. Ashton-miller, "Racial Differences in the Structure and Function of the Stress Urinary Continence Mechanism," *Obstetrics & Gynecology*, vol. 95, no. 5, pp. 713–717, 2005.

[46] H. P. Dietz, "Pelvic floor trauma following vaginal delivery.," *Current opinion in obstetrics & gynecology*, vol. 18, pp. 528–537, 2006.

[47] H. P. Dietz and V. Lanzarone, "Levator trauma after vaginal delivery.," *Obstetrics and gynecology*, vol. 106, no. 4, pp. 707–712, 2005.

[48] J. A. Ashton-Miller and J. O. L. DeLancey, "On the Biomechanics of Vaginal Birth and Common Sequelae," *Annu Rev Biomedical Eng*, vol. 11, pp. 163–176, 2009.

[49] Centers for Disease Control, "Growth Charts - Data Table of Stature-for-age Charts," 2001.

[50] J. M. Miller, C. Brandon, J. A. Jacobson, L. K. Low, R. Zielinski, J. Ashton-Miller, and J. O. L. DeLancey, "MRI findings in patients considered high risk for pelvic floor injury studied serially after vaginal childbirth," *American Journal of Roentgenology*, vol. 195, no. 3, pp. 786–791, 2010.

[51] G. Hilde, J. Staer-Jensen, F. Siafarikas, K. Gjestland, M. Ellström Engh, and K. Bø, "How well can pelvic floor muscles with major defects contract? A cross-sectional comparative study 6 weeks after delivery using transperineal 3D/4D ultrasound and manometer.," *BJOG : an international journal of obstetrics and gynaecology*, vol. 120, no. 11, pp. 1423–9, 2013.

[52] J. O. L. DeLancey, D. M. Morgan, D. E. Fenner, R. Kearney, K. Guire, J. M. Miller, H. Hussain, W. Umek, Y. Hsu, and J. a. Ashton-Miller, "Comparison of levator ani muscle defects and function in women with and without pelvic organ prolapse.," *Obstetrics and gynecology*, vol. 109, no. 2 Pt 1, pp. 295–302, 2007.

[53] L. T. Sirls, S. Tennstedt, M. Albo, T. Chai, K. Kenton, L. Huang, A. M. Stoddard, A. Arisco, and E. A. Gormley, "Factors associated with quality of life in women undergoing surgery for stress urinary incontinence.," *The Journal of urology*, vol. 184, pp. 2411–5, dec 2010.

[54] J. Luo, *Biomechanical Analysis of Posterior Vaginal Prolapse: MR Imaging and Computer Modeling Studies*. The University of Michigan, 2012.

[55] D. M. Spahlinger, L. Newcomb, J. A. Ashton-Miller, J. O. DeLancey, and L. Chen, "Relationship between intra-abdominal pressure and vaginal wall movements during Valsalva in women with and without pelvic organ prolapse : technique development and early observations," *International urogynecology journal*, vol. 25, pp. 873–881, 2014.

[56] H. P. Dietz, "Pelvic organ prolapse: a review," *Australian family physician*, vol. 44, no. 7, pp. 446–452, 2015.

[57] K. Rooney, K. Kenton, E. R. Mueller, M. P. FitzGerald, and L. Brubaker, "Advanced anterior vaginal wall prolapse is highly correlated with apical prolapse.," *American journal of obstetrics and gynecology*, vol. 195, pp. 1837–40, dec 2006.

[58] A. Summers, L. A. Winkel, H. K. Hussain, and J. O. L. DeLancey, "The relationship between anterior and apical compartment support," *American Journal of Obstetrics and Gynecology*, vol. 194, no. 5, pp. 1438–1443, 2006.

[59] J. Sendroy Jr. and L. P. Cechini, "Determination of human body surface area from height and weight," *J Appl.Physiol*, vol. 21, no. 1, pp. 1–12, 1966.

[60] C. E. Clauser, "Weight, volume, and center of mass of segments of the human body," *Air Force Systems Command Wright-Patterson Air Force Base, Ohio*, 1969.

[61] M. J. Egger, N. M. Hamad, R. W. Hitchcock, T. J. Coleman, J. M. Shaw, Y. Hsu, and I. E. Nygaard, "Reproducibility of intra-abdominal pressure measured during physical activities via a wireless vaginal transducer.," *Female pelvic medicine & reconstructive surgery*, vol. 21, pp. 164–9, jan 2015.

[62] L. Mouritsen, M. Hulb??k, S. Brostr??m, and J. Bogstad, "Vaginal pressure during daily activities before and after vaginal repair," *International Urogynecology Journal and Pelvic Floor Dysfunction*, vol. 18, no. 8, pp. 943–948, 2007.

[63] K. K. O'Dell, A. N. Morse, S. L. Crawford, and A. Howard, "Vaginal pressure during lifting, floor exercises, jogging, and use of hydraulic exercise machines.," *International urogynecology journal and pelvic floor dysfunction*, vol. 18, pp. 1481–9, dec 2007.

[64] R. L. Mizner, J. K. Kawaguchi, and T. L. Chmielewski, "Muscle strength in the lower extremity does not predict postinstruction improvements in the landing patterns of female athletes.," *The Journal of orthopaedic and sports physical therapy*, vol. 38, no. 6, pp. 353–361, 2008.

[65] K. K. O'Dell, A. N. Morse, S. L. Crawford, and A. Howard, "Vaginal pressure during lifting, floor exercises, jogging, and use of hydraulic exercise machines.," *International urogynecology journal and pelvic floor dysfunction*, vol. 18, pp. 1481–9, dec 2007.

[66] R. U. Margulies, Y. Hsu, R. Kearney, T. Stein, W. H. Umek, and J. O. L. DeLancey, "Appearance of the levator ani muscle subdivisions in magnetic resonance images.," *Obstetrics and gynecology*, vol. 107, pp. 1064–9, may 2006.

[67] M. Ikai and T. Fukunaga, "Calculation of muscle strength per unit cross-sectional area of human muscle by means of ultrasonic measurement.," *Internationale Zeitschrift fur angewandte Physiologie, einschliesslich Arbeitsphysiologie*, vol. 26, pp. 26–32, jan 1968.

[68] S. Brooks and J. Faulkner, “Skeletal muscle weakness in old age: Underlying mechanisms,” 1994.

[69] T. Kim, I. Sridharan, Y. Ma, B. Zhu, N. Chi, W. Kobak, J. Rotmensch, J. D. Schieber, and R. Wang, “Identifying distinct nanoscopic features of native collagen fibrils towards early diagnosis of pelvic organ prolapse.,” *Nanomedicine : nanotechnology, biology, and medicine*, vol. 12, no. 3, pp. 667–675, 2015.

[70] L. K. Low, R. Zielinski, Y. Tao, A. Galecki, C. J. Brandon, and J. M. Miller, “Predicting Birth-Related Levator Ani Tear Severity in Primiparous Women: Evaluating Maternal Recovery from Labor and Delivery (EMRLD Study),” *Open J Obstet Gynecol*, vol. 4, no. 6, pp. 266–278, 2014.

[71] V. C. Morris, M. P. Murray, J. O. L. DeLancey, and J. A. Ashton-Miller, “A comparison of the effect of age and levator ani and obturador internus muscle cross-sectional areas and volumes in nulliparous women,” *Neurourology and urodynamics*, vol. 31, pp. 481–486, 2012.

[72] 3D Slicer Community, “3D Slicer Transforms command,” 2016.

[73] 3D Slicer Community, “3D Slicer Reformat command,” 2016.

[74] J. Lopinto, “AnglePlanes documentation,” 2016.

[75] G. Rankin and M. Stokes, “Reliability of assessment tools in rehabilitation: an illustration of appropriate statistical analyses.,” *Clinical rehabilitation*, vol. 12, pp. 187–99, jun 1998.

[76] J. Martin Bland and D. Altman, “Statistical Methods for Assessing Agreement Between Two Methods of Clinical Measurement,” *The Lancet*, vol. 327, no. 8476, pp. 307–310, 1986.

[77] L. Hoyte, M. Jakab, S. K. Warfield, S. Shott, G. Flesh, and J. R. Fielding, “Levator ani thickness variations in symptomatic and asymptomatic women using magnetic resonance-based 3-dimensional color mapping,” *American Journal of Obstetrics and Gynecology*, vol. 191, no. 3, pp. 856–861, 2004.

[78] C. Alt, F. Hampel, P. Hallsheidt, C. Shon, B. Schele, and K. Brocker, “3T MRI-Based Measurements for the Integrity of the Female Pelvic Floor in 25 Healthy Nulliparous Women,” *Neurourology and urodynamics*, vol. 35, pp. 218–223, 2016.

[79] J. R. Fielding, H. Dumanli, A. G. Schreyer, S. Okuda, D. T. Gering, K. H. Zou, R. Kikinis, and F. A. Jolesz, “MR-based three-dimensional modeling of the normal pelvic floor in women: Quantification of muscle mass,” *American Journal of Roentgenology*, vol. 174, no. 3, pp. 657–660, 2000.

[80] J. A. Kruger, H. P. Dietz, and B. A. Murphy, “Pelvic floor function in elite nulliparous athletes,” *Ultrasound in Obstetrics and Gynecology*, vol. 30, pp. 81–85, jul 2007.

[81] A. L. Ackerman, U. J. Lee, F. C. Jellison, N. Tan, M. Patel, S. S. Raman, and L. V. Rodriguez, “MRI suggests increased tonicity of the levator ani in women with interstitial cystitis/bladder pain syndrome,” *International Urogynecology Journal and Pelvic Floor Dysfunction*, vol. 27, no. 1, pp. 77–83, 2016.

[82] H.-C. Hung, S.-M. Hsiao, S.-Y. Chih, H.-H. Lin, and J.-Y. Tsauo, “Effect of pelvic-floor muscle strengthening on bladder neck mobility: a clinical trial.,” *Physical therapy*, vol. 91, pp. 1030–8, jul 2011.

[83] B. Junginger, K. Baessler, R. Sapsford, and P. W. Hodges, “Effect of abdominal and pelvic floor tasks on muscle activity, abdominal pressure and bladder neck.,” *International urogynecology journal*, vol. 21, pp. 69–77, jan 2010.

[84] D. R. Claflin, L. M. Larkin, P. S. Cederna, J. F. Horowitz, N. B. Alexander, N. M. Cole, A. T. Galecki, S. Chen, L. V. Nyquist, B. M. Carlson, J. A. Faulkner, and J. A. Ashton-Miller, “Effects of high- and low-velocity resistance training on the contractile properties of skeletal muscle fibers from young and older humans.,” *Journal of applied physiology (Bethesda, Md. : 1985)*, vol. 111, pp. 1021–30, oct 2011.

[85] Y. Ozog, J. Deprest, K. Haest, F. Claus, D. De Ridder, and E. Mazza, “Calculation of membrane tension in selected sections of the pelvic floor,” *International Urogynecology Journal and Pelvic Floor Dysfunction*, vol. 25, no. 4, pp. 499–506, 2014.

[86] C. Betschart, L. Chen, J. A. Ashton-Miller, and J. O. L. DeLancey, “On pelvic reference lines and the MR evaluation of genital prolapse: a proposal for standardization using the Pelvic Inclination Correction System,” *International urogynecology journal*, vol. 18, no. 9, pp. 1199–1216, 2013.